

Functional Roles of NYD-SP8 in Cancer Development and Progression

CHUNG, Chin Man

A Thesis Submitted in Partial Fulfillment
of the Requirements for the Degree of
Doctor of Philosophy
in

Physiology

The Chinese University of Hong Kong
December 2009

UMI Number: 3436630

All rights reserved

INFORMATION TO ALL USERS

The quality of this reproduction is dependent upon the quality of the copy submitted.

In the unlikely event that the author did not send a complete manuscript and there are missing pages, these will be noted. Also, if material had to be removed, a note will indicate the deletion.



UMI 3436630

Copyright 2010 by ProQuest LLC.

All rights reserved. This edition of the work is protected against unauthorized copying under Title 17, United States Code.



ProQuest LLC
789 East Eisenhower Parkway
P.O. Box 1346
Ann Arbor, MI 48106-1346

Thesis/Assessment Committee

Professor WH Yung (Chair)

Professor HC Chan (Thesis Supervisor)

Professor SB Yu (Committee Member)

Professor XY Guan (External Examiner)

Content

Abstract	i
中文摘要	iii
Related Publications	v
Conference Abstract	vi
Awards	vi
Declaration	vii
Acknowledgements	ix
List of figures	x
List of abbreviations	xiii
Chapter 1 General Introduction	1
1.1 The epidemiology of cancer	1
1.2 The Cancer/Testis antigen for immunotherapy	1
1.3 Multi-steps of tumor development	2
1.4 Identification of NYD-SP8 in male reproductive tract	6
1.5 NYD-SP8 is hypothesized as a novel CT antigen	8
1.6 Objectives	11
Chapter 2 Materials and Methods	12
Chapter 3 Characterization of NYD-SP8 in cancer tissues – a novel interacting partner of uPAR	26
3.1 Introduction	26
3.1.1 GPI-anchored protein family.....	26

3.1.2 The urokinase Plasminogen Activator Receptor: an example of GPI-anchored proteins	27
3.1.3 Objectives.....	30
3.2 Experimental plan	31
3.3 Results	32
3.3.1 Expression of NYD-SP8 in multiple cancer tissues	32
3.3.2 NYD-SP8 is shed off by PI-PLC	36
3.3.3 NYD-SP8 is homologous to uPAR	36
3.3.4 NYD-SP8 protein interacts with uPA/uPAR complexes.....	40
3.4 Discussion.....	43
3.4.1 NYD-SP8 is a novel CT antigen	43
3.4.2 Stage specific expression of NYD-SP8	43
3.4.3 NYD-SP8 interacts with uPA/uPAR complexes	44
3.4.4 Post-translational modification of NYD-SP8	45
Chapter 4 Regulation of Programmed Cell Death by NYD-SP8.....	46
4.1 Introduction	46
4.1.1 Cell proliferation and cell cycle progression.....	46
4.1.2 Apoptosis	47
4.1.3 p53, a linker between cell cycle progression and apoptosis	47
4.1.4 NFkB, a well known mediator of apoptosis	49
4.1.5 The balance of Bcl-2 family leading to apoptosis	50
4.1.6 TNF α induced NFkB activation	50
4.1.7 Objective	52
4.2 Experimental plan	54

4.3.Results	55
4.3.1 NYD-SP8 promotes cell proliferation <i>in vitro</i>	55
4.3.2 Effect of NYD-SP8 in cell cycle progression and apoptosis.....	55
4.3.3 NYD-SP8 contributes to anchorage independent growth	62
4.3.4 Anti-apoptotic signaling in NYD-SP8 cells.....	62
4.3.5 Involvement of p53 in mediating the anti-apoptotic effect of NYD-SP8 ...	66
4.3.6 NYD-SP8 promotes tumor growth in vivo	66
4.4 Discussion	73
4.4.1 The growth promoting function of NYD-SP8 may be p53 dependent	73
4.4.2 Possible signaling mechanisms underlying NYD-SP8-mediated growth promoting effect	73
4.4.3 NYD-SP8 initiates uPAR dependent/independent downstream signalings	74
4.4.4 Limitations and future studies	75
4.4.5 More to know: Effect of tumor microenvironment on NYD-SP8 activity .	75
Chapter 5 NYD-SP8 inhibits cancer cell invasion and metastasis	77
5.1 Introduction	77
5.1.1 Cancer Invasion and Metastasis	77
5.1.2 Extracellular matrix (ECM) degradation	77
5.1.3 Serine Proteinases	79
5.1.4 The Matrix Metalloproteinase (MMPs) family	83
5.1.5 The Cysteine cathepsins Family	84
5.1.6 Objective	84
5.2 Experimental plan.....	86
5.3 Results.....	87

5.3.1 Suppressing functions of NYD-SP8 in uPAR family	87
5.3.2 NYD-SP8 suppresses MMPs activities	90
5.3.3 NYD-SP8 suppress Cathepsin B activity	93
5.3.4 NYD-SP8 inhibits cancer invasion and metastasis <i>in vivo</i>	84
5.4 Discussion	86

Chapter 6 Involvement of NYD-SP8 in Epithelial and Mesenchymal Transition ...105

6.1 Introduction	105
6.1.1 Epithelial-mesenchymal transitions	105
6.1.2 Induction and signaling mechanisms of EMTs	107
6.1.3 <i>In vitro</i> model of EMTs - The LIM1863 cell lines model	107
6.1.4 Cell matrix interactions in EMTs	110
6.1.5 Objectives	111
6.2 Experimental Plan	112
6.3 Results	113
6.3.1 Induction of EMTs by TGF- β in LIM1863 organoids	113
6.3.2 Accelerated EMTs under TNF- α /TGF- β treatment in LIM1863.....	115
6.3.3 NYD-SP8 affects cell-matrix interaction	115
6.4 Discussion	118
6.4.1 Loss of MYD-SP8 may be a pre-requisite for EMTs	118
6.4.2 Overexpression of NYD-SP8 results in immobilization of cancer cells ...	118
6.4.3 NYD-SP8 may serve as a new molecular marker of EMT	119

Chapter 7 Final Discussion and Conclusion120

7.1 Stage-specific expression of NYD-SP8	120
------------------------------------------------	-----

7.2 Stage-specific biological functions of NYD-SP8 in cancer development	120
7.3 Relationship between NYD-SP8 and uPAR	121
7.4 NYD-SP8 and its implications	122
7.4.1 NYD-SP8 may serve as a potential biomarker for early onset of tumor development and EMTs.....	122
7.4.2 NYD-SP8 may serve as a potential immunotherapeutic target.	122
7.5 Future Studies.....	123
7.6 Conclusion.....	123
Reference list.....	125
Appendix A Chemical and Reagents.....	152
Appendix B Antibodies lists	155
Appendix C Buffer Recipe	156
Appendix D Primer lists	159

Abstract

Cancer/testis (CT) antigens are encoded by genes that are normally expressed only in the human germ-line, but are also expressed in various tumor types. CT antigens are also being studied for their roles in carcinogenesis as well as for their potentials as targets for anti-cancer therapy. A novel CT gene, NYD-SP8, (Accession No. AY014285.1) has recently been identified. It is located to human chromosome *19q13.31* and encodes a 27 kDa glucosylphosphatidylinositol (GPI) anchored cell surface protein, which shows structural homology to urokinase plasminogen activator receptor (uPAR). This thesis describes the characterization and functional roles of NYD-SP8 involved in cancer development.

In the first set of experiments, the possible role(s) and underlying mechanism(s) of NYD-SP8 in regulating cell proliferation and apoptosis were investigated. Flow cytometric analysis, cell proliferation assay and Western blot analysis showed that NYD-SP8 promoted cell proliferation and protected cells against TNF α -induced apoptosis in Human embryonic kidney cells (HEK293) and human hepatocellular carcinoma cells (hHCC). *In vitro* studies showed that NYD-SP8 enhanced anchorage-independent growth of hHCC, further suggesting the pro-survival effect of NYD-SP8. These data demonstrated important functions of NYD-SP8 in promoting cell growth and preventing apoptosis during cancer development.

In the second sets of experiments, the possible role(s) and underlying mechanism(s) of NYD-SP8 in regulating cancer invasion and metastasis were investigated. The results showed that NYD-SP8 could suppress multiple "tumor associated" proteases. Overexpression of NYD-SP8 resulted in reducing activities of the three major classes of proteases known to be involved in ECM degradation, including uPA, matrix metalloproteinases (MMPs) and cathepsin B, leading to suppression of both *in vitro* and *in vivo* cancer cell invasion and metastasis. Co-immunoprecipitation experiments showed binding of NYD-SP8 to uPA/uPAR complexes and interfering with active uPA production. These data demonstrated an important function of

NYD-SP8 in regulating ECM degradation, providing a novel mechanism that modulates uPA/uPAR signaling in the suppression of cancer progression.

In the last part of thesis, the involvement of NYD-SP8 in epithelial-mesenchymal transitions (EMTs) was demonstrated. Upon TGF β stimulation or TGF β /TNF α co-stimulation, the mRNA and protein expression of NYD-SP8 was decreased in LIM1863 cells. Cell adhesion assay showed that the attachment ability of hHCC-SP8 was lowered in laminin and fibronectin coated plate, suggesting the possible role of NYD-SP8 in affecting cell-matrix interaction. These data indicate that NYD-SP8 is involved in the EMTs process and may serve as potential EMTs markers during cancer development.

In summary, the present findings have demonstrated the roles of NYD-SP8 in multi-step cancer development. Further investigations of NYD-SP8 in cancer development may provide new insights and ground for potential use of CT antigens in anti-cancer therapy.

(Abstract: 428 words)

中文摘要

CT 抗原是由一組在正常情況下只在生殖細胞表達，但也在多種腫瘤中表達的基因編碼的蛋白。目前關於它們在癌症發生的作用及其作為抗癌治療靶點的可能性正在研究之中。NYD-SP8 是一個新發現的 CT 抗原基因，它位於人類染色體的 19q13.31，編碼一個 27 kDa 的細胞表面的糖磷脂醯肌醇 (GPI) 錨定蛋白，這個蛋白在結構上與尿激型纖維溶原激活物受體 (uPAR) 具有同源性。本論文研究了 NYD-SP8 的特徵及其在癌症發展中的作用。

實驗的第一部分研究了 NYD-SP8 調節細胞增殖和細胞凋亡的作用及其機制。流式細胞分析，細胞增殖實驗和 Western blot 分析顯示，NYD-SP8 能夠在體內和體外調節細胞增殖和抑制由 $TNF\alpha$ 誘導的凋亡，保護人胚腎細胞 (HEK293) 和人肝癌細胞 (hHCC)。體外實驗顯示，NYD-SP8 增強了 hHCC 在軟膠 (soft agar) 的非貼附性細胞生長，進一步提示了 NYD-SP8 對細胞生存的作用。這些結果證明了在癌症發展中 NYD-SP8 對促進細胞生存的作用。

實驗的第二部分研究了 NYD-SP8 調節癌症侵襲和轉移的作用和機制。實驗結果顯示，NYD-SP8 是一個蛋白酶抑制物。超表達 NYD-SP8 導致三類多量的細胞外間質 (ECM) 降解的蛋白酶活性下降，包括尿激型纖維溶原激活物 (uPA)，基質金屬蛋白酶 (MMPs) 和細胞自溶酵素 B (Cathepsin B)，從而在體內和體外實驗中抑制癌症侵襲和轉移。免疫共沉澱實驗顯示 NYD-SP8 能夠結合 uPA/uPAR 複合物，並影響 uPA 的生成。以上結果證明了 NYD-SP8 在調節 ECM 降解中有重要作用，為抑制癌症進程中 uPA/uPAR 的信號通路提出了一個新的機制。

論文的最後一部分證明 NYD-SP8 參與了上皮-間質轉化 (EMTs)。在 $TGF\beta$ 刺激或 $TGF\beta/TNF\alpha$ 的共同刺激下，NYD-SP8 mRNA 和蛋白在 LIM1863 細胞株中表達下調。細胞貼附實驗顯示，hHCC-SP8 在 laminin 和 fibronectin 上的貼附能力下降，提示 NYD-SP8 影響細胞-基質相互作用的可能作用。以上結果表明 NYD-SP8 參與了 EMT 過程，並且有望成為癌症發展過程中 EMT 的一個標誌。

綜上所述，本論文中的發現證明了 NYD-SP8 在癌症發展過程中的多個層面的作用。對 NYD-SP8 在癌症發展中的進一步研究可能為 CT 抗原在抗癌治療中的應用提供新的認識和基礎。

Related Publications

1. Yin LL*, Chung CM*, Chen J*, Fok KL, Ng CP, Jia RR, Ren X, Zhou J, Zhang T, Zhao XH, Lin M, Zhu H, Zhang XH, Tsang LL, Bi Y, Zhou Z, Mo F, Wong N, Chung YW, Sha J, Chan HC. *A suppressor of multiple extracellular matrix-degrading proteases and cancer metastasis*. J Cell Mol Med. 2008 Nov 6. [Epub ahead of print]
**Co-first author publication*
2. Yin L, Chung CM, Huo R, Liu H, Zhou C, Xu W, Zhu H, Zhang J, Shi Q, Wong HY, Chen J, Lu Y, Bi Y, Zhao C, Du Y, Ma M, Cai Y, Chen WY, Fok KL, Tsang LL, Li K, Ni Y, Chung YW, Zhou Z, Sha J, Chan HC. *A sperm GPI-anchored protein elicits sperm-cumulus cross-talk leading to the acrosome reaction*. Cell Mol Life Sci. 2009 Mar;66(5):900-8

Conference Abstract

1. **Chung CM** and Chan HC. Identification and characterization of a novel and putative tumor suppressor gene. International Symposium on Frontiers in Life Sciences: Molecular Basis of Disease, Prevention and Treatment. *Cell Biol Int.* Vol 30 (8) S22 Aug 2006

Awards

Global Scholarship Program for Research Excellence, Sept 2008

Declaration

I hereby declare that this thesis represents my own work, except where due acknowledgement is made, and that it has not been previously included in a thesis, dissertation or report submitted to this University or to any other institution for a degree, diploma or other qualification.

Signature

CHUNG, Chin Man

*This thesis is dedicated to my beloved parents.
From the day I was born, you always treated me with love and kindness.*

Acknowledgements

I am indebted to Professor Hsiao Chang Chan for her valuable guidance, wonderful motivation and support in my PhD study.

My sincere thanks to Prof. X.Y.Guan (University of Hong Kong) for providing cDNA samples of liver cancer cell lines; Prof. K.W. Lo (The Chinese University of Hong Kong) for providing cDNA samples of nasopharyngeal cancer cell lines; Prof. Yang (The Chinese University of Hong Kong) for providing multiple leukemia cell lines; Prof J.H.Sha (Nanjing University of China) for providing NYD-SP8 antibodies and supporting the immunostaining of NYD-SP8 in mouse testis and various cancer tissues.

To my dearest friend Ellis Fok, thank you for your love and care, advice and encouragement, and always being there for me.

To all the wonderful members in ECBRC and my friends, thank you for all your support, warmth and friendship during these years.

List of figures

- Figure 1.1** abnormal expression of CT antigens in cancer cells recapitulated the germ line gametogenic program
- Figure 1.2** Different pathological stages of carcinogenesis
- Figure 1.3** The eukaryotic cell cycle progression and related signaling pathways
- Figure 1.4** Human testis cDNA microarray
- Figure 1.5** Testis-specific tissue distribution of NYD-SP8
- Figure 1.6** Immunohistochemical staining of mouse testis using NYD-SP8 Ab
- Figure 2** Cloning vector map
- Figure 3.1** The GPI-anchored proteins
- Figure 3.2** Molecular structure of uPAR
- Figure 3.3** mRNA expression of NYD-SP8
- Figure 3.4** Immunohistochemical demonstration of NYD-SP8 protein expression in multiple human cancer tissue arrays
- Figure 3.5** Western blot analysis showing expression of NYD-SP8 protein
- Figure 3.6** Bioinformatic analyses showing the potential GPI-modification site of NYD-SP8 protein
- Figure 3.7** Western blot analysis of NYD-SP8 protein expression in different cell types
- Figure 3.8** Clustal W alignment showing about 30% homology of NYD-SP8 to uPAR
- Figure 3.9** NYD-SP8 expression in hHCC cells
- Figure 3.10** NYD-SP8 interacts with uPA/uPAR complexes
- Figure 4.1** Classical apoptosis of a leukemia cell with condensed chromatin, the cell shrinkage and the fragmentation of the cell into apoptotic bodies
- Figure 4.2** Bcl-2 family and apoptotic signaling pathways
- Figure 4.3** Schematic diagram showing the TNF-mediated signaling pathways
- Figure 4.4** Microscopic Imaging of hHCC cells and HEK293 cells stably expressing NYD-SP8
- Figure 4.5** Effect of NYD-SP8 in cell growth
- Figure 4.6** The effect of NYD-SP8 in cell cycle progression

Figure 4.7	The anti-apoptotic functions of NYD-SP8 in HEK293 cells
Figure 4.8	The anti-apoptotic functions of NYD-SP8 in hHCC cells
Figure 4.9	Soft agar anchorage-independent growth assay in hHCC cell lines
Figure 4.10	The cDNA oligoarray of hHCC and HEK293 cell lines
Figure 4.11	Western blot analysis showing NYD-SP8 down-regulated p53 expression
Figure 4.12	Signaling mechanisms of NYD-SP8 mediated apoptosis
Figure 4.13	The effect of NYD-SP8 in h1299 cells
Figure 4.14	Effect of NYD-SP8 in tumor growth <i>in vivo</i>
Figure 4.15	Western blot analyses showing the expression of Bcl-2, Bax and p53 protein in hHCC-SP8 tumor tissues and its control
Figure 4.16	<i>In vivo</i> studies of NYD-SP8 effect in tumor growth of h1299 cells
Figure 5.1	The schematic diagram of cancer invasion and metastasis
Figure 5.2	Involvement of tumor associated proteases in cancer invasion and metastasis
Figure 5.3	Schematic Diagram showing uPA/uPAR system mediated ECM degradation and involvement of integrins in several signaling pathways
Figure 5.4	NYD-SP8 suppresses serine proteases uPA activity at protein level
Figure 5.5	The NYD-SP8-uPA/uPAR complexes
Figure 5.6	RT-PCR analysis of mRNA expression of uPA, uPAR and PAI-1 in hHCC-SP8
Figure 5.7	NYD-SP8 suppresses MMPs activity
Figure 5.8	RT-PCR analysis of mRNA expression MMP2 and MMP9 in hHCC-SP8 cells
Figure 5.9	Suppressed mean cathepsin B activity in hHCC-SP8 cell line
Figure 5.10	Suppression of cancer invasion and metastasis <i>in vitro</i>
Figure 5.11	Bar chart showing the percentage of nude mice forming tumors 30 days after ip inoculation
Figure 5.12	NYD-SP8 suppresses experimental metastasis <i>in vivo</i>
Figure 5.13	Suppressed lung extravasations and metastasis of NYD-SP8-overexpressed cancer cells after tail vein injection
Figure 6.1	Transitions between epithelial and mesenchymal states during carcinoma progression

- Figure 6.2** Signaling networks regulating epithelial-mesenchymal transitions (EMTs)
- Figure 6.3** *In vitro* model of EMT using LIM1863 cell lines
- Figure 6.4** LIM1863 cells undergo EMT after addition of TGF- β
- Figure 6.5** LIM1863 cells undergo EMT after addition of TGF- β /TNF α co-stimulation
- Figure 6.6** Attachment assay of hHCC cells in Laminin and Fibronectin coated plate

List of Abbreviations

Bid	BH3 interacting domain death agonist
ACE	angiotensin I converting enzyme
APS	Ammonium persulfate
ATCC	American Type Culture Collection
bp	base pair
Brij-35	polyoxyethylene 23 lauryl ether
BSA	Bovine serum albumin
CaCl₂	calcium Chloride
cdc2	cell division cycle 2
CDK	Cyclin-dependent kinases
CDP	5' -pyrophosphates of adenosine
CMFDA	5-chloromethylfluorescein diacetate
CNE1	human nasopharyngeal cancer cell lines
CO₂	Carbon Dioxide
DAPI	4',6-diamidino-2-phenylindole
DEPC	Diethyl pyrocarbonate
dH₂O	Deionized water
DNA	Deoxyribonucleic acid
Dnase	Deoxyribonuclease
dNTPs	Deoxynucleoside triphosphate
DTT	DL-Dithiothreitol
ECM	extracellular matrix
ECL	Chemiluminescence
EDTA	Ethylene-diamine-tetraacetic acid
ELISA	Enzyme-linked immunosorbent assay
FACS	Flow analysis cytometry system
FBS	Fetal Bovin Serum
FITC	Fluorescein-5-isothiocyanate
G1/S	Checkpoint between G1 (Gap 1) phase and S (DNA synthesis) phase in a cell cycle
G2/M	Checkpoint between G2 (Gap 2) phase and M (mitosis)

	phase in a cell cycle
G418	Geneticin
GDP	Guanosine diphosphate
GEA	Gene expression analysis
GPI	glucosylphosphatidylinositol
GTP	Guanosine triphosphate
HCl	Hydrochloric acid
hr	hour
HRP	Horse-radish peroxidase-linked antibody
IgG	Immunoglobulin G
Kb	Kilobase-pair
KCl	Potassium chloride
MgCl₂	Magnesium chloride
min	minute
miRNA	micro RNA
M-MLV	Moloney Murine Leukemia Virus
MMPs	matrix metalloproteinases
MTS	3-(4,5-dimethylthiazol-2-yl)-5-(3-carboxymethoxyphenyl)-2-(4-sulfophenyl)-2H-tetrazolium)
NaCl	Sodium chloride
NaOH	Sodium hydroxide
NP40	Nonidet-P40
NYD-SP8	Ni Da Yi -Sperm specific Protein no.8
PBS	Phosphate buffer saline
PCD	programmed cell death
PCNA	Proliferating Cell Nuclear Antigen
PCR	Polymerase Chain Reaction
pEGFP-C2	plasmid Green fluorescence Protein -Clone 2
PMSF	Phenylmethylsulfonyl fluoride
PS	phospholipid phosphatidylserine
PVDF	Polyvinylidene fluoride
RIPA	Radioimmunoprecipitation
RNA	Ribonucleic acid
RNAse	Ribonuclease A

rpm	rotation per minute
RT-QPCR	Reverse transcription quantitative polymerase chain reaction
SDS-PAGE	Sodium dodecyl sulphate – polyacrylamide gel electrophoresis
TBS	Tris- buffered saline
TBST	Tris-buffered saline Tween
TEMED	Tetramethylethylenediamine
TGF-β	Trasforming Growth Factor beta
TNFα	Tumor Necrosis Factors
TNF-α	Tumor Necrosis Factor alpha
TRAF2	tumor necrosis factor receptor associated factor 2
TRAIL	tumor necrosis factor-related apoptosis-inducing ligand
Tris-HCl	2-amino-2-(hydroxymethyl) propane-1, 3-diol-hydrochloroic acid
uPAR	urokinase plasminogen activator receptor
UV	Ultra Violet
SD	standard deviation
SEM	standard error of the mean
DEAE-cellulose	<i>O</i> -(diethylaminoethyl)-cellulose

Chapter 1 General Introduction

1.1 The Epidemiology of Cancer

Cancer is one of the major causes of disease and death worldwide. Cancer accounted for 9.7 million deaths, which was about 13% of all deaths in 2007 (World Health Organization (WHO), Retrieved June 2009, from <http://www.who.int>). Lung, stomach, liver, colorectal and breast cancer are the frequent causes of the cancer deaths every year. In addition, the WHO also estimates that cancer will cause 12 million global deaths by 2030. Although conventional therapeutic methods such as surgery, chemotherapy and radiation therapy efficiently control cancer development in some circumstances, it is not successful all the time when the cancer metastasizes. Therefore, it is very important to elucidate the causes and underlying mechanisms of cancer development; and to develop novel anti-cancer therapy that is completely different from conventional methods to improve patient's survival rate.

1.2 The Cancer/Testis Antigen for Immunotherapy

One of the novel methods is cancer immunotherapy. The principle is to make use of T cells to recognize cancer antigens,^{46,88,123,164} such as the cancer/testis (CT) antigens, mutated antigens, tumor virus antigens and differentiation antigens.¹⁸³ Currently, CT antigens are recognized as the ideal targets for cancer immunotherapy.

The CT antigens are a family of cancer antigens with highly restricted expression in testis and in various cancer tissues including melanoma, carcinomas of bladder, lung and liver.¹⁷¹ The CT antigens have distinct expression patterns in different stages of spermatogenesis and carcinogenesis. Most of the CT antigens expressions are mainly regulated by epigenetic mechanisms such as DNA methylation.¹¹⁴ However, the underlying mechanisms leading to hypomethylation in cancer cells are unclear.

To date, more than 44 distinct CT antigens families have been identified, based on immunogenic properties,⁴⁵ expression profiles,¹⁸⁶ and bioinformatic analysis.³⁰

Since CT antigens are immunogenic and their expression are highly restricted in cancer tissues, CT antigens are ideal targets as potential biomarkers for cancers and potential therapeutic targets for antigen-based tumor vaccines.³³ It has been proposed that the abnormal expression of CT antigens in cancer recapitulated the germ line gametogenic program and might contribute to properties of tumor progression including immortality, cell proliferation, migration, invasiveness and metastasis (Figure 1.1).^{33,147,177} Therefore, understanding the role of CT antigens in tumor development is important for improvement of cancer immunotherapy.

1.3 Multiple Steps of Tumor Development

Tumor development is a multi-steps process with distinct histological stages, from normal cells, hyperplasia, and dysplasia to tumor cells (Figure 1.2). Every stages accumulates both genetic and epigenetic alterations.²²⁶ Moreover, tumor progression is associated with the tumor and microenvironment interactions.

In normal cells, the eukaryotic cell cycle is divided into four non-overlapping phases.⁴³ The DNA synthesis phase (S phase) and Mitosis phases (M phase) are separated by G1 and G2 phases in which mRNAs and proteins accumulate continuously (Figure 1.3).^{32,121,172} Each phase is monitored by intracellular checkpoints to maintain the integrity and completion of DNA synthesis before mitosis and to prevent inappropriate cell proliferation.¹⁴⁶ After passing these checkpoints, the cells are irreversibly moved to the next phase.¹⁴⁶ The S phase checkpoint responds to DNA damage and the DNA replication fork, and lead to cell cycle arrest until the DNA is repaired or DNA replication is completed.²¹¹ DNA damages or abnormal cell division can trigger even apoptotic cascades leading to cell death.^{166,176}

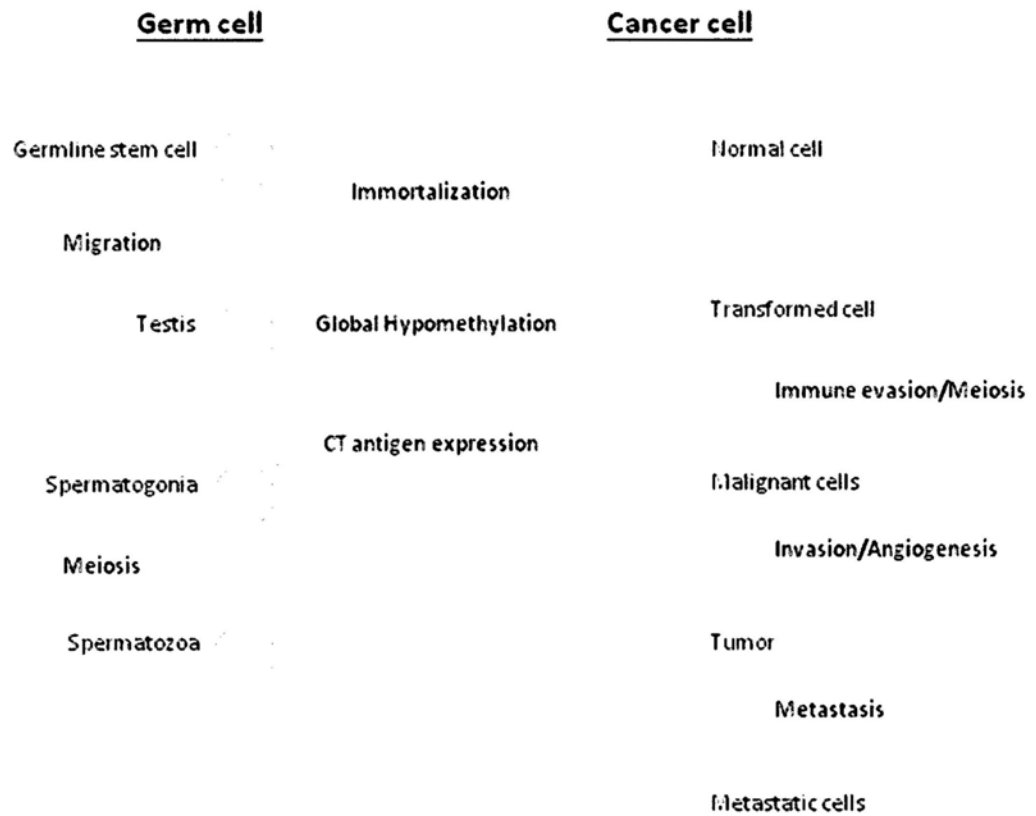


Figure 1.1 Abnormal expression of CT antigens in cancer cells recapitulated the germ line gametogenic program (*Adapted and modified from ¹⁷⁷*).

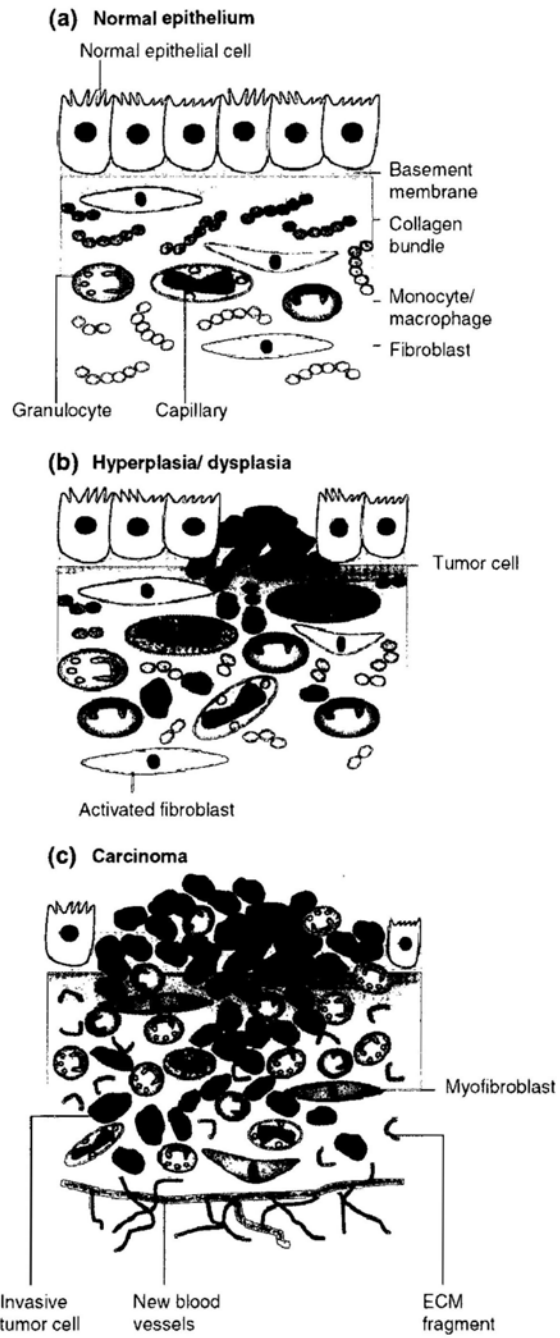


Figure 1.2 Different pathological stages of carcinogenesis from (a) normal cells; (b) hyperplasia and dysplasia to; (c) carcinoma (Adapted from ¹²⁸).

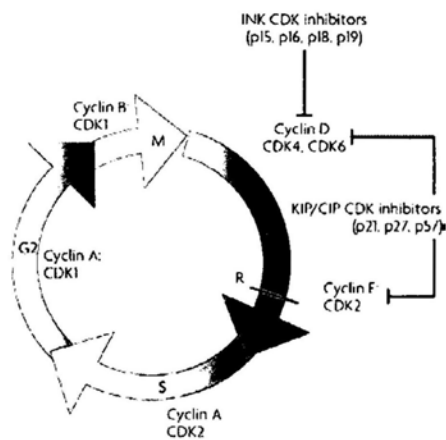


Figure 1.3 The eukaryotic cell cycle progression and related signaling pathways. Two cell-cycle checkpoints control the progression of G1/S and G2/M transition. Cell cycle progression is coordinated and driven by cyclin-dependent kinases (CDKs) and their activating cyclin subunits (such as cyclin D, cyclin E and CKIs). CDK activity is inhibited by CDK inhibitors (CKIs), with the INK4 family controls CDK4 and CDK6, and the CIP/KIP family controls broader range of CDKs (*Adapted from* ⁴³).

The coordination and transitions between the cell cycle phases depend on cyclin-dependent kinases (CDKs).^{32,205} Each cyclin-dependent kinase complex consists of an enzyme kinase and a modifying protein known as cyclin. The two parts target specific cellular proteins for phosphorylation and causes changes and direct a specific transition in the cell cycle at the proper time during each cell cycle.⁷⁸

While the programmed cell death in the cell cycle is critical in eliminating damaged cells and keeping normal cell functions,⁹⁸ defects in cell cycle checkpoint genes, damaged DNA repair mechanisms or programmed cell death might lead to inappropriate cell proliferation and early tumor development.^{174,219}

Advanced tumor development might result in cancer cell invasion, metastasis and therapeutic resistance. Cancer invasion is a dynamic process in which tumor cells adjust their adhesion ability to the cells and the extracellular matrix (ECM), their proteolytic ability to the surrounding tissues¹¹⁵ and their motility to migrate into the circulating system.¹⁸⁰ It is hypothesized that tumor cells undergo epithelial-mesenchymal transitions (EMTs) in order to survive and migrate in the invasion process and successfully metastasize in a distant organ.¹⁹⁴ EMTs is important steps during embryogenesis. Increasing evidences suggest a vital function in tumor progression. Cell characteristics are vastly changed during EMTs, resulting in changed cell-cell and cell-matrix interactions, cell motility and invasiveness. The induction of EMTs depends on the nature of tumor, the genetic background of tumor as well as the interaction with the ECM.² Successful colonization significantly depends on the cell-matrix interactions in the distant organ. While cancer metastasis is the major cause of death in cancer patients, increasing therapeutic strategies targeting the microenvironment of cell-matrix interactions have been highly developed for clinical testing in the past decades.⁷⁵

1.4 Identification of NYD-SP8 in the Male Reproductive Tract

NYD-SP8 was first identified from the differential hybridization of human testis cDNA microarray for its seven-fold difference in expression level between fetal and adult testis (Figure 1.4 a and b).¹⁷⁵ The DNA sequence of *NYD-SP8* consists of 1,123

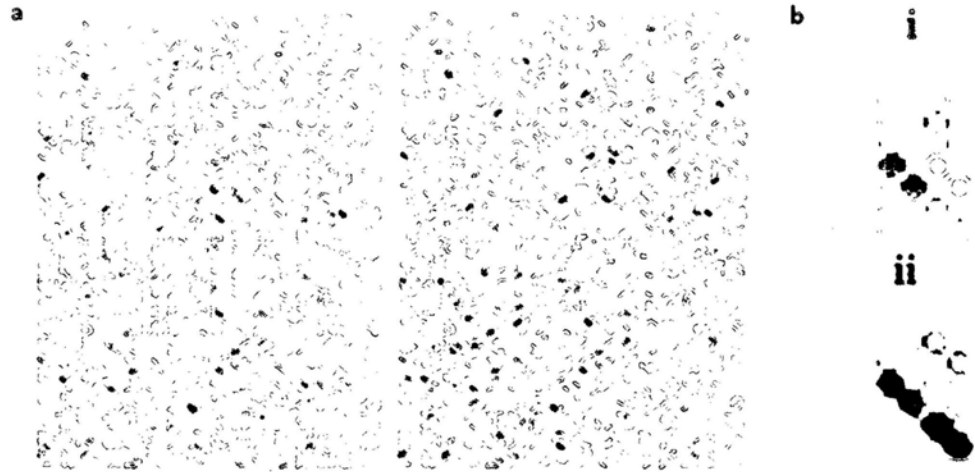


Figure 1.4 (a) Human testis cDNA microarray hybridized with the ^{33}P probes from embryo and adult testis, with the hybridization result of the embryonic testis (left) and the adult testis(right). (b) cDNA microarray hybridization showing seven fold-higher expression of NYD-SP8 in adult (ii) than the embryo testis (i) (*Adpated from* ²²⁰).

nucleotides (Gen-Bank Accession No.AY014285), which spans seven exons. The *NYD-SP8* gene contains an open reading frame of 249 amino acids and encodes a 27 kDa protein with an isoelectric point of 4.8.¹⁷⁵ *NYD-SP8* protein appears to be the human homologue of a mouse testis specific protein TES101RP,¹⁰³ which has been shown to be a surface protein on developing male germ cells with no definitive function demonstrated.²²¹

1.5 *NYD-SP8* is Hypothesized as a Novel CT Antigen

Tissue distribution studies using RT-PCR showed that *NYD-SP8* was expressed in the human testis but not in other normal tissues (Figure 1.5a). Other reports suggested that TES101RP demonstrated differential expression patterns between testes and ovaries.¹⁹⁸ For further characterization, antibodies against human *NYD-SP8* protein were raised.²²⁰ A single specific band at around 30 kDa in both human and mouse testes (and sperm) was detected by this antibody (Figure 1.5b), suggesting a high homology of human *NYD-SP8* protein to its mouse homologue (Figure 1.5c).²²⁰ Consistent with Yoshitake's finding in 2008,²²¹ Immunostaining confirmed its specific expression in both human and mouse testis, including spermatocytes, spermatids and spermatozoa (unpublished data from our collaborator Professor J. Xia) (Figure 1.6). It is hypothesized that *NYD-SP8* is a glycosylphosphatidylinositol (GPI) -anchored protein,²²¹ which is involved in the sperm-cumulus crosstalk leading to acrosome reaction.²²⁰ The use of RH position markers placed *NYD-SP8* in human chromosome 19q13.31 where many CT antigens have been mapped.²²⁰ In addition, preliminary observations in our laboratory revealed mRNA expression of *NYD-SP8* in some cancer patient samples, which was consistent with Yoshitake's finding in 2008.²²¹ This prompted us to investigate the biological functions of *NYD-SP8*. We hypothesize that *NYD-SP8* may act as a novel CT antigen in cancer development.

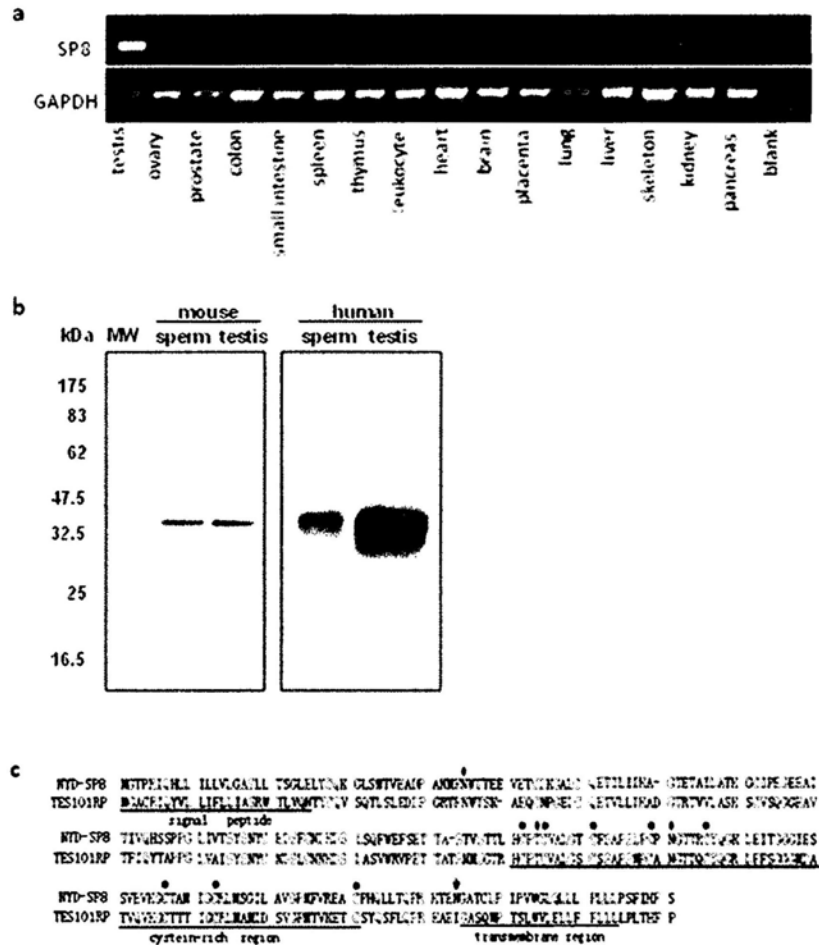


Figure 1.5 (a) RT-PCR revealed testis-specific expression of NYD-SP8, with GAPDH as control. (b) Western blot analysis of mouse and human sperm and testes showing the specificity of NYD-SP8 antibody. (c) Protein sequence alignment of human NYD-SP8 and its mouse homologue. High consensus residues are in red, and similar residues are in blue. Potential glycosylated sites are marked with rhombus, and predicted GPI-link site is marked with an arrow. Conserved cysteines were indicated by asterisks (Adapted from ²²⁰).

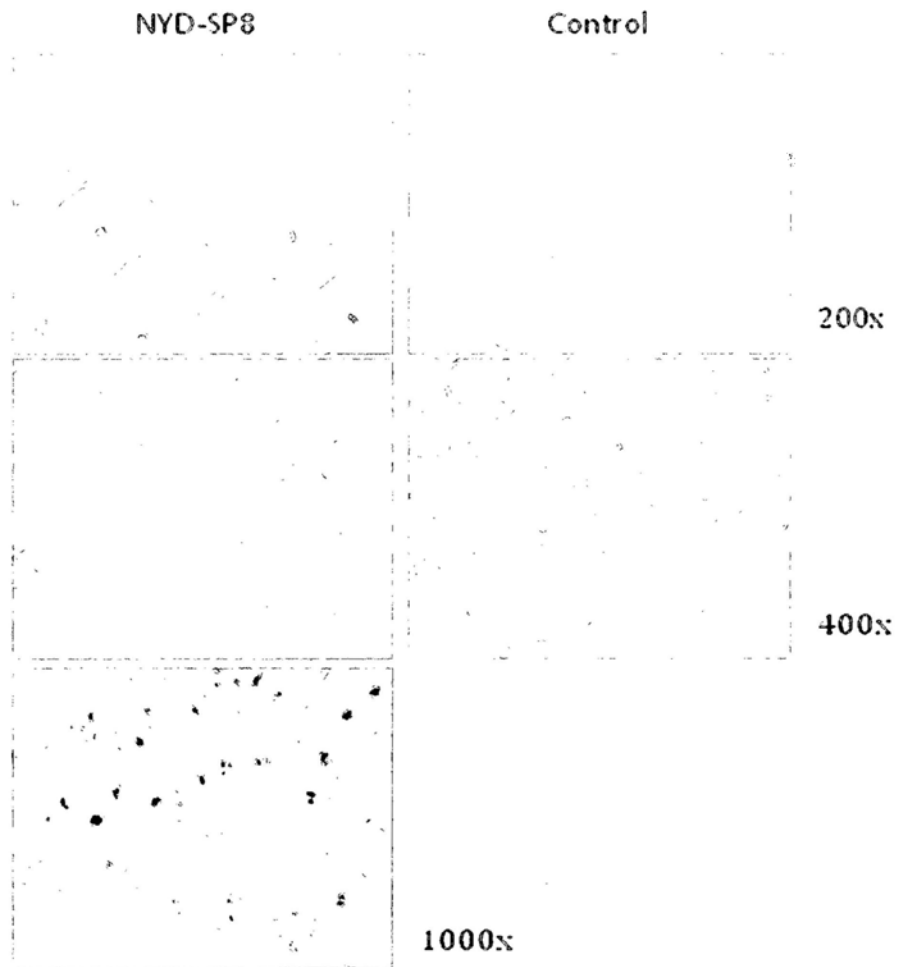


Figure 1.6 Immunohistochemical staining of mouse testis using NYD-SP8 antibody. NYD-SP8 is expressed in spermatocytes, spermatids and spermatozoa (*Unpublished data, acknowledgement to Professor J Sha from Nanning University of China*).

1.6 Objectives

This thesis describes the methodology for and experimental results from the studies of NYD-SP8 in tumor development. Three objectives were proposed.

To study the expression profile of NYD-SP8 in various cancer tissues and characterize the structure and biological functions of NYD-SP8.

To investigate the potential functions and underlying mechanisms of NYD-SP8 in early tumor development, including cell cycle regulation, apoptosis and tumor growth.

To investigate the potential functions and underlying mechanisms of NYD-SP8 in advanced tumor progression, including tumor invasion and metastasis.

Chapter 2 Materials and Methods

2.1 Materials

2.1.1 Reagents and Chemicals

Reagents and chemicals used in this study were purchased from the companies listed in the Appendix A.

2.1.2 Antibodies

Recombinant protein of NYD-SP8, rabbit anti-NYD-SP8 polyclonal antibody and mouse anti-NYD-SP8 polyclonal antibody were kindly provided by Professor J. Sha from the Nanning University of China. Other antibodies were purchased from the companies listed in Appendix B.

2.1.3 Primers for cloning, PCR and Real time PCR

All the primers were either designed using the Gene Runner software (Hastings Software Inc., Hastings-on-Hudson, NY, USA) or adapted from the quoted publications as listed in Appendix D.

2.1.4 Animals

Nude mice were purchased from the Laboratory Animal Service Center (LASEC), the Chinese University of Hong Kong. All experimental procedures were under ethical approval from LASEC (ethical no. 06/049/MIS).

2.1.5 Cell culture

Human embryonic kidney cells (HEK293) were cultured in DMEM (Gibco, Carlsbad, CA, USA). Human hepatocellular carcinoma cell line (hHCC), human liver cancer cell lines (SMMC-7721), human nasopharyngeal cancer cell lines (CNE1) and human colon carcinoma cell lines LIM1863 were cultured in RPMI 1640 (Gibco). All cell lines were cultured in medium supplemented with 10% heat-inactivated FBS (Gibco) and Penicillin-Streptomycin (Gibco). For the LIM1863 cell line, 5% heat inactivated FBS was used. All cell lines were incubated in 37°C and a 5% CO₂ incubator.

2.2 Methods

2.2.1 *In vitro* transfection

For overexpression using the pEGFP-C2 vector system (BD Biosciences, Clontech, Palo. Alto, CA, USA), NYD-SP8 was PCR amplified using primer sets as listed in Appendix C. PCR products were subsequently cloned into pEGFP-C2 vector (Figure 2a).

For overexpression using the pQCXIH vector system (BD Biosciences), NYD-SP8 was PCR amplified using primer sets as listed in Appendix C. PCR products were subsequently cloned into pQCXIH vector (Figure 2b) using *NotI* and *BamHI* double enzyme digestion method.

For the NYD-SP8 knockdown system, the sequence of NYD-SP8 miRNA knockdown NYD-SP8 was designed using Invitrogen software (Invitrogen, Carlsbad, CA, USA) Two miRNA sequence designs are as follow:

Design miR466

(5'-CCTGTACTGTAGGAGCAGATCAGTCAGTCAGTGGCCAAAAGTATCGTGACCTCCTACAGTAC-3');

Design miR689

(5'-TGCTGTCCACAGACGACTCAATGCCAGTTTTGGCC ACTGACTGACTGGCATTGTCGTCTGTGGA-3').

The miRNA were then cloned into pcDNATM6.2-GW/EmGFP-miR vector (Invitrogen) according to the manufacturer's protocol (Figure 2c).

2.2.2 Establishment of stable clones

For pEGFP-C2 clones in HEK293 and hHCC cells, the transfected cells were selected in full medium containing G418 at 1 mg/mL (Calbiochem, Schwalbach, Germany). Fresh medium containing 1 mg/mL G418 was changed every 3 days. After 2–3 weeks of drug selection, G418 resistant cells growing in single colony were isolated. Cells raised from a single colony were then transferred to a 12-well plate for expansion.

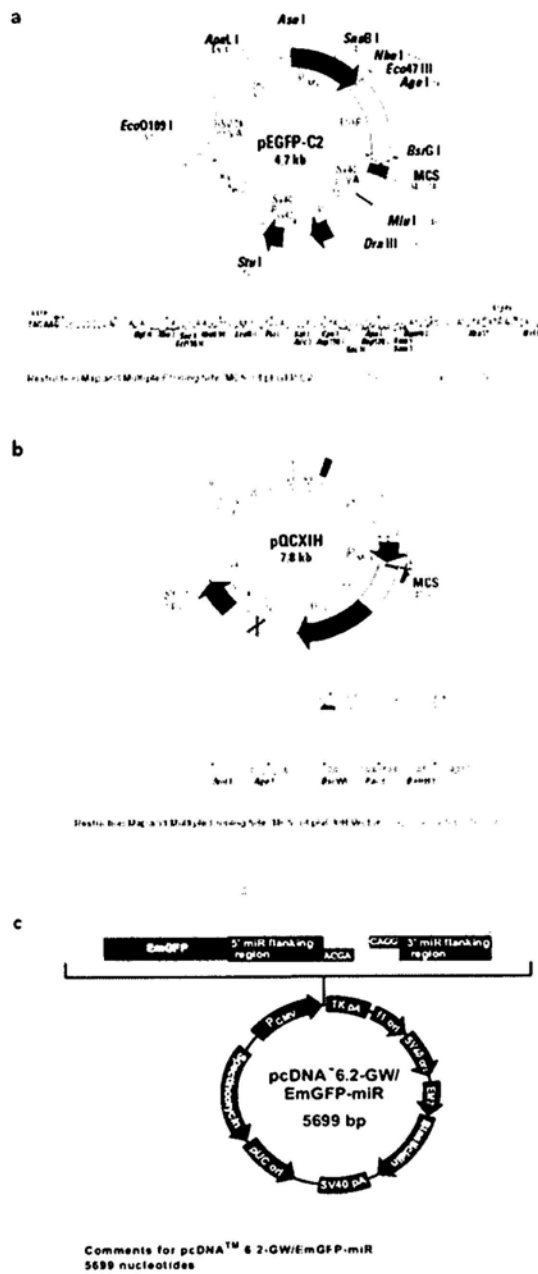


Figure 2 Cloning vector map. (a) The pEGFP-C2 expression vector; (b) the pQCXIH retrovirus expression vector; and (c) the pcDNA6.2-GW/EmGFP-miR expression vector

Confluent cells in 12-well plate were transferred to 6-well plates and allowed to grow until confluence. Cell lysates from every single clone were harvested for Western blot analysis to check for the expression of the transfected gene. The expression of gene cloned in the pEGFP-C2 vector was confirmed by Western blot analysis using anti-NYD-SP8 antibodies and anti-GFP antibodies (Santa Cruz, CA, USA). Stable cell lines were then maintained in 500 µg/mL G418 for subsequent study.

For pQCXIH clones, virus-transduced cells were selected and maintained in full medium containing 500 µg/mL Hygromycin B (Calbiochem). Different colonies were isolated and transfected to a 6-well plate for expansion. Cell lysates from each clone were collected for Western blot analysis to check for the expression of NYD-SP8. The expression of NYD-SP8 was confirmed by Western blot analysis using anti-NYD-SP8 antibodies. Stable cell lines were then maintained in 600µg/mL Hygromycin B for subsequent studies.

2.2.3 Immunohistochemistry

The NYD-SP8 antibody was purified using Montage antibody purification kits (Millipore, Billerica, MA, USA) for immunohistological detection according to the manufacturer's instructions of PicTure^(™)-plus kit (ZYMED/Invitrogen, CA, USA). For immunostaining and Immuno-fluorescence staining, NYD-SP8 antibody at a dilution of 1:100 was used.

2.2.4 PI-PLC treatment

Treatment of Sperm

2×10^8 sperm were incubated with 1 unit/mL of PI-PLC (Molecular Probes, Eugene, OR, USA) for 30 min at 22°C, with untreated sperm as control. Sperm pellets and their supernatants were then collected by centrifugation at 1,000 g for 30 minutes at 4°C. Proteins in the sperms were reconstituted in lysis buffer (Appendix C) for Western blotting.

Treatment of NYD-SP8 transfected cell lines

Cells at 90% confluence were washed twice with 1 x PBS and incubated with 1 unit/mL of PI-PLC (Molecular Probes) for 30 minutes at 22°C in serum free conditioned medium, with heated inactivated PI-PLC as control. The cell pellets and their supernatants were then collected by centrifugation at 1,000 xg for 30 minutes at 4°C. The proteins were reconstituted in RIPA buffer (Appendix C) for Western blot analysis.

2.2.5 Western blot analysis

Protein extraction and concentration measurement

Cultured cells were harvested at 90% confluence. Cell pellets were lysed in either RIPA buffer (Appendix C) containing 50 µg/mL PMSF and proteinase inhibitors or other buffers as indicated. The protein concentration was determined using the DC Protein Assay according to manufacturer's recommendation (BioRad Laboratories, CA, USA). Bovine serum albumin (BSA) with known concentration was used as a protein standard. Absorbance reading at 595 nm was measured and the protein concentration was calculated accordingly.

SDS-PAGE and protein blotting

Proteins were separated by 5%, 8%, 12% or 15% SDS-PAGE using Mini-PROTEAN II apparatus (BioRad), according to the manufacturer's recommendation. Protein samples were mixed in SDS loading buffer and heat denatured at 95°C for 5 minutes. Rainbow Marker (Invitrogen) was used as size standard marker. After protein transfer, the membrane was blocked in 5% non-fat milk in 1 x TBST for 30 minutes and then was probed with the indicated antibodies. Target bands were detected using Enhanced Chemiluminescence (ECL) system plus (Amersham Biosciences, Amersham UK) and exposed using x-ray film (Fuji, Tokyo, Japan). For all Western blot analysis, representative examples of at least three independent experiments are shown.

Co-immunoprecipitation

Cultured cells were harvested at 90% confluence. Cell pellets were washed twice with 1 x ice cooled PBS and lysed in ice-cooled uPA lysis buffer (Appendix C). Antibody against NYD-SP8 and uPAR-399R (5 µg per reaction) were incubated together with the cell lysate and protein G-Sepharose (Amersham) overnight at 4°C. Bound proteins were analyzed by Western blot analysis using monoclonal antibody to NYD-SP8, uPAR, uPA at a dilution of 1:500.

2.2.6 RNA extraction and RT-PCR

The cultured cells were harvested at 90% confluence. Total RNA was isolated using TRIzol (Invitrogen) according to the manufacturer's protocol and dissolved in DEPC-treated dH₂O. The RNA concentration was measured by NanoVue UV/Vis spectrophotometer (GE healthcare, Piscataway, NJ, USA) at a ratio of A₂₆₀ and A₂₈₀. The integrity of the isolated total RNA was confirmed by gel electrophoresis by the intact 28S and 18S ribosomal RNA bands in the RNA preparation. 5 µg of total RNA and RT buffer 1 (Appendix C) and M-MLV reverse transcriptase (Life Technologies, Cergy-Pontoise, France) were used for reverse transcription. The primer sets were designed by Gene Runner software (Hastings Software). The amplified products were separated through 1.5% agarose gel. One µg of DNA ladder (1 kb+) was used as a molecular weight marker. Results were visualized on an ultraviolet transilluminator (Alpha Innotech, Corp., CA, USA).

2.2.7 Real time quantitative PCR

Total RNA extraction and cDNA synthesis

The total RNA was dissolved in DNase/RNase free dH₂O. Five µg of total RNA, random hexamers (Applied Biosystems), RT-buffer 2 (Appendix C) and M-MLV reverse transcriptase (Life Technologies, Cergy Pontoise) were used for reverse transcription. All samples were diluted 1:10 in DNase/RNase free dH₂O and stored in aliquots at -70°C.

Primers and Probes

Primers for amplification using SYBR Green I was based on published sequences as listed in Appendix D. The primers and fluorogenic probes for Taqman assay were designed using Primer Express version 1.0 (Applied Biosystems) listed in Appendix D.

Real-time PCR quantification using Taqman fluorogenic probes

Reaction conditions for fluorogenic PCR mixtures are shown in Appendix C. The thermal cycling profile consisted of: stage 1, 50°C for 2 minutes; stage 2, 95°C for 10 minutes; stage 3, 95°C for 15 seconds followed by 60°C for 1 minute. Stage 3 was repeated for 40 cycles. In experiments using fluorogenic probes and primer sets, the universal Master Mix (Appendix C) was used. Amplification was performed in biological triplicates.

Real-time PCR quantification using SYBR Green I

The reaction conditions and buffers used are shown in Appendix C. SYBR Green I Universal Master Mix was used. The optimum temperature, determined from melting point analysis, was then used for quantitative PCR using the following thermal cycling program: stage 1: 50°C for 2 minutes; stage 2: 95°C for 10 minutes; stage 3: 95°C for 15 seconds followed by 60°C for 1 minute. Stage 3 was repeated for 40 cycles. Amplification was performed in biological triplicates. The specificity of the PCR reaction was confirmed by gel electrophoresis revealing a single PCR product size and also by melting curve analysis. The expression levels of cDNA of the candidate genes were internally normalized using *GAPDH*. Expression levels of candidate genes in the tumor cell line were represented as $2^{-\Delta\Delta Ct}$, where the ΔCt represents differences between thresholds of the candidate gene and *GAPDH* ($C_{t \text{ candidate}} - C_{t \text{ GAPDH}}$). $\Delta\Delta Ct$ represents the differences of ΔCt between SP8 expressing cell line and vector-expressing cell line ($\Delta C_{t \text{ SP8}} - \Delta C_{t \text{ vector}}$) after normalized with the *GAPDH*. The significance of fold changes of expression levels were calculated using the unpaired *t* test, where a *p* value ≤ 0.05 was regarded as statistically significant.

2.2.8 Cell proliferation assay

Typan blue cell counting

To determine the cell proliferation rate, 3×10^4 cells were seeded in each well of a 6-well plate on day 1 and cultured in 2 mL of full medium. Cells were counted on consecutive days for a week using a hemacytometer. Living cells were counted using Trypan blue staining (in 1:1 ratio). The number of cells per mL was equal to the average cell count $\times 1 \times 10^4 \times 2$ (dilution factor).

MTS proliferation assay

The growth rate of cells was measured using the CellTiter 96 MTS Aqueous One solution cell proliferation assay (Promega Biotech, Piscataway, NJ, USA) at the indicated time points. This assay is based on the bio-reduction of 3-(4,5-dimethylthiazol-2-yl)-5-(3-carboxymethoxyphenyl)-2-(4-sulfophenyl)-2H-tetrazolium by metabolically active cells to form a product, in the presence of phenazine methosulfate, that is soluble in tissue culture medium and can be measured by spectrophotometry. The quantity of the formazan product is directly proportional to the number of living cells in culture. In brief, 5×10^3 cells were seeded into each well of a 96-well plate and 100 μ L of full medium. 20 μ L of MTS reagents was added and the plate was incubated for 2 hours at 37°C. Intensity at 490 nm was measured.

For both the cell counting and MTS proliferation assay, each time point was set up in at least in three wells and each experiment was duplicated.

2.2.9 Flow cytometry

Cell cycle analysis

For cell cycle analysis, 2×10^5 cells were seeded in each well of a 6-well plate and grown for 24 hours. The cells were washed twice with ice-cooled PBS and then harvested. The cells were then resuspended in 1 mL 1 X PBS. Ethanol fixation was then performed by adding 3 mL of cold absolute ethanol to the cell suspension gently and vortexed. The cells were fixed at 4°C for 1 hour. After fixation, the cells were washed twice with 1 X PBS and stained with 1 mL of Propidium Iodide (PI; 20 μ g/mL) staining solution with RNase A (10 μ g/mL) at 37°C for 20 minutes. Flow

cytometry was then performed by using BD FACS Calibur system (BD Biosciences).

Apoptotic flow cytometry

Annexin-V conjugated with fluoresceine isothiocyanate (Annexin V-FITC) and PI staining kit (BD Biosciences) was used to detect living and apoptotic cells using flow cytometry. 4×10^5 cells were seeded in each well of a 6-well plate and grown for 24 hours. The cells were then cultured in serum depleted medium for 48 hours and then different samples from each of the wells were treated with TNF α for further a 24, 48 and 72 hours, respectively. The cells were then harvested and washed twice with 1 X PBS. The cells were then resuspended in 1mL of 1 X binding buffer and stained with FITC Annexin V (BD Biosciences) and PI according to manufacturing protocol. Living cells were negative for Annexin V-FITC and PI. Early apoptotic cells were detected after binding with Annexin V-FITC. Secondary necrotic cells stained positively for both Annexin V-FITC and PI. It is presumed that secondary necrotic cells died in an apoptotic process. Necrotic cells were stained with PI. Flow cytometry was then performed using BD the FACS Calibur system (BD Biosciences). All experiments were performed at least in triplicates.

2.2.10 Oligo GEArray

Tumor Metastasis Oligo GEArray OHS-028 (Superarray Bioscience, Bethesda, USA) and human signal transduction assay OHS-044 (Superarray Bioscience) designed for gene-expression relative quantification of 128 genes potentially involved in various cancer progression process were used in this study.

RNA extraction and quality control

Cell pellets of NYD-SP8 transfected cells and their control were harvested at 90% confluence. RNA was isolated using TRIzol (Invitrogen) according to the manufacturer's protocol and dissolved in DEPC-treated dH₂O. The RNA concentration and purity were measured by UV spectrophotometry ($A_{260}:A_{280} > 1.8$, $A_{260}:A_{230} > 2.0$). RNA integrity was checked and no DNA contamination signs were

observed.

Sample labeling, cRNA hybridization and Image processing

Total RNA was converted to amplified- and biotin-labeled- cRNA using TrueLabeling-AMP 2.0 (SuperArray Bioscience) and purified by ArrayGrade™ cRNA cleanup kit (SuperArray Bioscience) according to the manufacturer's instructions. cRNA probes were subsequently denatured, and hybridized to nylon membranes spotted with gene-specific 60-mer oligonucleotides. Arrays were then washed and chemiluminescence detection obtained by alkaline phosphatase-conjugated streptavidin and CDP-Star chemiluminescent substrate (Tropix, Inc., Bedford, MA) was captured using x-ray film (Fuji).

Data analysis

Web-based software GEArray Expression Analysis Suite (SuperArray Bioscience) was used for raw image analysis, background subtraction (spot with minimum value) and data normalization. Data were normalized using housekeeping genes expression levels and spots with lower intensity than 10% of the median value were excluded. Genes with statistically significant changes in expression, with at least a 2-fold difference in expression, were selected for subsequent analysis.

2.2.11 Adhesion assay

96-well plates were coated with Laminin (20 µg/mL), Fibronectin (10 µg/mL), Poly-L-lysine (25 µg/mL; as+ control), or Bovine Serum Albumin Fraction V (BSA; as -ve control) and incubated overnight at 4°C. Plates were blocked by incubation with 0.1% BSA in PBS at 37°C for 1 hour. Cells (50,000 cell/well) were seeded into the wells and incubated at 37°C for 1 hour. Non-adherent cells were removed by washing three times in 1 X PBS. The amount of viable cells attached was evaluated using CellTiter 96 MTS Aqueous One solution cell proliferation assay (Promega), incubated at 37°C for 4 hours and quantified by light absorbance using ELISA reader at 595 nm.

2.2.12 Soft agar anchored-independent assay

A total of 1×10^4 cells were mixed with 0.4% soft agar at around 37°C to 40°C, and immediately seeded on a layer of 1% bottom agar in a 35-mm plate. After 14–21 days incubation at 37°C, the cells were stained with 0.01% crystal violet and colony formation was evaluated by counting the number/frequency of colonies containing more than 20 cells. Assays were performed in triplicates.

2.2.13 Matrigel invasion assay

The Matrigel is a mixture of basement membrane components isolated from the EHS sarcoma. The major components of matrigel includes laminin, collagen type IV and proteoglycans. Matrigel also contains matrix degrading enzymes and several growth factors. At room temperature, Matrigel polymerizes to produce biologically active matrix materials resembling the basement membrane. Matrigel provides a suitable ECM environment for studies of cancer cell invasion *in vitro*.

The *in vitro* invasion potential of cancer cells was determined using the Cell Invasion assay kit, Fluorigenic (Chemicon) according to the manufacturer's instructions. A total of 1×10^5 cells were seeded into each well of the 96-well plates. Results were obtained 48 hours after incubation. Data is shown as three separate experiments, each of which is in triplicate.

2.2.14 Gelatin zymography

Enzymatic activities of MMP-2 and MMP-9 were detected by gelatin zymography. The same number of NYD-SP8 transfected hHCC lines and their control were incubated in equal amount of serum-free media for 24 hours and same volume of conditioned media was separated by 7.5% SDS-PAGE gels containing 0.1% gelatin (Sigma, St.Louis, MO, USA) under non-reducing conditions. The gels were washed twice with 2.5% (v/v) Triton X-100, and then incubated in zymography digestion buffer (Appendix C) for 18 hours at 37°C. Gels were stained in 0.5% Coomassie Blue R-250 solution for 2 hours, then destained. Area of clear bands against a blue

background indicates the activity of proteases. The experiment was done in triplicates.

2.2.15 uPA activity assay

uPA activity was examined using uPA activity assay kit (Chemicon)) according to the manufacturer's instruction. Results were obtained after 24 hours of incubation. The photometric absorbance of the reaction mixtures at 405 nm was measured using a SpectraMax ELISA reader (MWG Biotech, Ebersberg, Germany). Data is shown as three separate experiments and each of which is in triplicate.

2.2.16 Cathepsin B activity assay

Cathepsin B activity in protein lysates was measured using the InnoZyme™ Cathepsin B activity assay kit, Fluorogenic (Calbiochem) according to the manufacturer's instructions. Cell pellets were lysed in MES buffer (pH 6.0, containing EDTA) and the enzyme activity was determined using the specific substrate Z-Arg-Arg-AMC. Results are displayed as fluorescence units per µg total protein per time. Data is shown as three separate experiments and each of which is in triplicate.

2.2.17 Xenograft experiment in nude mice

Tumorigenicity of NYD-SP8 transfected cells were investigated by tumor xenograft experiments. Approximately 1×10^6 NYD-SP8 expressing cells and the same amount of vector control cells were injected subcutaneously into 6–8 week-old nude mice respectively. Five mice were injected with saline as a sham control Tumor volume (V) was estimated from the length (l) and width (w) of the tumor using the formula: $V = (\pi/6) \times ((l + w)/2)^3$. Tumor formation in nude mice was monitored over a 4-week period. Tumor weight to body weight ratios was measured.

2.2.18 *In vivo* metastasis assay

Fluorescent labeling

Cells were incubated together with fluorescent cell tracker dyes CMRA (a

rhodol-based fluorophore, red fluorescent) or CMFDA (5-chloromethyl- fluorescein diacetate, green fluorescent) at 2 μ M (Molecular Probes) according to manufacturer's instruction. After washing, cells were incubated for an additional 30 minutes. with dye-free medium, washed and trypsinized.

In vivo micrometastasis assay

For tumor carcinomatosis assays, 5×10^5 tumor cells were intra-peritoneally injected into the abdomen cavity of nude mice. After 60 days, the mice were sacrificed and the lungs from each group of mice were excised and RT-PCR was performed. For experimental metastasis assay, hHCC-SP8 or hHCC-vector were labeled *in vitro* with CMRA or CMFDA as described above. Cell labeled with red and green fluorescent dyes were mixed at a ratio of 1:1.

Approximately 2×10^6 cells suspended in HBSS were injected by tail vein. The ratio of green-to-red fluorescence tumor cells in the injected suspensions was measured by counting in a fluorescence microscope. Lungs were harvested at 10 minutes or 6 hours after injection. The trachea and pulmonary artery were cannulated and perfused in situ with ice-cool 1 X PBS followed by 4% PFA (in PBS) gently. Lung tissues were sectioned at 5 μ m in a cryostat and fluorescent cells in 15 random fields of each slice were counted.

2.2.19 *In vivo metastasis assay*

Approximately 2×10^6 cells suspended in HBSS were injected via the tail vein injection into each mouse. Lungs were harvested 2 months after injection. The trachea and pulmonary artery were cannulated and perfused in situ with ice-cool 1 X PBS followed by 4% PFA (in PBS) gently. Lungs were fixed in bouin solution (Sigma) and numbers of surface tumor was counted.

2.2.20 Induced epithelial-mesenchymal transitions (EMTs) in LIM1863 cells

LIM1863 cells is a human colon carcinoma cell line and were grown as nonadherent organoids in RPMI 1640 (Cambrex, Walkersville) supplemented with 5% FCS,

L-glutamine, penicillin, and streptomycin. TGF β (2 ng/mL), or in combination with TNF α (10 ng/mL), were used to induce EMTs for indicated time points. Microscopic photos were taken and cells were harvested for subsequent assay.

Statistical analysis

All data are expressed as mean \pm S.E.M. or \pm S.D. ($n = 3$ or more). Statistical analysis was performed using Student's t test and one way ANOVA analysis. Results are representative examples of more than three independent experiments, each with triplicates. A $p \leq 0.05$ are considered to be statistical significant.

Chapter 3 Characterization of NYD-SP8 in cancer tissues — a novel interacting partner of uPAR

3.1 Introduction

In the previous study, NYD-SP8 was demonstrated to be a GPI-anchored protein with important biological function in mediating sperm-cumulus crosstalk in the male reproductive system in mice.^{220,221} NYD-SP8 is identified in both human and mouse testes and hypothesized to be a novel CT antigen, but the expression profile and structural characteristics in cancer tissues remain unclear. Moreover, the biological role of NYD-SP8 in tumor development is unknown.

3.1.1 GPI-anchored protein family

The GPI-anchored protein family is a diverse group of proteins and accounts for about 20% of all membrane bound proteins.¹⁴² This protein family includes coat proteins, receptors, adhesion proteins, ecto-enzymes, differentiation antigens, and adaptors. The C-terminus of GPI-anchored proteins covalently link to the membrane via the GPI-anchoring (Figure 3.1).¹⁴²

The GPI-anchoring is the most complex post-translational modification described to date.^{125,143} The GPI-anchoring are pre-assembled in the endoplasmic reticulum (ER) by a series of highly conserved enzymes following a multi-steps GPI-anchoring pathway.¹⁴³ The GPI anchoring pathway starts on the cytoplasmic side of the ER and finishes in the ER lumen. This process requires glycolipid turnover across the ER membrane. Finally, the GPI proteins are transported via the secretory pathway to the cell surface¹⁴³.

More than 200 GPI-anchored glycoproteins have been identified in mammals.^{10,60,125} GPI-anchored proteins are involved in cell adhesion, cell surface hydrolysis, intracellular sorting, cell wall remodeling, and transmembrane signaling processes.^{61,68,82,142} Unlike the transmembrane proteins that span the membrane lipid-bilayer, GPI anchors penetrate only into a single membrane leaflet and cannot interact directly with cytosolic partners that recognize intracellular signals.¹²⁵ As a

result, GPI-anchored proteins must either interact with transmembrane proteins or be sorted into vesicles by an alternative mechanism.

The position of the putative GPI-anchoring site are highly conserved among mammalian species.^{90,198} Site-direct mutagenesis studies have shown that there are certain sequence constraints of the attachment site of GPI-anchoring.^{53,202} Many bioinformatic softwares for GPI-anchored protein predictions are commercially available, such as DGPI.¹⁰² Big-Pi,⁵⁴ and GPI-SOM.⁵⁹ The predicted candidates are commonly verified by enzymatic treatment that specifically recognizes GPI anchoring structures and catalyzes the cleavage of the diphosphoester bond, thereby releasing the protein from the lipid membrane. By now, common enzymatic treatments for GPI-cleavage include phosphatidylinositol specific phospholipases C (PI-PLC),⁸⁶ phospholipase D (PLD), and angiotensin converting enzyme (ACE) cleavage¹⁰⁸ (Figure 3.1b).

3.1.2 The urokinase plasminogen activator receptor - an example of GPI-anchored proteins

One of the best known examples of GPI-anchored proteins is the urokinase plasminogen activator receptor (uPAR). uPAR is a heavily glycosylated 55–60 kDa GPI-anchored protein.^{1,209} The uPAR contains three cysteine rich domains (D1,D2, and D3) which are connected by short linkers region¹⁴⁹ (Figure 3.2). Each domain contains approximately 90 residues with Ly-6/uPAR/ α -neurotoxin and a three-finger fold.¹⁵⁰ The uPAR does not contain any transmembrane or cytosolic domains.^{126,208} In order to mediate intracellular signal transduction, the uPAR undergoes conformational changes and interacts with the adaptor proteins such as integrins family.¹⁵⁴

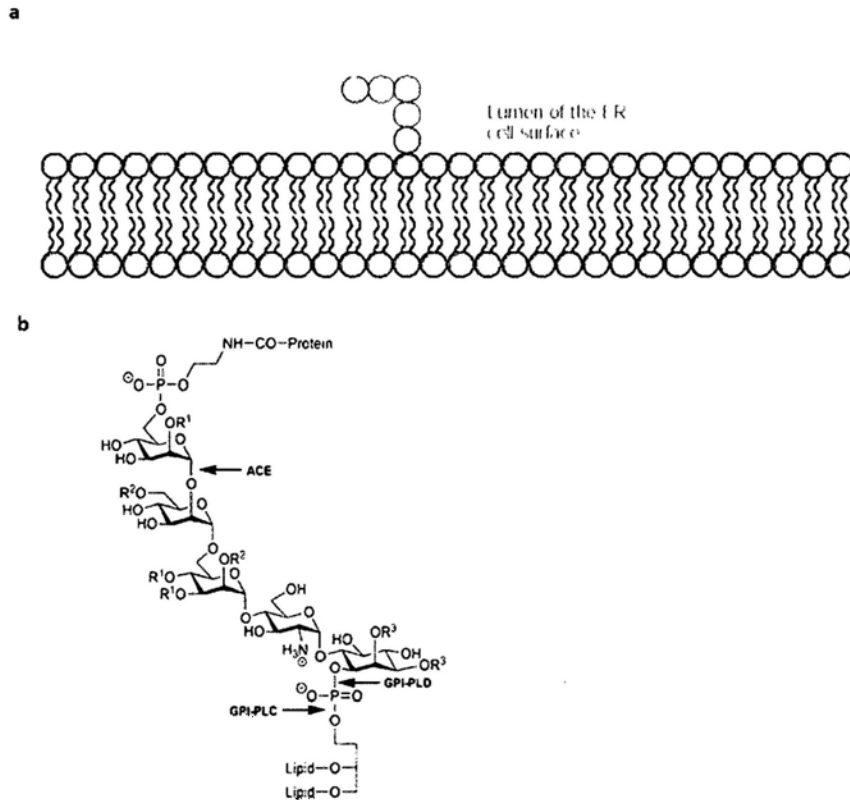


Figure 3.1 The GPI-anchored proteins. (a) GPI-anchored proteins are embedded in the extracellular of membranes through their GPI-moiety (*Adapted from* ¹²⁵). (b) Core structure for GPI-anchored proteins. Cleavage sites of GPI phospholipase C (GPI-PLC), GPI-phospholipase D (GPI-PLD) and angiotensinconverting enzyme (ACE) are marked by arrows. (*Adapted and modified from* ¹⁰⁸).

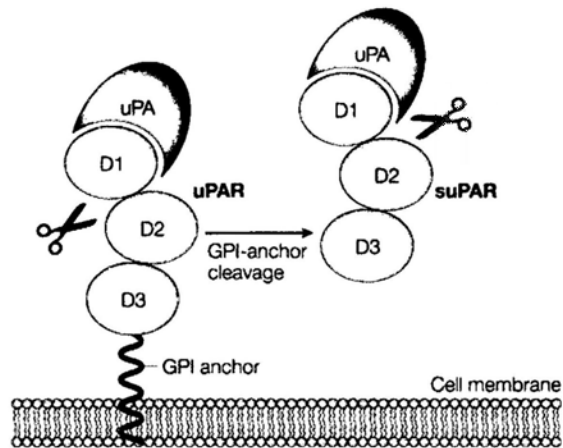


Figure 3.2 Molecular structure of uPAR. The uPAR consists of three internally disulphide-bonded domains and is attached to the cell surface by a GPI anchor. Soluble uPAR (suPAR) is released from the plasma membrane by cleavage of the GPI anchor. Both uPAR and suPAR can be cleaved in the region that links domains D1 to D2 (scissors) to yield a D1 and D2D3 fragment, which has direct chemotactic activity (*Adapted from* ¹⁶).

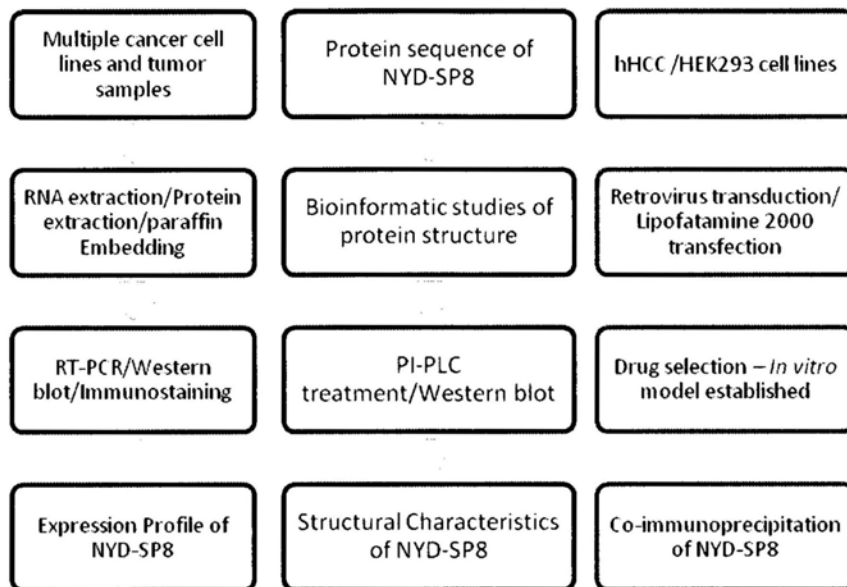
uPAR is a multifunctional proteins. It play important roles in many physiological processes such as cell migration and adhesion via ECM degradation, regulation of cAMP levels and intracellular calcium and activation of integrins, tyrosine kinases and serine/theorine kinases-mediated signaling pathways.⁴⁰ There are very low or no expression of uPAR in normal cells.^{67,127} However, high levels of uPAR expression are detected in various tumor tissues. It is widely believed that uPAR is involved in the pathology of human cancers.^{16,149,151,163} High levels of uPA, the activation substrate of uPAR, in various tumor tissues from patients are associated with poor prognosis and high recurrence rate.^{16,145,162} The uPA/uPAR complex induces the conversion of plasminogen zymogen to active plasmin,³¹ which degrades most ECM proteins and promotes cancer invasion and metastasis.

3.1.3 Objective

The aims of this study are: (1) to characterize the expression profile of NYD-SP8 in normal tissues and multiple cancer tissues; (2) to identify the structural characteristics of NYD-SP8 protein; and (3) to study the molecular interactions between NYD-SP8 and uPAR using *in vitro* model.

3.2 Experimental Plan

Detailed materials and methods are described in Chapter 2. A schematic diagram of experimental plan is shown below.



3.3 Results

3.3.1 Expression of NYD-SP8 in multiple cancer tissues

At transcriptional level, RT-PCR analysis showed that *NYD-SP8* mRNA was expressed in multiple cancer cell lines and cancerous tissues from human patients. Figure 3.3a to d shows the expression of *NYD-SP8* in multiple cancer cell lines (Figure 3.3a), including liver cancer cell lines 8024, 7721, 7705 and 32G (Figure 3.3b), colon carcinoma cells line LIM1863 (Figure 3.3a) and nasopharyngeal cancer cell lines NP1, NP2, CNE1 and CNE2 (Figure 3.3 a and c). Among the NYD-SP8 positive cell lines, LIM1863 showed the strongest NYD-SP8 expression.

Figure 3.3d shows the expression of NYD-SP8 in patient samples with different type of cancer. Results have shown that NYD-SP8 is expressed in malignant lymphoma, adenocarcinoma of kidney, colon carcinoma and esophageal cancer but not in lung cancer and gastric cancer.

We also investigated the expression profile of the NYD-SP8 protein in multiple human cancer tissues. Immunohistochemical studies of multiple human cancer tissue arrays showed that NYD-SP8 protein is expressed in lung cancer, breast cancer, pudendum cancer, colon cancer and esophagus squamous cell carcinoma. NYD-SP8 protein was not detected in their normal tissue counterparts (Figure 3.4 a and b). Western blot analysis showed weak expression of NYD-SP8 protein in the lymphocytes of B cell lymphoma patients (Figure 3.5a) and Acute lymphoblastic leukemia patients (ALL) (Figure 3.5b) but neither chronic lymphocytic leukemia (CLL) patients (Figure 3.5c) nor normal lymphocytes (Figure 3.5c).

Taken together, RT-PCR, immunostaining and Western blot analysis showed that NYD-SP8 is expressed in teste but not other normal tissues. Interestingly, it is expressed in various cancer tissues and cancer cell lines, with the strongest expression in LIM1863 cell line. These data indicated that expression of NYD-SP8 is re-activated in cancer tissues, suggesting that NYD-SP8 is a novel CT antigen with unknown biological function in tumor development.

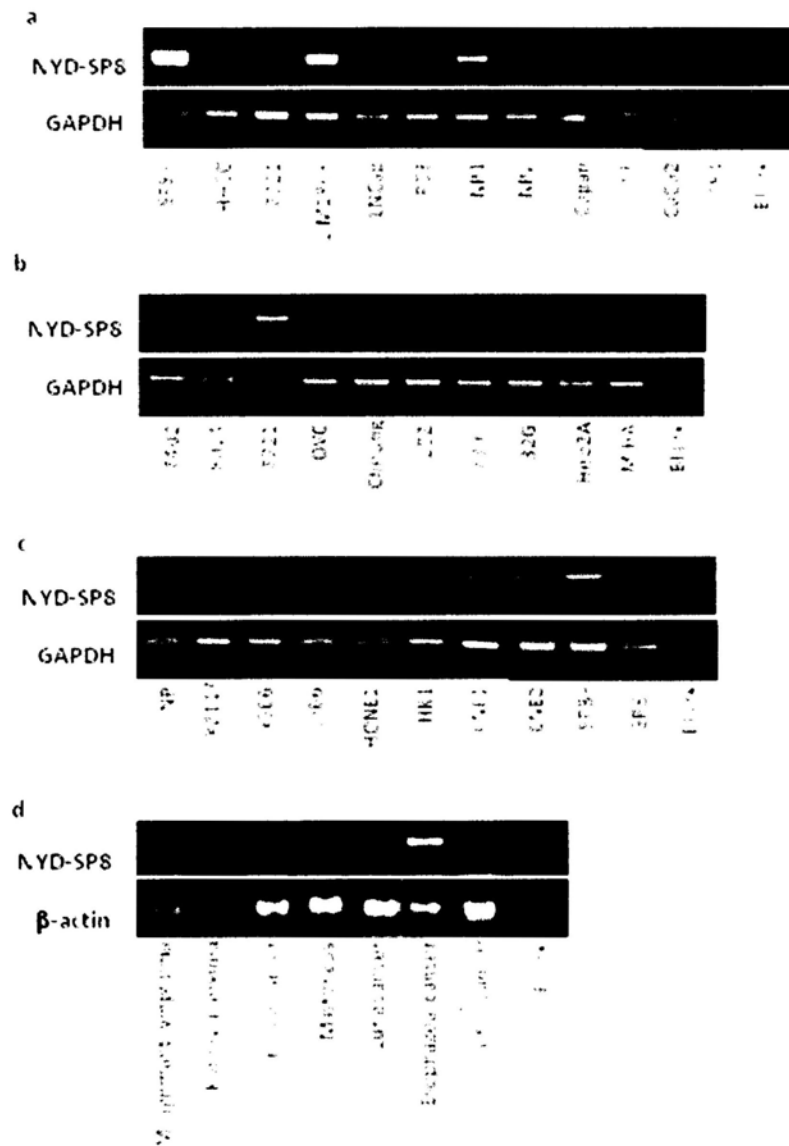


Figure 3.3 mRNA expression of NYD-SP8. mRNA expression of NYD-SP8 (a) in multiple cancer cell lines; (b) in liver cancer cell lines; (c) in nasopharyngeal cancer cell lines and; (d) in multiple cancer patient tissues.

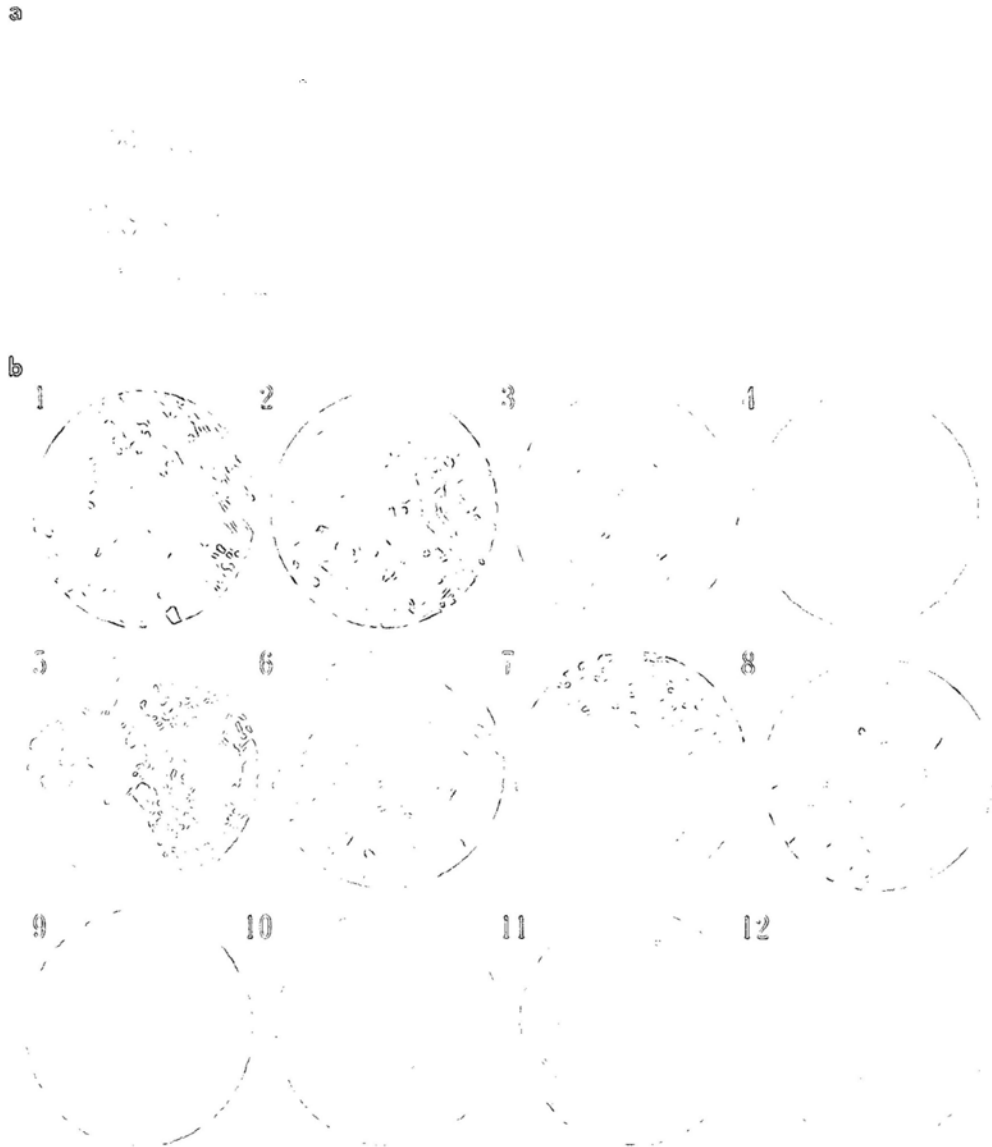


Figure 3.4 (a) Immunohistochemical demonstration of NYD-SP8 protein expression in multiple human cancer tissue arrays. (b) Representative fields from with various cancer tissues and their normal tissues counterparts: cervical cancer (1-2), pudendum cancer (3), colon cancer (4), lung cancer (5), breast cancer (6), esophageal squamous cell carcinoma ESCC (7-8), normal colon mucosa (9-10), and normal esophageal mucosa (11-12). Original magnification = 400x.

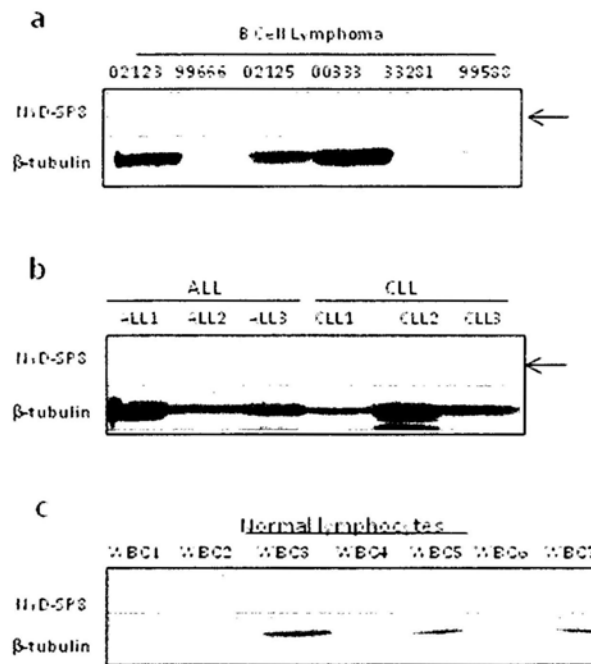


Figure 3.5 Western blot analysis showing expression of NYD-SP8 protein in (a) B cell lymphoma; (b) acute lymphoblastic leukemia (ALL) but not in chronic lymphocytic leukemia (CLL) or (c) normal lymphocytes.

3.3.2 NYD-SP8 is shed off by PI-PLC

In order to understand the biological function of NYD-SP8, bioinformatic analyses were used to study the structural characteristics of NYD-SP8 proteins. Bioinformatic analysis of Uniprot and Swissprot suggested that NYD-SP8 is a cell surface membrane protein and is predicted to have 9 phosphorylation sites and 2 putative N-glycosylated sites. These indicated that NYD-SP8 may be involved multiple post-translational modifications. However, NYD-SP8 does not contain any transmembrane helix structure. DGPI software indicated that NYD-SP8 is a putative GPI-anchored membrane protein, with a potential GPI-modification site at amino acid 222 (<http://www.ebi.uniprot.org>.) (Figure 3.6).¹⁸⁷ We therefore investigated whether NYD-SP8 would be susceptible to PI-PLC, which removes GPI-anchored proteins from the membrane²¹⁶.

Western blot analysis comparing the expression level of NYD-SP8 protein in different cellular fractions of sperm and hHCC-SP8 cells indicated that NYD-SP8 is predominantly expressed on the cell membrane (Figure 3.7 a and b). Besides, NYD-SP8 was also detected in the supernatant of both human and mouse sperm after PI-PLC treatment (Figure 3.7c), and in the serum free medium of HHCC-SP8 and HEK293-SP8 (Figure 3.7d), confirming its GPI-membrane anchored nature of NYD-SP8 protein.

3.3.3 NYD-SP8 is homologues to uPAR

In addition to the GPI-anchored nature, Swissprot analysis suggested that NYD-SP8 contains a UPAR/Ly6 domain, which is an extracellular disulphide bond rich domain. According to Clustal W analysis, the NYD-SP8 protein has about 30% structural homology to uPAR (Figure 3.8a); both of them contain a GPI-modification site, a membrane peptide signal, and UPAR/Ly6 domains. In addition, NYD-SP8 has a potential Trail factor binding domain 2 (TRAF2) (Figure 3.8b). The uPAR has been implicated in cancer proliferation, invasion and metastasis,¹⁰⁵ the homologies between NYD-SP8 and uPAR suggests that NYD-SP8 may be implicated in cancer development.

Prediction of potential C-terminal GPI-Modification Sites

Query sequence gi|13508450:1-249 (length 249 amino acids):

MGTPRIQHLL ILLVLGASLL TSGLELYCQK GLSMTVEADP ANMFNWTTEE VETCDKGALC
QETILIKAG TETAILATKG CIPEGEEAIT IVQHSSPPGL IVTSYSNYCE DSFCNDKDSL
SQFWEFSETT ASTVSTTLHC PTCVALGTCT SAPSLPCPNG TTRCYQGKLE ITGGGIESSV
EVKGCTAMIG CRLMSGILAV GPMFVREACP HQLLTQPRKT **EN**GATCLPIP VWGLQLLLPL
LLPSFIHFS

Best predicted site is shown in red

Use of the prediction function for METAZOA Potential GPI-modification site was found.

Quality of the site : P

Sequence position of the omega-site : **222**

Score of the best site : **8.20** (PValue = 3.560426e-04)

Figure 3.6 Bioinformatic analyses showing the potential GPI-modification site of NYD-SP8 protein.

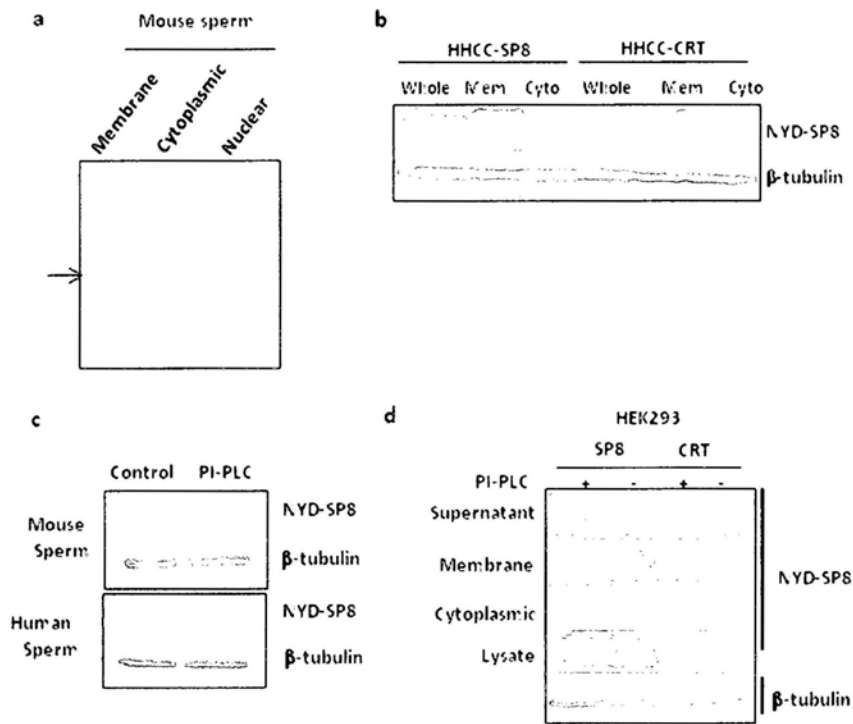
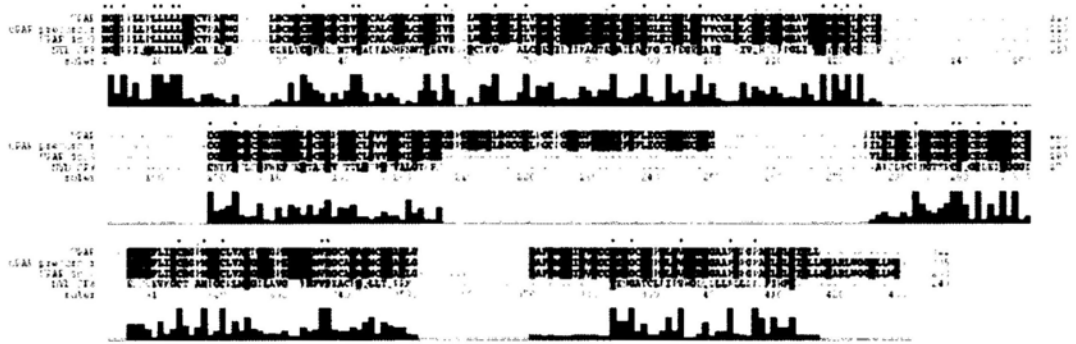


Figure 3.7 Western blot analysis of NYD-SP8 protein expression in different cell types. NYD-SP8 was expressed in the membrane fraction of (a) mouse sperm and (b) hHCC-SP8 cell lines, whole = whole cell lysate; Mem = membrane fraction; Cyto=cytoplasmic fraction. (c) NYD-SP8 in the supernatant of mouse (upper) and human (lower) sperm treated with PI-PLC (PI-PLC-treated), with β -tubulin as the control for the amount of sperm used in the assay. (d) NYD-SP8 was detected in the supernatant of HEK293-SP8 after PI-PLC treatment.

a



b



Figure 3.8 (a) Clustal W alignment showing about 30% homology of NYD-SP8 to uPAR. Asterisk indicates complete matches and semicolon indicates highly similar region. (b) Structural diagram showing the predicted conserved domains of NYD-SP8 from bioinformatic analysis. Ly-6/uPAR = lysine 6 domain of uPAR; TRAF2 BD = Trail factor binding domain; GPI = GPI-modification site.

Therefore, we raise a question: Is NYD-SP8 also involved in multiple steps of cancer development, through uPAR-dependent and/or -independent pathways?

3.3.4 NYD-SP8 protein interacts with uPA/uPAR complexes

To answer the above question, *in vitro* cell line models were established. We employed a human hepatocellular carcinoma cell line (hHCC) which is highly invasive but does not have detectable NYD-SP8 expression. NYD-SP8 was transfected into hHCC cells using retrovirus transduction and the expression level of NYD-SP8 was confirmed by RT-PCR and Western blot analysis (Figure 3.9 a and b). Clones were established after drug selection and only clones with strong NYD-SP8 expression were chosen for functional studies (Figure 3.9c). Clone 2 was chosen as the cell line model for subsequent studies because western blotting showed that clone 2 had the strongest NYD-SP8 expression.

Because of the high structural homology between NYD-SP8 and uPAR and both are on cell membrane, there are possible protein-protein interactions between NYD-SP8 and uPAR. This possibility was examined by co-immunoprecipitation experiments. Results showed that NYD-SP8 could pull down both uPA and uPAR in hHCC-SP8 (Figure 3.10a) suggesting that NYD-SP8 interacts with uPA/uPAR complexes. Similarly, anti-uPAR antibody, but not anti-IgG, could pull down both NYD-SP8 and uPA in hHCC-SP8 (Figure 3.10b), further confirming protein-protein interaction between uPA/uPAR complexes and NYD-SP8.

Taken together, these data suggested a new biological function of NYD-SP8 in tumor development. NYD-SP8 protein interacts with uPA/uPAR complexes and may be involved in regulating uPA/uPAR complexes assembly and the downstream signaling pathways.

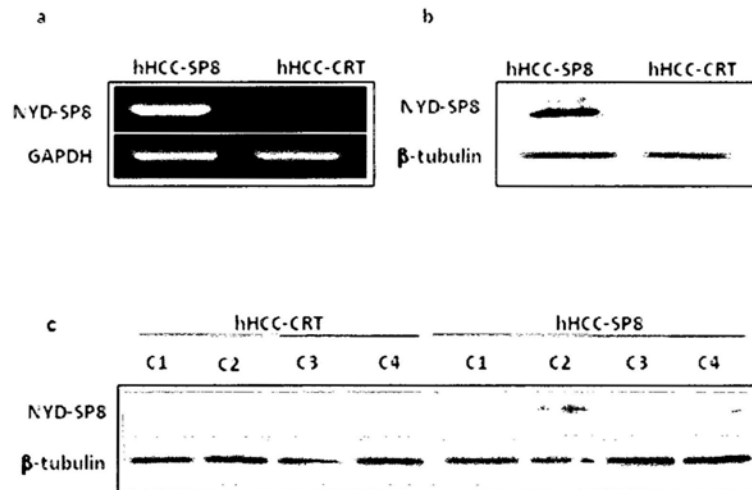


Figure 3.9 RT-PCR (a) and Western blot analysis (b) confirm the NYD-SP8 expression in hHCC cells. (c) Western blot analysis showing the expression of NYD-SP8 in multiple clones of hHCC stably expressing NYD-SP8, with β -tubulin as loading control.

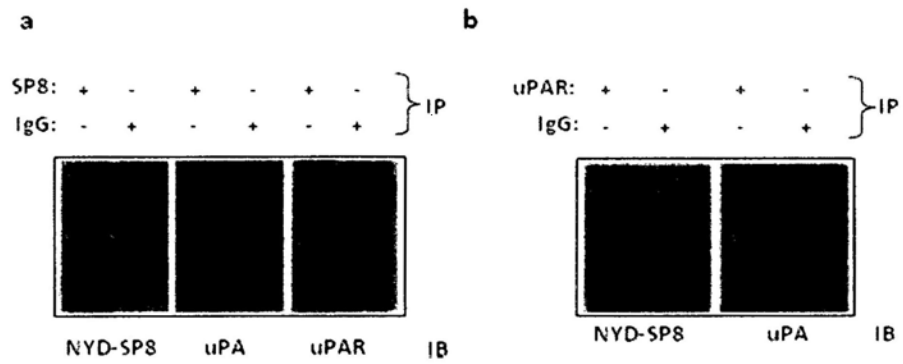


Figure 3.10 NYD-SP8 interacts with uPA/uPAR complexes. (a) Protein-protein interaction between NYD-SP8 and uPA/uPAR complexes. 300 μ g of hHCC/SP8 cell lysate were immunoprecipitated (IP) with NYD-SP8 antibody (SP8), resolved by SDS-PAGE and immunoblotted (IB) with NYD-SP8, uPA or uPAR antibodies. (b) Reversed co-immunoprecipitation of NYD-SP8 and uPA with uPAR. Antibodies for normal mouse or rabbit IgG were used as control correspondingly. Molecular size detected: NYD-SP8, 30 kDa; uPA, 30kDa; uPAR, 55 kDa.

3.4 Discussion

3.4.1 NYD-SP8 is a novel CT antigen

In this chapter, the expression profiles of NYD-SP8 in healthy and cancerous tissues were investigated. Expression of NYD-SP8 is highly restricted to the testes. De-regulation of NYD-SP8 resulted in its expression in various cancerous tissues. These results are consistent with a recent report showing that NYD-SP8 transcript was expressed in some small cell lung cancer,¹⁹⁰ indicating that NYD-SP8 may be involved in cancer development. Moreover, results in our previous study indicated that the NYD-SP8 protein is immunogenic,²²⁰ further confirming its potential use as a CT antigen in cancer immunotherapy. However, the biological functions of NYD-SP8 in cancer remain unclear. It is of therapeutic value to investigate the biological functions of NYD-SP8 in cancer development.

Since most of the expressions of CT antigens are regulated by epigenetic mechanisms such as promoter methylation, it is important to know the fundamental mechanisms that contribute to NYD-SP8 expression in cancer tissues. A recent report has suggested that the promoter region of the *NYD-SP8* forms three major transcripts with CAAT boxes positioned in the potential activating cis-regulatory region, and neither TATA box nor a GC rich region was found.¹⁹⁸ Therefore, it is obvious that NYD-SP8 is regulated by other epigenetic mechanisms rather than DNA methylation. Elucidation of the molecular mechanism(s) contributing NYD-SP8 expression may provide new insight into relationships between epigenetic regulations and CT antigens expression.

3.4.2 Stage specific expression of NYD-SP8

RT-PCR analysis showed that LIM1863 cells have the strongest expression of NYD-SP8. LIM1863 cells are a highly differentiated colon carcinoma cell line, suggesting that expression of NYD-SP8 may be correlated with the differentiation status of cancers. Interestingly, RT-PCR analysis demonstrated that transcriptional expression of NYD-SP8 in a couple of less invasive hepatocellular cancer cell lines (7721, 8024 and 7705 cell lines; Figure 3.3b) was much higher than the more

invasive hHCC cell line and tumors from late stage liver cancer patients (hHCC and Cheung; Figure 3.3b). Moreover, the transcriptional expression of NYD-SP8 in a couple of less invasive nasopharyngeal cell lines (NP1 and NP2; Figure 3.3a) was much higher than the more invasive nasopharyngeal cell line (CNE1 and CNE2; Figure 3.3c). This raises an interesting notion that the expression profile of NYD-SP8 may be correlated to different stages of cancer development with different metastatic potentials. Further investigation on NYD-SP8 expression profiles in different cancer tissues with different stages and different differentiation statuses may provide answers for the question.

3.4.3 NYD-SP8 interacts with uPA/uPAR complexes

Bioinformatic analyses have shown that NYD-SP8 is a GPI-anchored protein. Since GPI-anchored proteins do not have transmembrane or intracellular domains, it is unclear how NYD-SP8 mediates intracellular signaling. Recent reports suggested that uPAR transmits intracellular signaling via interactions with integrins.⁴⁰ Since NYD-SP8 protein interacts with uPA/uPAR complexes, it is possible that NYD-SP8 may mediate intracellular signaling via uPAR/Integrins downstream signaling pathways. Several possible hypotheses are proposed. First, NYD-SP8 may be a novel uPAR antagonist which alters the uPA/uPAR binding affinity and blocks the uPAR-mediated signaling transduction. Second, NYD-SP8 may be a novel uPA inhibitor. NYD-SP8 may bind to the active uPA/uPAR complexes, which may interfere the internalization and degradation of complexes in lysosomes.⁸¹ Further investigation on how NYD-SP8 interacts with uPA/uPAR complexes, uPAR/Integrins and other uPA family inhibitors may provide new understanding of molecular mechanisms of NYD-SP8 in regulating the uPA/uPAR system.

In addition, it has been suggested that GPI-anchored protein clusters recruit members of the Src-family, which is associated with lipid rafts and activate downstream intracellular signaling pathways.¹⁸¹ Further investigation on the interaction between the NYD-SP8 protein and the Src-kinase family may provide new understanding into the molecular mechanisms of NYD-SP8 in regulating the

intracellular signaling transduction.

3.4.4 Post-translational modifications of NYD-SP8 protein

The bands of NYD-SP8 protein observed in Western blot analysis are different in human and mouse sperm when compared to hHCC-SP8. A sharp band of 27 kDa was observed in both human and mouse sperm lysates while a broad band around 30KDa was observed in hHCC-SP8 and HEK293 transfectants (Figure 3.7). The molecular difference of NYD-SP8 protein in two systems could be explained by the additional post-translational modifications of NYD-SP8 protein in human cancer cell lines. In addition, two NYD-SP8 bands were observed in hHCC-SP8 and HEK293 cell lysates, indicating that there may be phosphorylation and/or N-linked glycosylation of NYD-SP8 protein which may be necessary for NYD-SP8 activities. Further investigation on the post-translational modification of NYD-SP8 may provide new insights into the upstream regulation of NYD-SP8 protein expression.

Chapter 4 Regulation of programmed cell death by NYD-SP8

4.1 Introduction

In chapter 3, the results demonstrated that NYD-SP8 is a novel CT antigen and is highly expressed in various cancer tissues but not the normal tissue counterpart. Recent reports have also suggested that the abnormal expression of CT antigens in cancer tissues confers phenotypic behaviors that are essential for cancer cell growth and survival. In addition, NYD-SP8 protein is highly homologous to uPAR and interacts with uPA/uPAR complexes. Since uPAR is a multifunctional protein and plays important roles in affecting cancer proliferation, invasion and metastasis,¹⁰⁵ NYD-SP8 may also be involved in multistep cancer development via the uPAR-dependent and/or uPAR-independent signaling pathways. It would be interesting to investigate the role of NYD-SP8 in both early and late stage of cancer development. This chapter describes the investigation on the biological functions of NYD-SP8 in early stage of tumor development.

4.1.1 Cell proliferation and cell cycle progression

Cellular proliferation is a tightly regulated biological process that involves both cell-cycle progression and checkpoint transitions. The eukaryotic cell cycle is divided into four non-overlapping phases (The G1/S and G2/M) as described in Chapter 1.3⁴³. The highly conserved cell cycle progression is delicately controlled by cell-cycle regulators, such as cyclins/cyclin-dependent kinases (CDKs) and the checkpoint proteins, such as tumor-suppressor p53 and pRb⁶⁶. These cell cycle regulators and checkpoint proteins either permit or arrest cell cycle progression and ensure the normal cell division. For example, cyclin A activates two CDKs and regulates both the G1 phase and the mitosis phase while cdk2 and cyclin E regulate S phase initiation¹⁰⁹. In the other mechanism, the checkpoint protein pRb binds to the transactivation domain of E2F family of transcription factor, blocking the ability of E2F to stimulate transcription and regulating DNA synthesis and cell cycle progression.⁷⁷ pRb also recruits the chromatin remodeling factors and thereby represses transcription.⁷⁷ The p53 protein is a transcription factor, which controls

the expression of key apoptosis proteins such as Bcl-2 and Bax^{107,224} and thereby regulates signal transduction from cell cycle progression to apoptotic mechanisms.

Both extracellular factors (such as growth factor, stress stimuli) and intracellular factors (such as oncogenes and tumor-suppressor genes) affect cell cycle progression. Deregulation of cell cycle progression results in uncontrolled cellular proliferation, a hallmark of cancer cells.¹²¹ In fact, many cell cycle regulators and tumor suppressor genes are mutated or inactivated in tumors.⁷⁶ In addition, the accumulation of both genetic and epigenetic changes in their oncogenes and tumor-suppressor genes not only affect cell cycle progression, but also apoptosis and differentiation of tumor cells.¹²¹ Impairment of apoptotic pathways can promote cancer cell survival¹⁸⁴ and also confer therapeutic resistance⁷².

4.1.2 Apoptosis

Programmed cell death, also called apoptosis, is initiated upon external stimuli such as the ligand-death receptor interactions or internal stimuli such as the DNA damage and cell cycle arrest.^{166,176} Initiation of apoptosis results in activation of caspases, which cleave numerous structural and regulatory proteins, leading to apoptotic cell death.^{34,38} Apoptosis is characterized by cell shrinkage, chromatin condensation, DNA fragmentation, loss of cell membrane^{97,169} and formation of apoptotic bodies (Figure 4.1)³⁴. The apoptotic cells transport the membrane phospholipid phosphatidylserine (PS) from the inner to the outer side of the plasma membrane, thereby attracting neighboring phagocytes to engulf and digest the apoptotic cells³⁴. Translocation of PS is the hallmark of early apoptotic event.

4.1.3 p53 — a linker between cell cycle progression and apoptosis

Molecular linkage between cell cycle and programmed cell death has been intensely studied recent years.¹²¹ It has been suggested that the tumor suppresser protein p53 is an important linker between cell cycle arrest and apoptosis^{121,189}. The p53 is a sequence-specific DNA binding protein that regulates various physiological process including cell growth, DNA repair, cell cycle arrest and apoptosis.¹⁸⁹ In



Figure 4.1 Classical apoptosis of a leukemia cell with condensed chromatin, the cell shrinkage and the fragmentation of the cell into apoptotic bodies (*Adapted from ^{3d}*).

normal cells, p53 is functionally inactive due to MDM2-induced degradation. However, cellular stress such as DNA damage resulted in failure of MDM2-mediated degradation and p53 accumulation, thereby initiating cell cycle arrest and apoptosis.¹⁸⁹ The p53 gene is often mutated or inactivated in various human cancers, indicating its central role as a tumor suppressor.¹⁸⁹

4.1.4 NFκB, a well known mediator of apoptosis

The signaling mechanisms leading to apoptosis are complex and difficult to examine *in vivo*. NFκB-mediated signaling is one of the well-known signaling pathways leading to apoptosis. NFκB is a homo- or heterodimeric complex formed by a family of transcription factors, which included RelA (p65), RelB, c-Rel, NFκB1 (p50/p105) and NFκB2 (p52/p100).¹¹⁶ In normal situations, NFκB transcription factors are arrested by the protein family IκB, which are inhibitors in the cytoplasm. Various cellular stimuli such as cytokines, UV irradiation and DNA damage can activate NFκB-related signaling. After stimulation, IκB inhibitors are phosphorylated and NFκB transcription factors are then translocated into the nucleus and bind to *cis*-acting DNA regulatory elements. These in turn regulate various biological functions such as cytokine-induced inflammation, differentiation, immune response, and cell growth tumorigenesis and apoptosis.¹⁹⁷ The dimers bind at kappa-B sites of their target genes and the different dimers combinations act as transcriptional activators or repressors. In general, activation of NFκB exerts an anti-apoptotic function and results in reduced apoptosis and promoted tumor growth.^{20,148}

Overexpression of NFκB1 has been found in various human cancer including non-small cell lung carcinoma, colon cancer, prostate cancer, breast cancer and brain cancer.²⁹ The NFκB p50-p50 homodimer is a transcriptional repressor, but can act as a transcriptional activator in some cases. NFκB heterodimeric p65-p50 and RelB-p50 complexes are transcriptional activators.^{29,116} It is important to study the dimer combinations in order to determine the way of dual function proteins in the NFκB related signaling pathways.

4.1.5 The balance of Bcl-2 family members leading to apoptosis

NFκB transcription factors also activate several genes that promote cell survival, such as the anti-apoptotic Bcl-2 families.²⁰ Generally, activation of NFκB exerts an anti-apoptotic function and results in reduced apoptosis and promoted tumor growth^{20,148} via the regulation of Bcl-2 family (Figure 4.2).

The Bcl-2 family regulates apoptosis in response to a number of external stimuli such as DNA damage by UV/gamma-irradiation, growth-factor deprivation, cytokine withdrawal and tumor necrosis factor family members such as Fas, TNF and TRAIL.^{62,222} The Bcl-2 family of proteins consists of pro- and anti-apoptotic family members.¹⁵⁷ The anti-apoptotic subfamily contains Bcl-2, Bcl-XL, Bcl-w, Mcl-1, Bfl1/A-1 and Bcl-B proteins. The pro-apoptotic subfamily contains Bax, Bak, Bok, Bim, Bad and Bid.^{73,95} The balance of pro-apoptotic death signals and anti-apoptotic survival signals determines the fate of the cells.^{73,141} Overexpression of the anti-apoptotic Bcl-2 protein and other pro-survival Bcl-2 family members are known to protect cells from apoptosis. In addition, it has been correlated with human malignancies and therapeutic resistance.⁶²

4.1.6 TNFα induce NFκB activation

In experimental designs, TNFα is a major activator of NFκB signaling. The TNFα ligand binds to the TNF receptor (TNFR) and induces its trimerization, thereby recruits other signaling molecules to form active TNFR complexes and initiates downstream signaling pathways. On the one hand, TNFR complexes interact with TRADD and FADD proteins, which induce cellular cytotoxicity and initiate apoptosis. On the other hand, TNFR complexes interact with TRAF2 and RIP proteins which are involved in the activation of the NFκB and anti-apoptotic activities³ (Figure 4.3). It has been suggested that the opposing function of TNFR complexes depend on the dosage of TNFα and the cell type.⁹ Moreover, TNFα may also affect p53 transcription activity through an NFκB-dependent signaling pathway.^{48,167} As a result, there are close relationships and interactions between NFκB-dependent and p53-dependent anti-apoptotic signaling pathways.

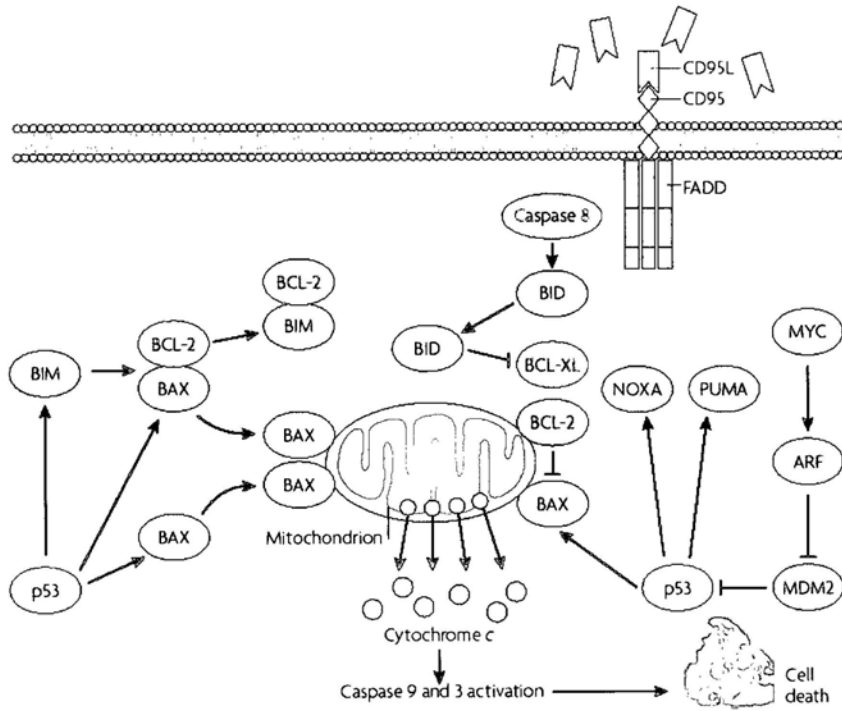


Figure 4.2 Bcl-2 family and apoptotic signaling pathways (Adapted from ³⁴).

4.1.7 Objective

Since NYD-SP8 may be involved in multistep cancer development, the involvement of NYD-SP8 in early tumor development was investigated, including: (1) the effect of NYD-SP8 on cell proliferation and cell growth; (2) the effect of NYD-SP8 on cell cycle progression and apoptosis; (3) their underlying molecular mechanisms.

To achieve these goals, NYD-SP8 was stably expressed in HEK293 cells and hHCC cells to allow subsequent studies. The genetic background of HEK293 and hHCC is significantly different. The HEK293 cell line originated from human embryonic kidney cells and were generated by transformation of cultures using adenovirus.⁷¹ HEK293 is an immortalized cell lines with molecular characteristics of normal cells such as the expression of endogenous p53 proteins and normal cell cycle progression. The fast growing and easy transfecting properties allow general cell biology and molecular biology studies such as cell proliferation and gene expression and protein-protein interactions. The hHCC cell line originated from human hepatocellular carcinoma patients. It has a relatively low endogenous expression of wide type p53. The invasive and highly metastatic potential properties *in vivo* allow studies in cancer invasion and metastatic capacity. As p53 is one of the key players in cell cycle progression and apoptosis, the two cell line systems allows us to compare the p53-dependent and p53-independent effects of NYD-SP8 in early tumor development.

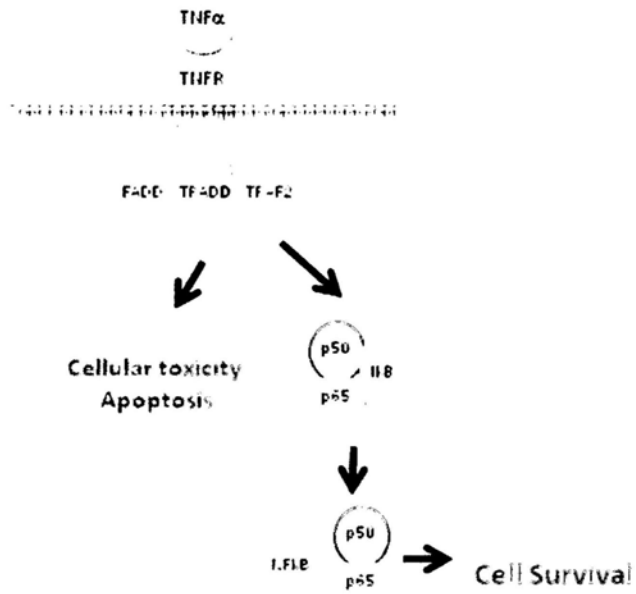
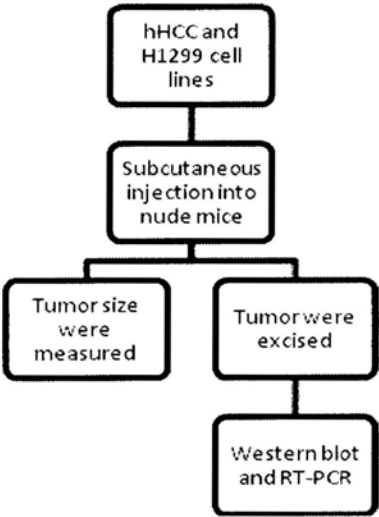
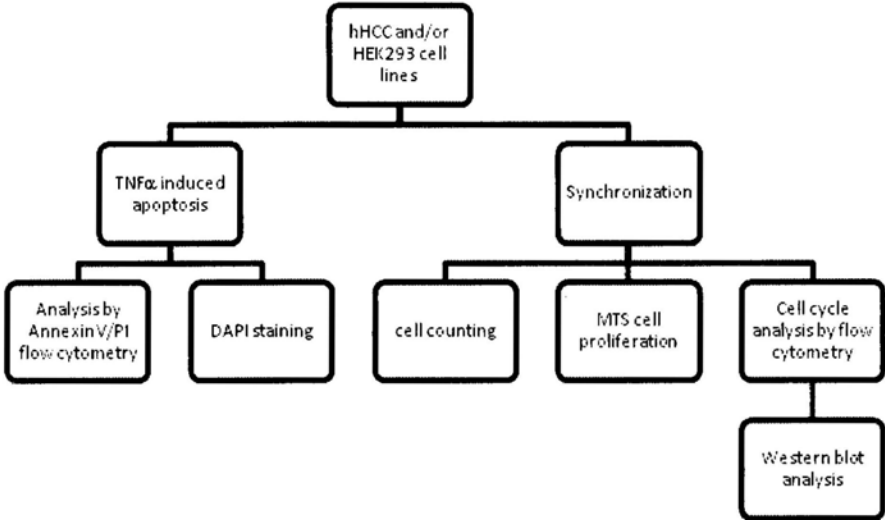


Figure 4.3 A schematic diagram showing the TNF-mediated signaling pathways. The TNF binds to TNF receptor (TNFR) and mediates growth regulatory signaling in the cytoplasm. In normal cells TNF is mitogenic. However, TNF initiates apoptosis in transformed cells causing DNA fragmentation cytotoxicity. The TNF-induced cell survival pathway is mediated by the transcription factor NF- κ B. Activation of NF- κ B occurs via phosphorylation of I κ B, resulting in the dissociation and subsequent nuclear localization of active NF- κ B (*Modified from Sigma*).

4.2 Experimental Plan

Detailed materials and methods are described in Chapter 2. A schematic diagram of experimental plan is shown below.



4.3 Results

4.3.1 NYD-SP8 promotes cell proliferation *in vitro*

First, the cell morphology of HEK293-SP8 and hHCC-SP8 cell lines were studied to investigate whether NYD-SP8 could affect cell shape and cell size *in vitro*. Microscopic studies showed that NYD-SP8 expressing cells did not have observable changes in cell morphology (Figure 4.4), indicating that NYD-SP8 has no effects on cell shape and cell size in HEK293 and hHCC cell lines.

The effect of NYD-SP8 on affecting cell growth was determined by both cell counting and MTS cell proliferation assays for both the HEK293 cells and hHCC cell lines. In the cell counting assay, the proliferation rate of HEK293-SP8 was significantly higher than its vector control from day 2 onwards (Figure 4.5b), while the proliferation rate hHCC-SP8 was only slightly higher than its vector control (Figure 4.5a). Similar results were obtained using MTS proliferation assay (Figure 4.5 a and b). These results indicated that NYD-SP8 promotes cell proliferation *in vitro*, with more noticeable effect in HEK293 cells than in hHCC cells.

4.3.2 Effect of NYD-SP8 on cell cycle progression and apoptosis

NYD-SP8 does not affect cell cycle progression

To address the underlying mechanisms of how NYD-SP8 enhances cell growth, we studied cell cycle progression and apoptosis in NYD-SP8 expressing cells using flow cytometry. The results showed that there were no significant changes in the G1/S progression or the G2/M phases of NYD-SP8 expressing HEK293 and hHCC cells when compared to its vector controls (Figure 4.6a), indicating that NYD-SP8 does not significantly affect cell cycle progression. Consistent with the Western blot analysis results (Figure 4.6b), NYD-SP8 did not alter changes in protein expression of several G1/S and G2/M phase regulating proteins, including cyclin E, CDK4, cdc2 and PCNA, further confirming that NYD-SP8 may not be involved in regulating cell cycle progression.

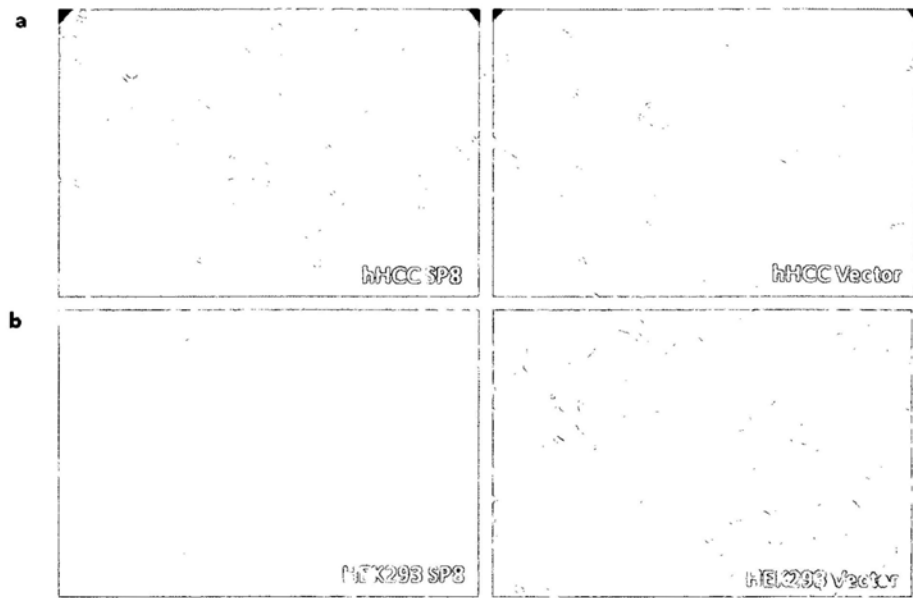


Figure 4.4 Microscopic Imaging of (a) hHCC cells stably expressing NYD-SP8 (left) and its vector control (right); (b) HEK293 cells stably expressing NYD-SP8 (left) and its control (right). Original magnification = 200x.

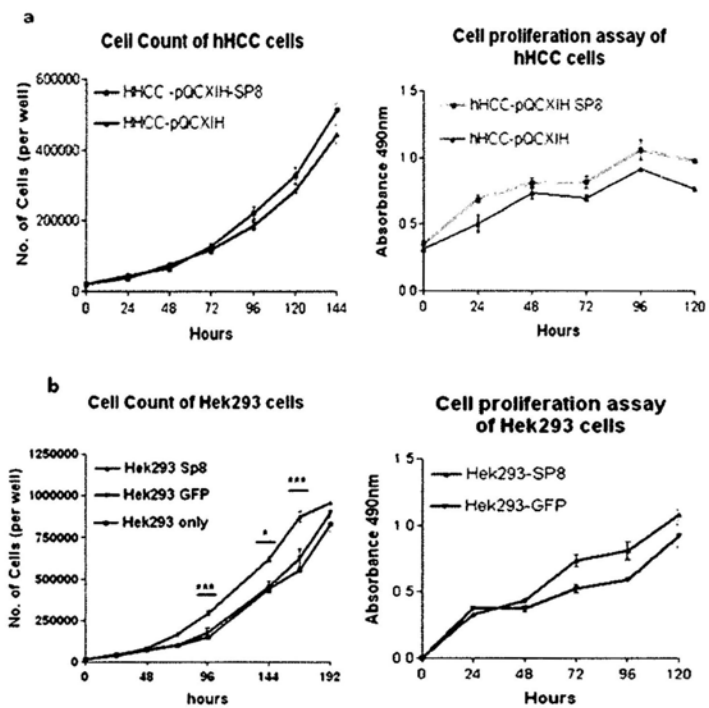


Figure 4.5 Effect of NYD-SP8 in cell growth. Cell count (left column) and MTS cell proliferation (right column) assay revealed the effect of NYD-SP8 in cell growth in (a) hHCC cells, (b) HEK293 cells. * $p < 0.05$; ** $p < 0.01$.

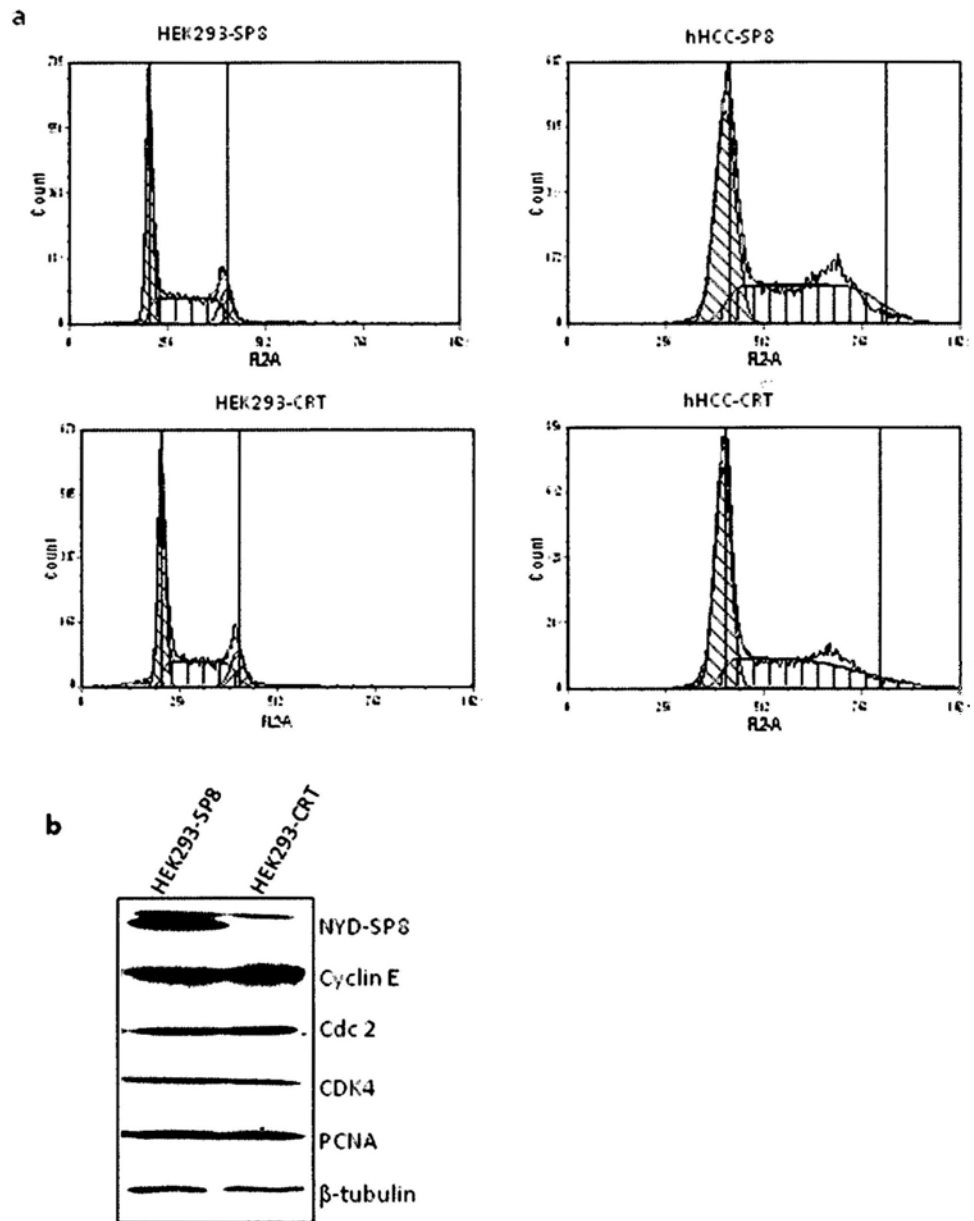


Figure 4.6 The effect of NYD-SP8 in cell cycle progression (a) Flow cytometric analysis showing the effect of NYD-SP8 in cell cycle progression in HEK293 cells (left) and hHCC cells (right). (b) Western blot analysis showing the effect of NYD-SP8 in cell cycle proteins expression in HEK293 cells.

NYD-SP8 protects cells against TNF α -induced apoptosis

In cell apoptotic flow cytometry, the propidium iodide (PI) staining and Annexin-V binding were used. It has been suggested that Annexin-V is a Ca²⁺-dependent phospholipids-binding protein that has a high binding affinity for the exposed PS³⁴. Therefore, Annexin-V staining is a reliable tool for detecting apoptosis. Results showed that the PI staining and Annexin-V binding of SP8 over-expressing cells and its control group were not identical, indicating significant difference in the apoptotic rate between NYD-SP8 over-expressing cells and its control group (Figure 4.7a). NYD-SP8 group showed higher cell viability after TNF α -induced apoptosis, with 64% of viable cells in NYD-SP8 group compared to 38% of viable cells in control group. The NYD-SP8 group also had a lower percentage of apoptotic cells, with 4.79% apoptotic cells compared to 31.64% apoptotic cells in control group. Moreover, NYD-SP8 group has less secondary necrotic cells than the control group, with 2.09% in NYD-SP8 group compared to 4.8% in control group. The data are summarized in Figure 4.7b. DAPI staining of TNF α -treated HEK293 cells further confirmed the anti-apoptotic effect of NYD-SP8. The NYD-SP8 group had less apoptotic nuclear fragmented bodies found than its control (Figure 4.7c). These data indicate that NYD-SP8 has potent anti-apoptotic effect in HEK293 cells.

In the hHCC cell line, NYD-SP8 also induced a significant decrease in apoptotic cells (Figure 4.8 a and b). However, the anti-apoptotic effect of NYD-SP8 was less prominent than that in the HEK293 cells (Figure 4.7). NYD-SP8 group showed higher cell viability after TNF α -induced apoptosis, with 92.14% of viable cells in NYD-SP8 group compared to 85.58% of viable cells in control group. NYD-SP8 group also has lower percentage of apoptotic cells, with 0.28% of apoptotic cells compared to 6.79% of apoptotic cells in control group. Moreover, the NYD-SP8 group had less secondary necrotic cells than the control group, with 6.68% in NYD-SP8 group compared to 7.13% in control group (Figure 4.8a). The data are summarized in Figure 4.8b. NYD-SP8 appeared to have anti-apoptotic functions in both HEK293 and hHCC cell lines, with a more prominent effect in HEK293 system.

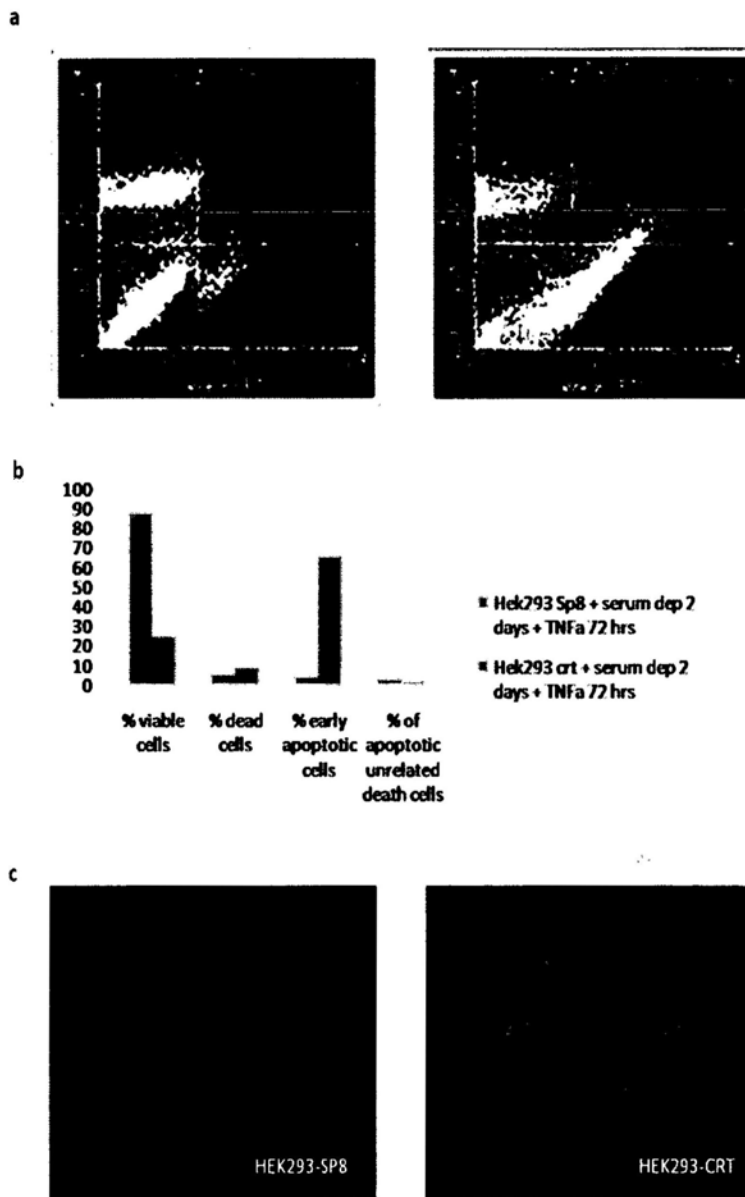


Figure 4.7 The anti-apoptotic functions of NYD-SP8 in HEK293 cells. (a) Annexin V binding and PI staining showing the effect of NYD-SP8 in HEK293 cells after TNF α induced apoptosis. (b) Summarized data of (a). (c) DAPI staining showing presence of fragmented nuclear bodies in HEK293 cells after TNF α -induced apoptosis.

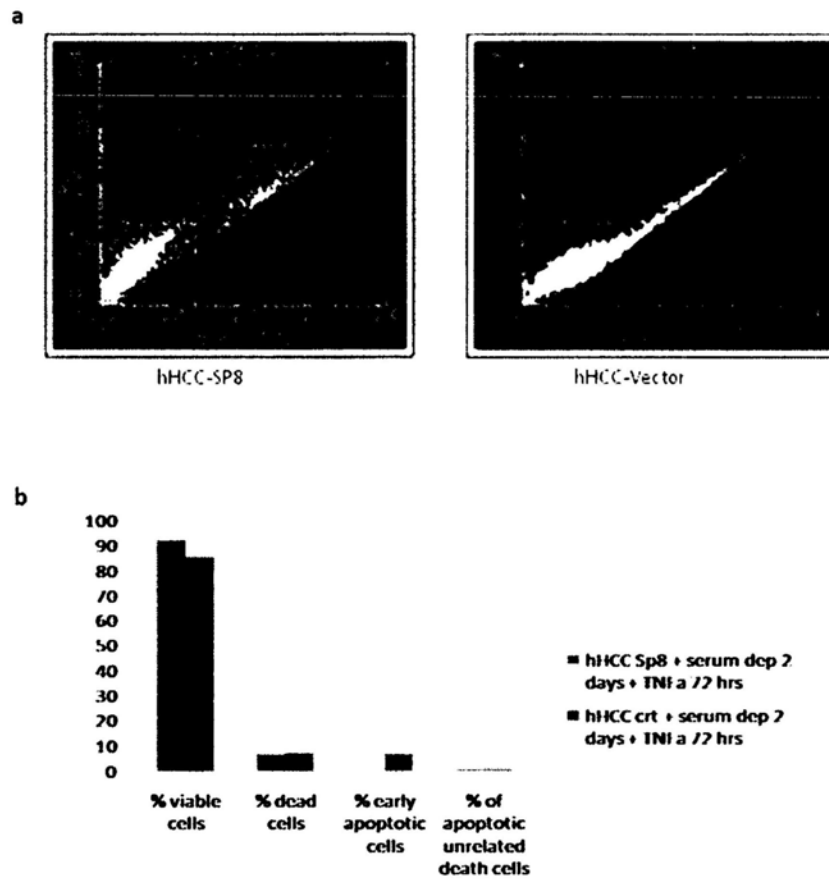


Figure 4.8 The anti-apoptotic functions of NYD-SP8 in hHCC cells. (a) Annexin-V binding and PI staining showing the effect of NYD-SP8 in hHCC cells after TNF α induced apoptosis. (b) Summarized data of (a).

4.3.3 NYD-SP8 contributes to anchorage-independent growth

Most normal epithelial cells are anchorage-dependent; however, transformed cells lose their contact inhibition and gain anchorage-independent growth ability.^{75,161} Anchorage-independent growth is one of the hallmarks of tumor transformation, after which tumor cells increase their anti-apoptotic ability in order to survive in semi-solid matrix gel. Since NYD-SP8 contributes to the anti-apoptotic functions in tumor cells, a soft agar anchorage-independent growth assay was used to study the effect of NYD-SP8 in tumor transformation *in vitro*. Results showed that NYD-SP8 increased the number of colonies formed in soft agar when compared to its corresponding control (Figure 4.9a), with an average 12 colonies/well in hHCC-SP8 while 4 colonies/well in hHCC-CRT group, $n = 4$, $p < 0.05$; Figure 4.9b). These data have shown that NYD-SP8 enhance anchorage-independent growth and may contribute to tumor transforming properties.

4.3.4 Anti-apoptotic signaling in NYD-SP8 cells

Based on the functional results, cDNA oligoarrays were used to elucidate the underlying molecular mechanisms of cell proliferation and anti-apoptotic function in NYD-SP8 cells (Figure 4.10).

A total of 10 up-regulated genes and 5 down-regulated genes were found in HEK293-SP8 group when compared to the vector control group. Among those candidate genes, the Tumor Suppressor *p53* (*TP53*) was selected for further studies because it is the major regulator in cell proliferation and apoptosis. The expression of *TP53* was further confirmed by Western blot analysis. Results showed that *TP53* was down-regulated in HEK293-SP8 cells, indicating that NYD-SP8 suppresses *TP53* protein expression (Figure 4.11).

A total of 5 up-regulated genes and 13 down-regulated genes were found in hHCC-SP8 group. Among these candidate genes for anti-apoptotic signaling, *NFκB-1* and *Bcl-2* were selected for further studies. *NFκB-1* and *Bcl-2* are major participants

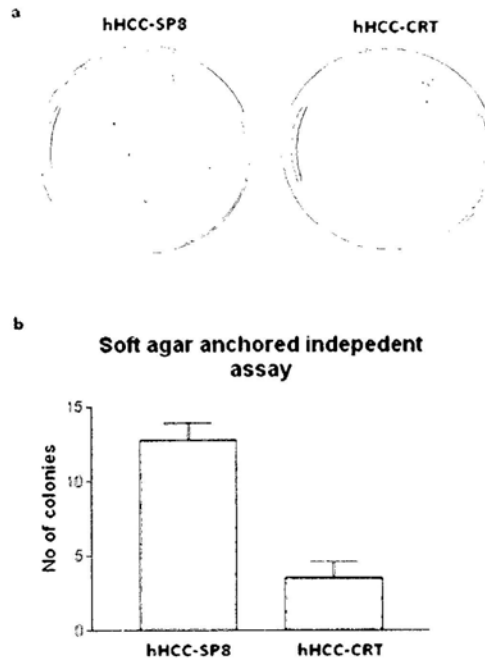


Figure 4.9 (a) Soft agar anchorage-independent growth assay in hHCC cell lines. (b) Summarized data as shown in chart.

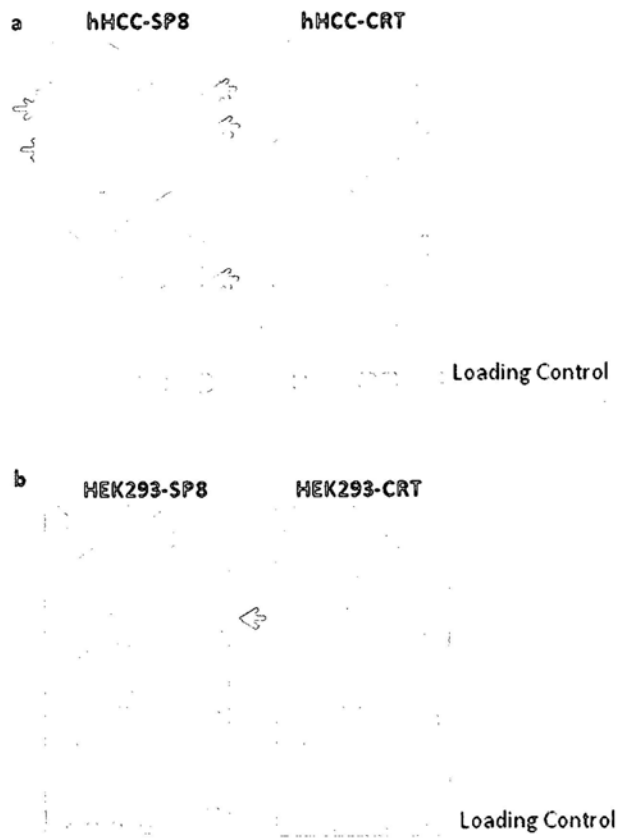


Figure 4.10 The cDNA oligoarray of (a) hHCC and (b) HEK293 cell lines.

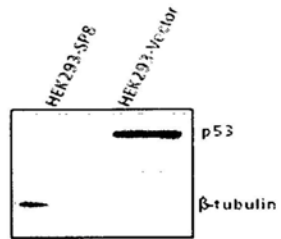


Figure 4.11 Western blot analysis showing NYD-SP8 down-regulated p53 expression.

in pro-survival and apoptosis signaling in various cancer tissues, therefore, the expression of *Bcl-2* and *NFκB-1* was further confirmed using semi-quantitative PCR and real time quantitative PCR in the hHCC cell lines. Semi-quantitative PCR results showed up regulation of *Bcl-2* and real time quantitative PCR results showed more than a 2 fold increase in *NFκB-1* transcripts (> 2 fold) in NYD-SP8 over expressing cell lines (Figure 4.12 a and b), indicating that the anti-apoptotic role of NYD-SP8 may occur through up-regulation of *NFκB* signaling pathway.

4.3.5 Involvement of p53 in mediating the anti-apoptotic effect of NYD-SP8

The p53 protein is a key regulator in cell cycle and apoptosis. Altered expressions of the p53 protein have decisive effects upon tumor growth. Since most cancer cells have either mutated or no expression of p53, the effectiveness of the anti-apoptotic function of NYD-SP8 may rely on the p53 expression profile in the cells. HEK293 has a relative high level of wide type p53 expression while hHCC has relative low level wide type p53 expression. Western blot analysis showed that NYD-SP8 has a less significant effect in downregulating p53 expression in hHCC cell lines (Figure 4.12c). We hypothesize that the different potency of NYD-SP8 in cell survival mainly depends on the p53 expression level of the cells. In order to test this hypothesis, a p53-negative human lung carcinoma cell line h1299 was used. Cell proliferation assays showed that NYD-SP8 has no effect on cell growth in the p53-negative h1299 cell lines (Figure 4.13a). RT-PCR and Real time quantitative PCR results showed that the mRNA expression of *Bcl-2* and *NFκB-1* in h1299-SP8 cell line did not alter when compared to its vector control cell line (Figure 4.13 b and c). These data further suggested that the anti-apoptotic properties of NYD-SP8 may be p53-dependent.

4.3.6 NYD-SP8 promotes tumor growth *in vivo*

To test how NYD-SP8 would affect the cell proliferation of tumor cells *in vivo*, hHCC-SP8 and hHCC-vector cells were subcutaneously (s.c.) inoculated into nude mice. Four mice were included in each group and the experiment was done in duplicates. The proliferation rates of tumors were monitored and tumor sizes were

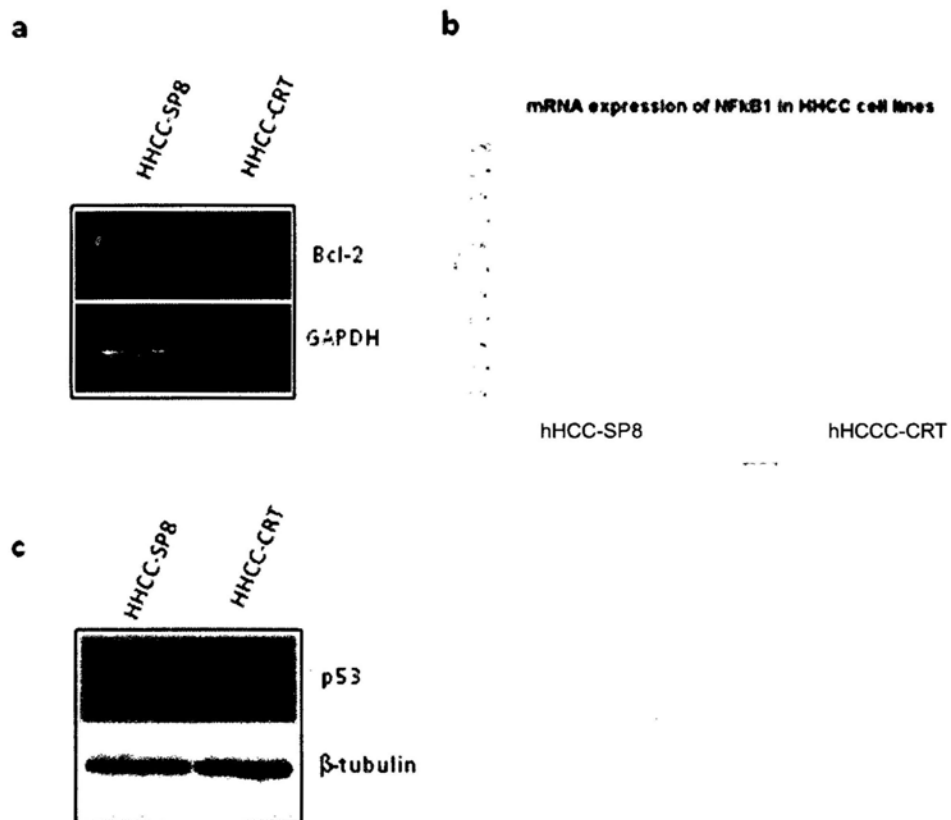


Figure 4.12 Signaling mechanisms of NYD-SP8-mediated apoptosis. (a) Semi-quantitative PCR showed an increase in Bcl-2 expression in HHCC-SP8 and (b) real time quantitative PCR showing an 2-fold increase in NFkB expression in HHCC-SP8. (c) Western blot analysis showing p53 expression in HHCC-SP8 cell lines.

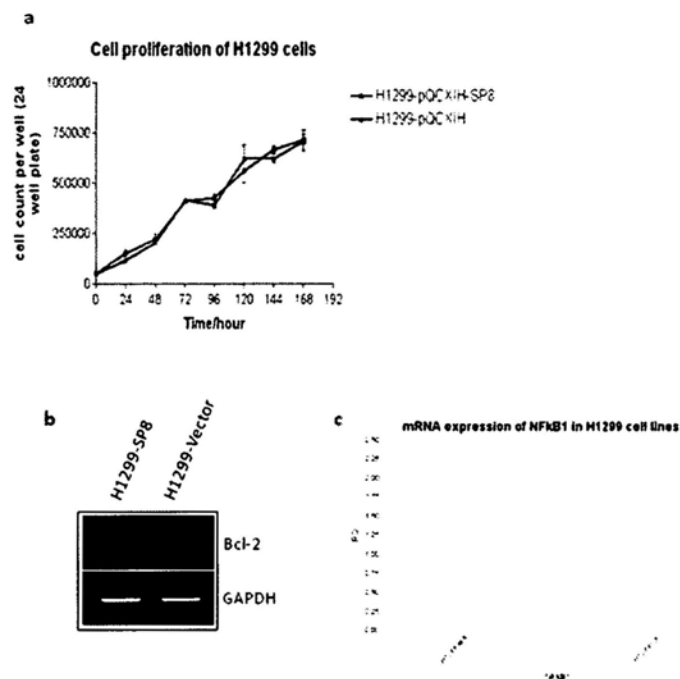


Figure 4.13 The effect of NYD-SP8 in h1299 cells. (a) Growth curve of h1299 cells showing NYD-SP8 does not alter the cell proliferation rate significantly. (b) RT-PCR showing the effect of NYD-SP8 in expression of Bcl-2 in h1299 cells. (c) Quantitative real time PCR showing the effect of NYD-SP8 in h1299 cells.

measured 2 weeks after inoculations. As shown in Figure 4.14a, the mice were euthanized and the tumors were excised out 2 weeks after inoculations. The tumor measurement and weights are displayed in Figure 4.14b. The hHCC-SP8 group demonstrated significantly faster tumor growth than the vector control group and higher tumor-to-body ratio, suggesting that NYD-SP8 enhances tumor growth *in vivo*.

In order to confirm the anti-apoptotic role of NYD-SP8 *in vivo*, the expression of Bcl-2, Bax and p53 in tumor tissues were analyzed using Western blot analysis. Results showed that hHCC-SP8 tumors showed an elevated anti-apoptotic Bcl-2 protein expression, but have no significant changes in pro-apoptotic Bax protein and p53 protein expression (Figure 4.15). These data further confirmed the anti-apoptotic role of NYD-SP8 *in vivo*.

To test the hypothesis that the effect of NYD-SP8 on tumor growth *in vivo* is also p53-dependent *in vivo*, h1299-SP8 and h1299-vector cells were subcutaneously (s.c.) inoculated into nude mice. Five mice were included in each group. The proliferation rates of tumors were monitored and tumor sizes were measured 2 weeks after inoculations. As shown in Figure 4.15, the mice were euthanized and the tumors were excised out 2 weeks after inoculations. The tumor measurement and weights are displayed in Figure 4.16. The h1299-SP8 group did not have significantly changes in tumor growth rate when compare to the vector control group, consistent with the *in vitro* cell proliferation and cell count results. These data further suggested that the growth promoting functions of NYD-SP8 may be p53-dependent.

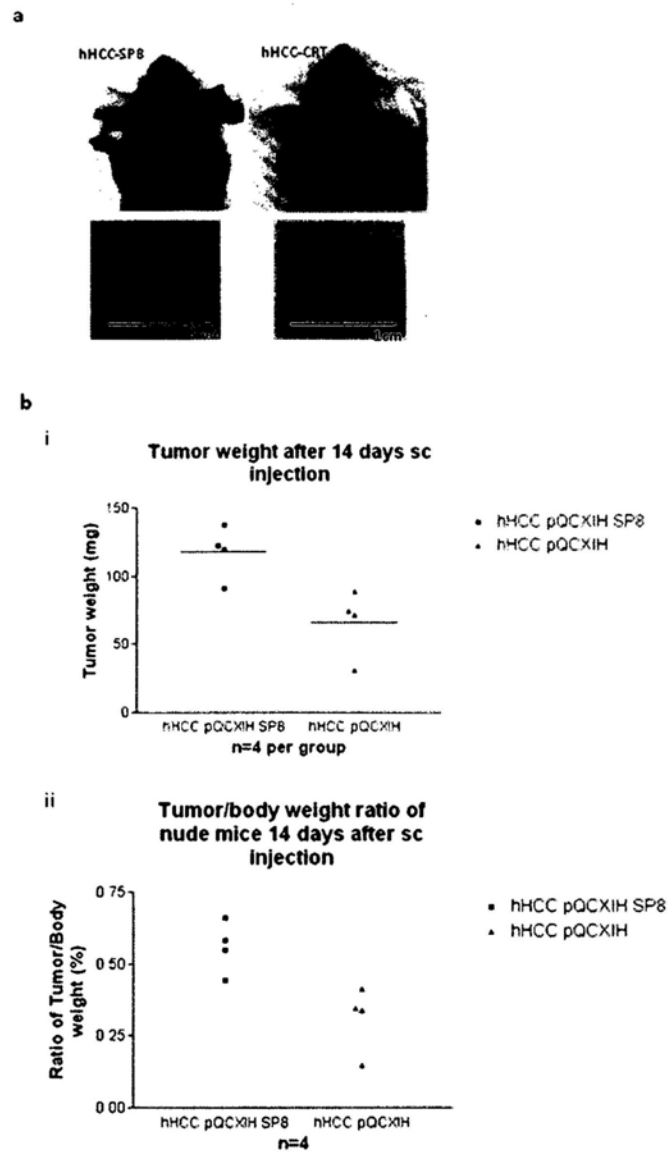


Figure 4.14 Effect of NYD-SP8 in tumor growth *in vivo*. (a) Representative diagram showing tumor growth and tumor size in nude mice. (b) Summarized data showing the tumor weight of hHCC-SP8 and control group (i) and tumor-to-body weight (ii).

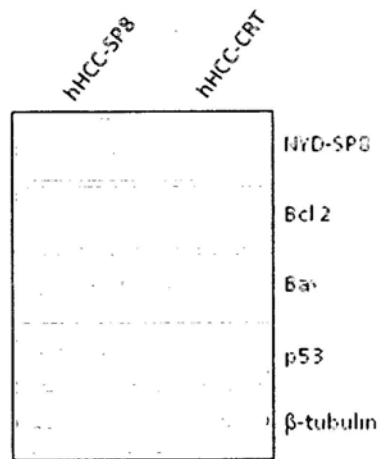


Figure 4.15 Western blot analysis shows the expression of Bcl-2, Bax and p53 protein in hHCC-SP8 tumor tissues and its control.

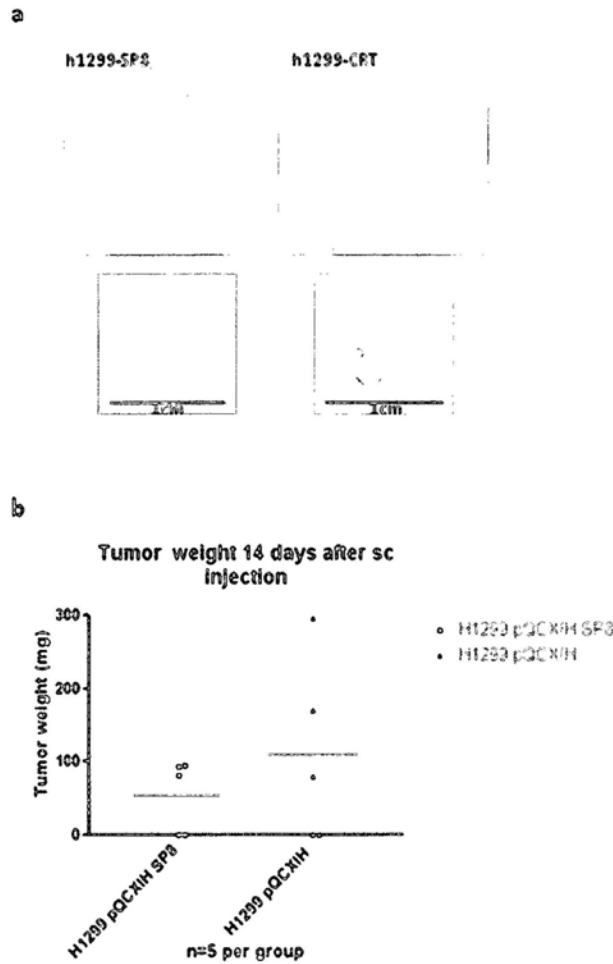


Figure 4.16 *In vivo* studies of NYD-SP8 effect in tumor growth of h1299 cells. (a) Representative diagram showing tumor growth and tumor size in nude mice. (b) Summarized data showing the tumor weight of h1299-SP8 and its control group.

4.4 Discussions

4.4.1 The growth promoting function of NYD-SP8 may be p53dependent

In this chapter, both the cell proliferation assays and cell counts demonstrated that NYD-SP8 has a promoting effect on cell growth of HEK293 and hHCC cell line, but not in the h1299 cell lines. It is hypothesized that the amount of p53 protein expression is correlated with growth promoting and anti-apoptotic function of NYD-SP8.

The HEK293 cell line has relatively higher p53 protein expression. Therefore it is more sensitive to p53-dependent growth response. The hHCC cell line has a mutant form of p53 protein. If the growth promoting effect of NYD-SP8 depends on the NYD-SP8-mediated wild type p53 suppression, the mutant p53 protein may not be sensitive to NYD-SP8-mediated suppression. Therefore, the growth promoting effect is diminished. Indeed, the growth promoting effect of NYD-SP8 in h1299 cell line, which has no detectable p53 expression, was not observed. These results indicate that part of the growth promoting effect of NYD-SP8 may be p53-dependent. Furthermore, these results also indicate that NYD-SP8 may have a more pronounced effect during the early stage of tumor growth when wild type p53 is expressed. In more advanced stage of tumor development in which most p53 protein is mutated or silenced, the p53-dependent effect of NYD-SP8 is abolished. It would be interesting to study further the relationship between NYD-SP8 and p53 in different stages of tumor development.

4.4.2 Possible signaling mechanisms underlying NYD-SP8-mediated growth promoting effect

Results in the flow cytometric analysis have showed that NYD-SP8 enhances anti-apoptotic properties in both HEK293 and hHCC cell lines and protect cells against TNF α -induced apoptosis. Although hHCC has a very weak p53 expression, the *in vivo* tumor growth of hHCC-SP8 cell line was enhanced significantly when compared to its corresponding control. Oligoarray data, RT-PCR and real time PCR results showed that NYD-SP8 enhanced *Bcl-2* and *NF κ B-1* mRNA expression in hHCC

cell lines but not in h1299 cell line, which is p53 negative. These data further suggests that the growth promoting effects of NYD-SP8 may be p53-dependent. Moreover, the downstream signaling pathway leading to the anti-apoptotic functions in hHCC cells may be dependent on the up-regulation of Bcl-2 anti-apoptotic proteins via NFκB related signaling.

4.4.3 NYD-SP8 initiates uPAR-dependent/independent downstream signalings

An important question was raised: as a GPI-anchored cell surface protein, how can NYD-SP8 trigger its intracellular signaling and regulate p53 expression? Based on the structural homology and protein-protein interactions between NYD-SP8 and uPAR as described in Chapter 3, one possible mechanism may be through the regulation of uPAR-mediated intracellular signaling transduction. Apart from its proteolytic activity, uPAR is involved in cell adhesion and intracellular signaling transduction. Recent reports have demonstrated that uPAR acts as a survival factor for melanoma by downregulating p53.¹² These findings may offer an explanation for our observation that NYD-SP8 may serve as a homolog/antagonist of uPAR, interfering or mimicking the anti-apoptotic functions of uPAR by regulating p53. However, more in depth investigation is required to understand the detail relationship between NYD-SP8 and p53 protein.

Surprisingly, HEK293 has no uPAR protein expression, but the growth promoting effect of NYD-SP8 in HEK293 is even much stronger than that in the hHCC cell lines *in vitro*. These results indicate that NYD-SP8 may also regulate cell growth, majority, via other signaling mechanism, which may be uPAR-independent. The putative TRAF2 binding domain of NYD-SP8 structure may provide some hints. The TRAF2 protein is a member of TRAF protein family. TRAF2 interacts with TNF receptors and mediates signal transduction and TNFα-mediated NFκB activation and anti-apoptotic functions. Thus, NYD-SP8 may regulate TRAF2-mediated signal transduction and thereby enhancing its anti-apoptotic activity in cells lacking uPAR. Further investigation of the signaling mechanism of NYD-SP8 and TRAF2 interactions is important in understanding the uPAR-independent growth promoting effect of

NYD-SP8.

4.4.4 Limitations and future studies

The existing data have several limitations. Firstly, the p53-dependent growth promoting effect is demonstrated in three different cell lines with totally different molecular backgrounds. It is not conclusive in confirming the p53-dependent signaling of NYD-SP8 using only these cell lines. Further investigation on the relationship between NYD-SP8 and p53 by RNAi conditional knockdown technology in the same cell line system is necessary.

Secondly, p53 is a transcription factor while NYD-SP8 is a membrane bound cell surface receptor. The underlying mechanisms of how NYD-SP8 triggers its downstream signaling leading to p53-dependent growth promoting effect is unclear. Further investigation on the relationship between NYD-SP8, uPAR and other interacting partners of NYD-SP8 by RNAi conditional knockdown technology in the same cell line system is necessary to answer this question.

4.4.5 More to know: Effect of tumor microenvironment on NYD-SP8 activity

Interestingly, cell proliferation and cell count assay have showed that the growth promoting function of NYD-SP8 is less significant in hHCC cells. However, the *in vivo* tumor growth of hHCC-SP8 cell line was enhanced significantly when compared to its corresponding control. These observations indicated that the *in vivo* tumor microenvironment is very important in promoting/enhancing the functions of NYD-SP8. The cell-matrix interactions are necessary to cell surface proteins as to function properly in tumor microenvironment. It would be interesting to investigate the interactions of NYD-SP8 with the tumor microenvironment, such as cell-cell and cell-matrix interactions during tumor development.

As shown in Figure 4.13a, the tumors in the hHCC-SP8 group were more angiogenic than the control group. The rapid tumor growth in NYD-SP8 group may result in intracellular hypoxia, which initiates a series of cell signaling event that promote angiogenesis. However, the underlying mechanism(s) of how NYD-SP8

induces rapid tumor growth and angiogenesis remain unclear.

Taken together, NYD-SP8 appear to promote cell proliferation and cell growth by regulating the anti-apoptotic functions of cells possibly through p53-dependent NF κ B related Bcl-2 signaling pathways.

Chapter 5 NYD-SP8 inhibits cancer cell invasion and metastasis

5.1 Introduction

In Chapter 4, the results have demonstrated that NYD-SP8 promotes tumor growth and cell survival. It is hypothesized that NYD-SP8 may have stage-dependent effects in tumor development. It would be interesting to study the function of NYD-SP8 in advanced stages of tumor development. In this chapter, the role of NYD-SP8 in affecting proteolytic ECM degradation, cancer invasion, metastasis and the underlying mechanisms are discussed.

5.1.1 Cancer Invasion and Metastasis

The incidence of cancer is rising rapidly worldwide, and metastasis remains the cause of 90% of deaths from solid tumors. However, the underlying mechanisms of metastasis are still unclear.^{75,178} Metastasis is a multi-step process, with the spread of cancer cells from the primary site to a distant secondary site. These steps include detachment of cancer cells from the primary tumors, local invasion, angiogenesis, intravasations into the circulating system, increase cell survival, extravasations and establishment of new clones at a secondary site (Figure 5.1).⁴⁹

5.1.2 ECM degradation

In order to enter and exit the circulating system, tumor cells must penetrate through the basement membrane. Tumor invasion and metastasis is often facilitated by proteolysis of the ECM. The ECM consists of mainly collagens, glycoproteins such as laminin and fibronectin, as well as proteoglycans. Collagens are the most abundant proteins in the ECM and they are essential structural components in all connective tissues.^{133,160}

Recent reports suggested that alterations of ECM composition is the main promoter of carcinogenesis.¹²² The ECM composition is mainly regulated by a panel of "tumor-associated proteases".^{122,119} Tumor cells produce and secrete various proteases to degrade the ECM and allow tumor cells to invade nearby connective tissues and blood vessels.^{18,25,156,182,212} These proteases are generally classified into

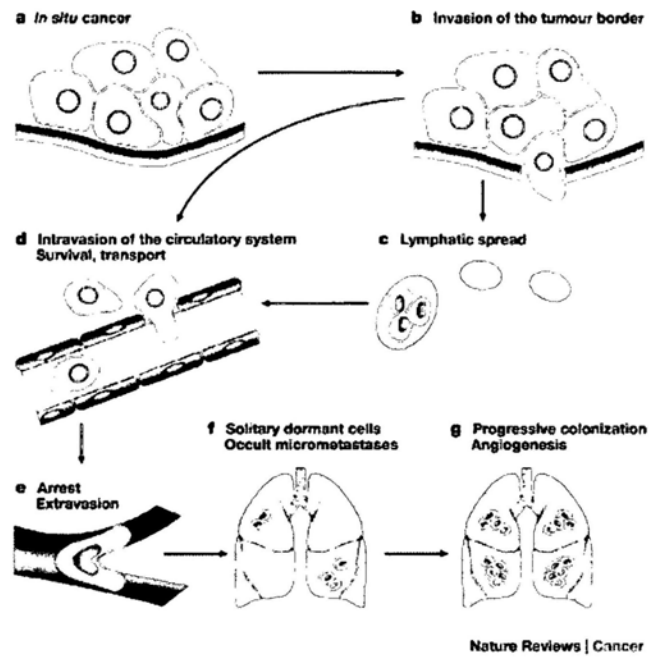


Figure 5.1 The schematic diagram of cancer invasion and metastasis. (a) A tumor in primary site surrounded by the basement membrane. (b) Local invasion of cancer cells by decrease cell-cell adhesion, increase cell-matrix interaction, and destroy the ECM. (c) Extravasations of tumor cells into either lymphatics, or (d) the blood circulation. (e) Survival and extravasations of tumor cells at a distant site. (f) Micrometastasis of tumor cells. (g) Establishment of proliferation of new clones at a distant site. (Adapted and modified from ²⁶)

three major groups by their catalytically active site. They are serine proteases [e.g. urokinase plasminogen activator (uPA) family],^{16,173} cysteine proteases (cathepsins),⁵⁰ and matrix metalloproteinases (MMPs).^{50,120} There are various possible mechanisms by which these proteases can promote tumor cell invasion and metastasis, including disruption of cell-cell adhesion by cleaving cell-adhesion molecules such as E-Cadherin, degradation of ECM and basement membranes and internal signaling processing for cell migration and metastasis (Figure 5.2). Inhibitions or ablations of these proteases lead to an obvious decrease in tumor cell invasion and metastasis.^{52,69,92} For that reason, targeting these proteases is a promising strategy in anti-cancer therapy. Recent development of small molecular inhibitors for the treatment of cancer, in particular uPA specific inhibitor (PAI-1) and MMPs inhibitors have proven to be effective in experimental models.²⁰⁰ However, these inhibitors exhibited a lack of efficacy in the clinical setting. Therefore, novel proteases inhibitors have been increasingly recognized as new therapeutic target for anti-cancer therapy on top of conventional therapeutic methods.

5.1.3 Serine Proteinases

The plasminogen activator (PA) system is best characterized for their role in ECM regulation. There are two types of plasminogen activators: the urokinase-type (uPA) and the tissue type (tPA). Both of them are responsible for the translation of plasminogen zymogen to active plasmin proteinases. Evidence has suggested that tPA is responsible for plasminogen conversion during thrombolysis while uPA is involved in ECM degradation²⁰⁸.

The uPA family is composed of an enzyme (uPA), two receptors (uPAR) and three inhibitors (PAI-1, PAI-2 and protease nexin 1). The uPA enzyme is produced as inactive pro-uPA zymogen, which undergoes several post-translational modifications before releases. The pro-PA zymogen then binds to the uPAR and is cleaved by membrane bound plasmin to become active mature uPA. The active uPA/uPAR complexes induces a localized cell surface proteolysis by catalyzing the conversion of plasminogen zymogen to active plasmin³¹ Active plasmin degrade

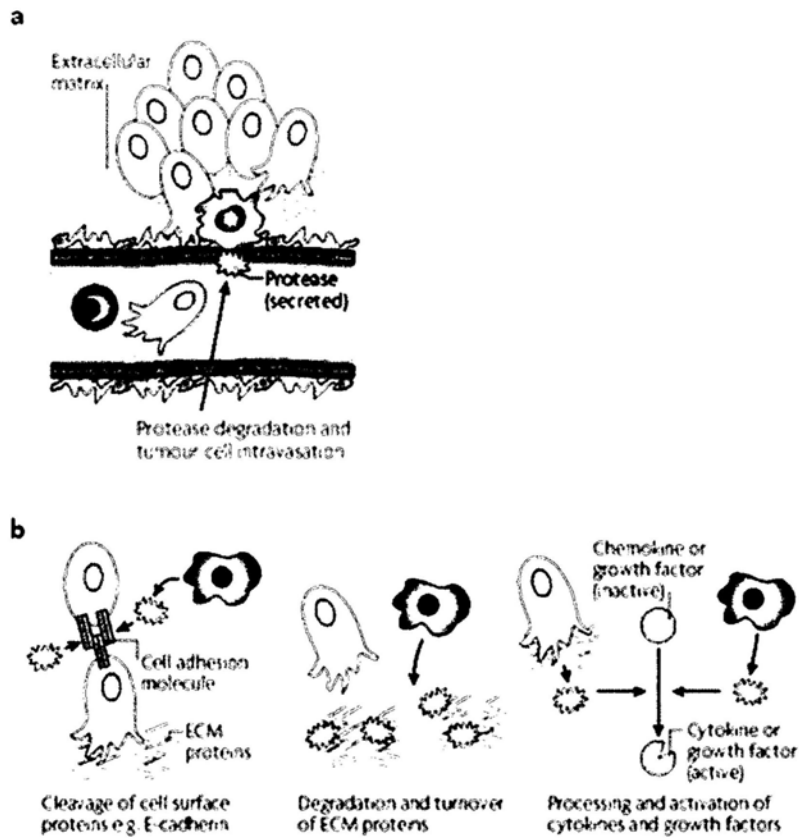
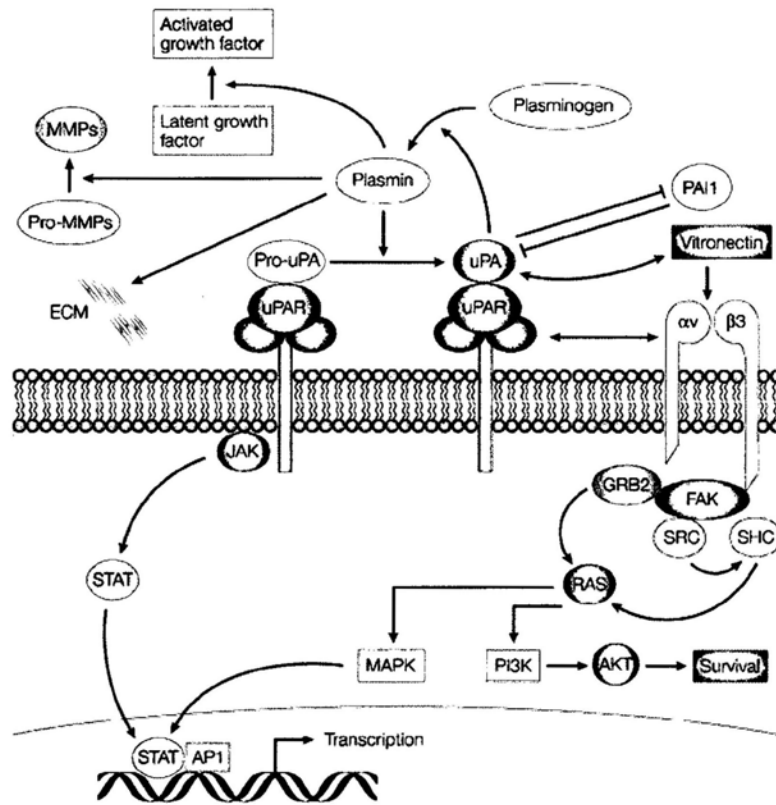


Figure 5.2 Involvement of tumor associated proteases in cancer invasion and metastasis. (a) Intravasations of cancer cells into circulating system. Proteolytic degradation of basement membrane by tumor associated proteases during intravasations. (b) Tumor associated proteases promote cancer cell intravasation and local invasion by several possible mechanism, including decrease cell-cell adhesion, degradation and turnover of ECM proteins and stimulation of internal signalings of cancer invasion of metastasis. (Adapted from ⁹³).

most ECM proteins such as fibronectin, vitronectin and fibrin.³⁹ Active plasmin also promotes ECM degradation indirectly via activation of other proteases such as MMPs (Figure 5.3).²³

Apart from promoting ECM degradation, uPA/uPAR complexes are associated with cell proliferation, differentiation, angiogenesis, implantation, wound healing, cellular adhesion, anoikis, tissue remodeling, inflammation and cell migration.^{44,179,207} Most of these cellular responses are modulated by direct contacts of uPAR (or in some cases uPA) with a variety of extracellular proteins and cell membrane receptors such as integrins, EGF receptor, caveolin and G-protein-coupled receptors.^{16,144} For example, uPAR promotes cellular adhesion to ECM proteins by a direct high affinity interaction between uPAR and Vitronectin²¹⁰ and lateral interactions with adhesion receptors from the integrins family.²⁸ The interaction between uPAR and integrins provide a basis for integrin-mediated transmembrane signal transduction after the binding of ligands to uPAR. The C-terminus sequence of active uPA is suggested to interact with $\alpha_v\beta_3$ integrin and is relevant for cell migration.¹⁹¹ Thus, downregulation of uPA or uPAR may lead to inhibited pericellular proteolysis, changes in signal transduction and decreased in cell migration which, among other changes may result in the loss of the invasive phenotype of tumor cells.

Most normal tissues have no detectable uPAR.¹²⁷ In tumor cells, enhanced activity of uPA has been associated with tumor invasion, metastasis and angiogenesis.^{40,129,203} Several studies has shown that inhibition of uPA activity and its binding to the uPAR by different strategies results in inhibition of cell surface plasminogen activation, tumor growth, invasion and metastasis.^{37,106,130,151} As a result, inhibition of uPA/uPAR system becomes ideal targets for potential anti-cancer therapy.



Nature Reviews | Cancer

Figure 5.3 Schematic Diagram showing uPA/uPAR system mediated ECM degradation and involvement of integrins in several signaling pathways (Adapted and modified from ¹⁵⁶).

5.1.4 The Matrix Metalloproteinase family

An important family of proteinases responsible for ECM degradation in cancer progression is the MMPs family. The MMP family is composed of both secreted or transmembrane proteins which play important roles in many physiological processes.^{57,140} They are classified into different group according to their protein structure and substrate specificity. For example, collagenases degrade fibrillar collagen while gelatinases degrade non-fibrillar and denatured collagen (gelatin).

In normal cells, MMPs are tightly controlled and produced at very low levels. In cancer cells, abnormal expression of MMPs is associated with basement membrane and ECM degradation during tumor invasion and metastasis.²⁷ Abnormal expression of MMPs has been shown in various carcinomas such as lung, colon, breast and pancreas.^{41,58,117,188} In addition, elevated MMPs levels are observed in the plasma and urine of cancer patients when compared with healthy subject.⁸⁰ Among the MMPs family, MMP-2 and MMP-9 specifically degrade type IV collagen, which is the main component of the basement membrane and the ECM.^{5,140} Active MMP-2 binds to integrin $\alpha_v\beta_3$ ¹⁹ while active MMP-9 is associated with CD44,²²³ indicating a role in promoting tumor invasion. It is because increase expression/activation of MMP-2 and MMP-9 appear to play important roles in tumor invasion and metastasis,^{5,11,87,91,112} novel inhibitors of MMP-2 and MMP-9 are ideal targets of anti-cancer therapy.

The expression of MMP-2 and MMP-9 is partly induced by Extracellular matrix metalloproteinases inducer (Emmprin). Emmprin, also called CD147, is a cell surface glycoprotein,¹⁵ which is implicated in different steps of tumor progression. Emmprin stimulates MMPs production,^{74,94,192} including MMP-2¹⁶⁸ and MMP-9,⁹⁶ via normal as well as pathological cellular interactions. Downregulation of Emmprin has been shown to reduce MMP-2 and MMP-9 production and thus inhibit cancer invasion and metastasis. While synthetic MMPs inhibitors lack encouraging effectiveness in anti-cancer treatment in the clinical setting, Emmprin could be an ideal target for reducing the production of MMPs in tumors and thereby inhibit cancer invasion and metastasis.

Targeting MMP activation is an alternative way to reduce MMP family related ECM degradation, cancer invasion and metastasis. Several studies have suggested that serine proteases, particularly plasmin, function to activate pro-MMPs.^{23,36,139} However, plasmin-mediated activation of pro-MMPs is not conclusive to date, so there may be other mechanisms in regulating MMPs activation.

5.1.5 The cysteine cathepsins Family

Another important family of proteases responsible for ECM degradation in cancer progression is the cysteine cathepsins family. The cathepsins family consists of 11 lysosomal proteases that is involved in various physiological process, such as wound healing and apoptosis, inflammation, and cancer progression.^{21,22,99,215,89}

In normal cells, cathepsins are regulated at multiple levels including transcription, post-transcriptional processing, translation, post-translational processing and trafficking. However, deregulation of cathepsins in different levels results in increased mRNA and protein expression, increased activity and altered intracellular distribution in tumor cells.¹⁰¹ Among the cathepsins family member, cathepsin B has been the most extensively studied and implicated in enhancing tumor invasion and metastasis.^{63,64,79,84,104,138}

Cathepsin B is produced as a zymogen and is activated in prelysosomal acidic vesicles. Pro-cathepsin B is activated by cathepsin D, elastase, cathepsins G and uPA.²⁰⁴ Active cathepsin B is stored in lysosomes and is responsible for proteolytic degradation of type IV collagen, which is the main component of basement membrane.²⁰⁴

In tumor cells, active cathepsin B has been suggested to initiate and facilitate proteolytic degradation on the tumor surface directly or indirectly via interacting with other tumor associated proteases such as serine proteases and MMPs.^{51,132,165} Elevated expression and secretion of cathepsin B leads to tumor cell growth, invasion and metastasis.^{47,131} Overexpression of cathepsin B has been associated with poor prognosis in cancer patients.^{22,57,100,111,159} Therefore, novel inhibitors for cathepsin B are ideal targets for potential anti-cancer and anti-metastatic

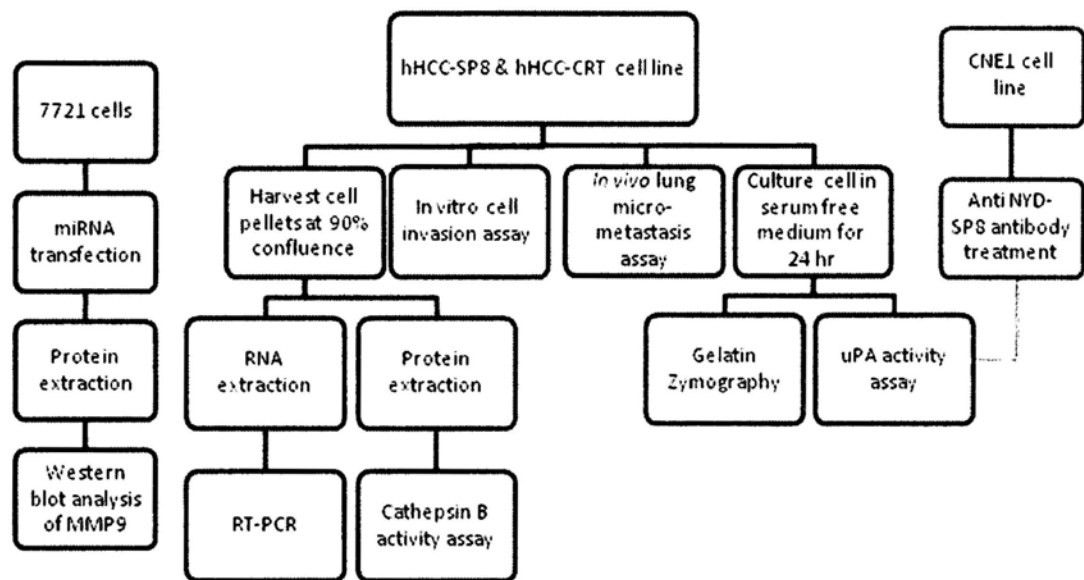
therapy.^{63,113}

5.1.6 Objective

The aim of this study is to investigate (1) the role of NYD-SP8 in regulating uPA system and other proteases activities; (2) the effect of NYD-SP8 in affecting cancer cell invasion and metastasis; and (3) the underlying molecular mechanisms.

5.2 Experimental plan

Detailed materials and methods are described in Chapter 2. A schematic diagram of experimental plan is shown below.



5.3 Results

5.3.1 Suppressing functions of NYD-SP8 in uPAR family

NYD-SP8 suppresses active uPA production

The possible effect of NYD-SP8 on the uPA/uPAR complexes was studied using the uPA activity assay kit (Chemicon) and Western blot analysis. The results showed significant reduction in the uPAR-mediated active uPA production in hHCC-SP8 cells when compared to vector control cells, (** $p < 0.01$, Figure 5.4a). The inhibiting effect could be reversed by anti-NYD-SP8 antibody, but not control IgG antibody, at a concentration of 5 $\mu\text{g}/\text{mL}$ (** $p < 0.01$, Figure 5.4a), suggesting that the suppressing effect of NYD-SP8 on active uPA production *in vitro* is specific. This was further confirmed by the use of recombinant NYD-SP8, showing concentration-dependent reduction in active uPA production with an increasing amount of NYD-SP8 used (Figure 5.4b). Interestingly, the NYD-SP8 antibody, but not IgG, also produced an increase in uPA activity in a nasopharyngeal cancer cell line (CNE1) expressing endogenous NYD-SP8 (Figure 5.4c), consistent with an inhibitory role of NYD-SP8 in the uPA/uPAR system.

Similar results were observed using Western blot analysis, with less active uPA detected in the NYD-SP8-expressing cells (Figure 5.4d) and when excess recombinant NYD-SP8 was added (20 $\mu\text{g}/\text{mL}$), active uPA production could also be blocked (Figure 5.4d), consistent with that revealed by uPA activity assay (Figure 5.4b). However, no significant alternations in pro-uPA and uPAR expression were observed (Figure 5.4d). Interestingly, when recombinant NYD-SP8 protein was added into culture medium, a diffuse band of $\approx 120\text{--}160$ kDa was observed in all the NYD-SP8-treated, but not BSA treated-samples under non-denaturing and non-reducing conditions, indicating complex formation between NYD-SP8 with uPA/uPAR complexes (Figure 5.5). Taken together, these results indicate that NYD-SP8 binds to and interferes with uPA/uPAR activation process and leading to the observed decrease in active uPA production in NYD-SP8 overexpressed or NYD-SP8 treated cells.

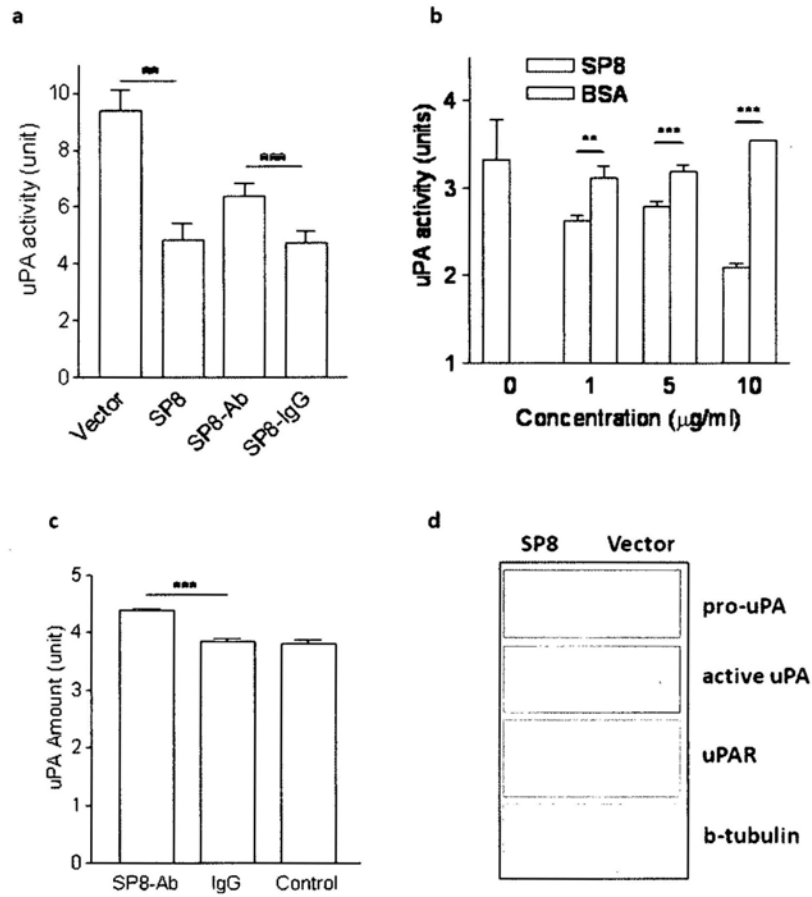


Figure 5.4 NYD-SP8 suppresses serine proteases uPA activity at protein level. (a) Comparison of the mean uPA activity in culture medium of hHCC/SP8 cell line (SP8) and its control (VECTOR), and reversal of uPA activity in the presence of 5 µg/mL of NYD-SP8 antibody (SP8-Ab) but not the normal mouse IgG (SP8-IgG) (values are mean S.D., n = 3, *** $p < 0.001$). (b) hHCC cells were treated with NYD-SP8 recombinant protein for 24 hours at indicated concentrations, with corresponding concentrations of BSA as controls, and enzymatic activity of uPA in culture medium was measured. (S.D., n = 3, *** $p < 0.001$). (c) NYD-SP8 antibody reversed the uPA activity in nasopharyngeal cancer cell line (CNE1) expressing endogeneous NYD-SP8 (d) Western blot analysis of pro-uPA, active uPA and uPAR in hHCC-SP8 cell line (SP8) or its control (Vector) (β -tubulin as a loading control).

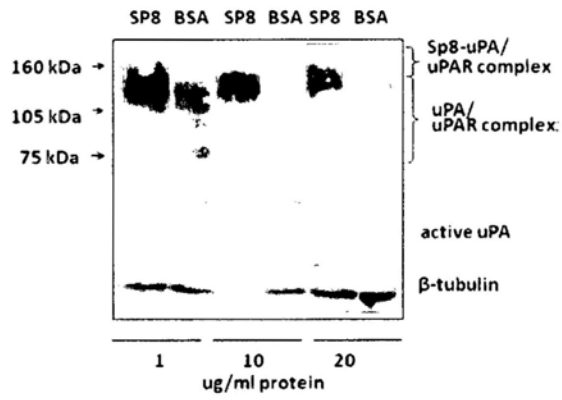


Figure 5.5 The NYD-SP8-uPA/uPAR complexes. hHCC cells were treated with NYD-SP8 recombinant protein for 24 hours at indicated concentrations, with corresponding concentrations of BSA as controls, and cell lysate were subjected to Western blot analysis with antibodies to uPA/uPAR complexes, active-uPA or to β -tubulin as a loading control ($n = 3$).

NYD-SP8 did not alter transcriptional expression of uPAR family

We also tested whether NYD-SP8 could affect uPA-related gene expression at transcription level. Semi-quantitative RT-PCR results showed that there was no significant difference in the mRNA expression profiles of uPA, uPAR and PAI-1 between hHCC-SP8 and hHCC-vector cells (Figure 5.6), suggesting that the decrease in active uPA production in the NYD-SP8 expressing cells was not due to a transcriptional change in the uPA/uPAR system or inhibitory effects from overexpression of PAI-1 inhibitors.

5.3.2 NYD-SP8 suppresses MMPs activities

NYD-SP8 suppress active MMPs production

Binding of uPA to uPAR activates the conversion of plasminogen to plasmin, and thereby enhancing ECM degradation through multiple signaling pathways such as promoting the expression/activation of MMPs, which are family of zinc-dependent endopeptidases that have been implicated in the proteolytic events of tumor cell invasion.⁵⁶ Among this family, Gelatinases A and B (MMP-2 and MMP-9) have been shown to play an important role in ECM degradation and participate in cancer progression in several neoplasia.²⁰¹ Gelatin zymography was used to investigate whether NYD-SP8 affects MMPs activity in conditioned medium, and the results showed that both MMP-2 and MMP-9 activities were reduced in hHCC-SP8 cells with more prominent effect on MMP-9 activity (Figure 5.7a). This was further confirmed by the use of recombinant NYD-SP8, showing significant reduction in both pro- and active MMP-9 productions with 10 µg/mL of NYD-SP8 used (Figure 5.7b). In addition, use of miRNA knockdown in SMMC-7721 cell lines, which has endogenous NYD-SP8 expression, showed an increase in active MMP-9 protein production in Western blot analysis, indicating that NYD-SP8 has inhibiting effects on both pro- and active MMP-9 production (Figure 5.7c).

NYD-SP8 alters MMP-2 and MMP-9 mRNA expression

To further assess the nature of NYD-SP8-induced suppression in MMP activity, the

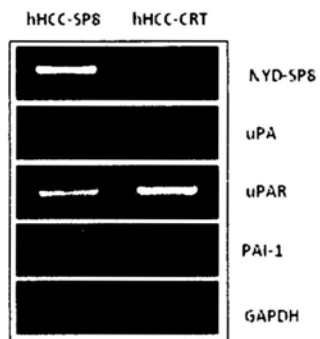


Figure 5.6 RT-PCR analysis of mRNA expression of uPA, uPAR and PAI-1 in hHCC-SP8 cell line (SP8) or its control (CRT), with GAPDH as an internal control ($n = 3$).

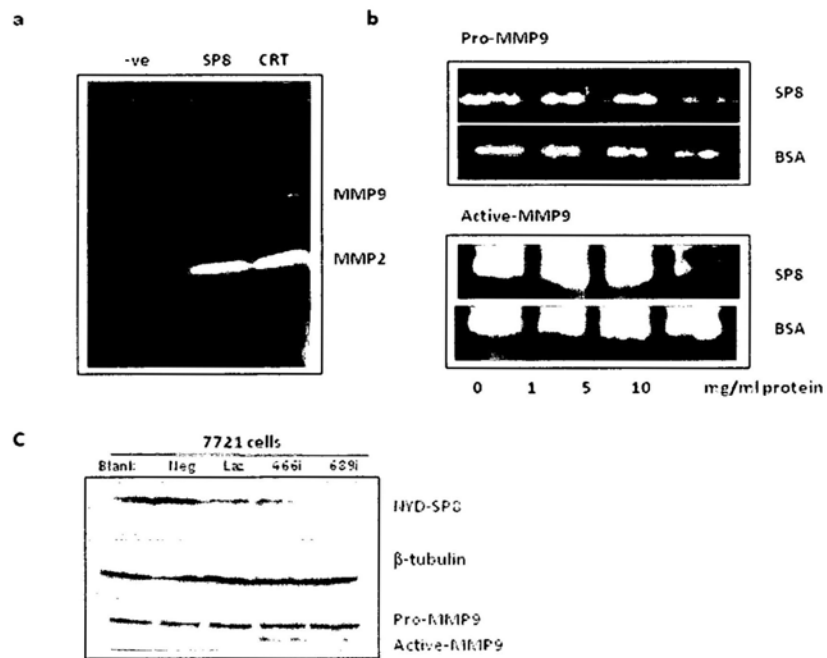


Figure 5.7 NYD-SP8 suppresses MMPs activity. (a) Representative zymographic analysis of active MMP-2 and MMP-9 release into conditioned media of hHCC-SP8 cell line (SP8) and its control (CRT) ($n = 3$). Negative control lane (-ve) was loaded with conditioned media only. (b) hHCC cells were treated with NYD-SP8 recombinant protein (SP8) for 24 hours at indicated concentrations, with corresponding concentrations of BSA as controls, and representative zymographic analyses of MMP-9 production conditioned medium are shown ($n = 6$), indicating reduced pro- and active MMP-9 with increasing NYD-SP8. (c) Western blot analysis of pro- and active MMP-9 expression in NYD-SP8 knockdown 7721 cells. Neg and Lac, knockdown control oligo; 466i and 689i, effective knockdown design.

mRNA expression of MMP-2 and MMP-9 was measured using semi-quantitative RT-PCR and the results showed that both MMP-2 and MMP-9 mRNA levels were significantly decreased in hHCC-SP8 (Figure 5.8a), indicating a suppressor role of NYD-SP8 in MMPs expression/production. Emmprin is known to be the inducer of MMP-2 and MMP-9, thus the effect of NYD-SP8 in the transcription of Emmprin was also studied. However, there were no significant changes in Emmprin mRNA expression in hHCC-SP8 cell lines, as reviewed by RT-PCR (Figure 5.8b). These data suggested that NYD-SP8 directly regulates MMP-2 and MMP-9 mRNA expression which is independent of Emmprin related signaling pathways.

5.3.3 NYD-SP8 suppress Cathepsin B activity

During cancer metastasis, other proteases, such as cathepsin B, have been demonstrated to mediate direct ECM degradation.¹⁶⁵ Cathepsin B is also suggested to be an important upstream regulator in the activation of pro-uPA, plasminogen and pro-MMPs, is thereby indirectly involved in mediating ECM degradation¹⁷³. Because NYD-SP8 appears to interfere with the uPA/uPAR system, it may also affect uPA/uPAR-related cathepsin B activity and ECM degradation. To test this, we measured the cathepsin B activity in hHCC-SP8 and hHCC-vector cells using a cathepsin B activity assay kit (Chemicon, San Diego, CA, USA). The results showed that the activity of cathepsin B in hHCC-SP8 was about 10-fold lower than that observed in the vector control (***) $p < 0.001$, Figure 5.9a). However, there was no significant alterations in mRNA levels of cathepsin B (Figure 5.9b), indicating that NYD-SP8 modified cathepsin B activation at protein level.

Taken together, we have demonstrated that NYD-SP8 is a potent suppressor of multiple ECM degrading proteases, namely uPA, MMPs and cathepsin B, indicating its potential role in suppressing cancer invasion/metastasis.

5.3.4 NYD-SP8 inhibits cancer cell invasion *in vitro*

To examine possible role of NYD-SP8 in suppressing cancer invasion *in vitro*, a matrigel invasion assay was performed. The results revealed that the invasion

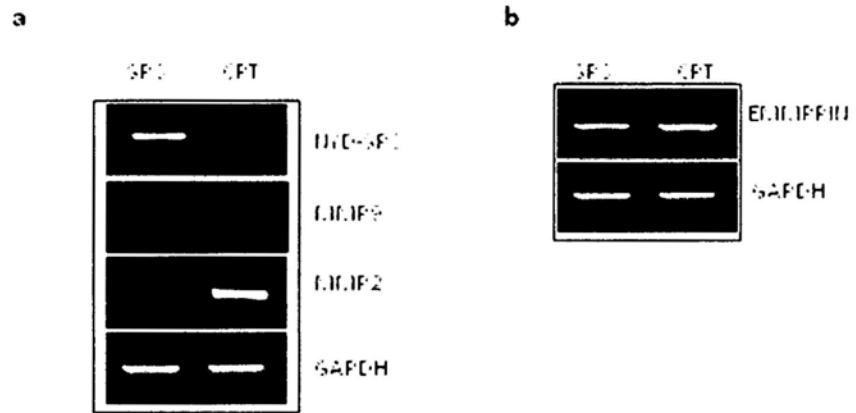


Figure 5.8 RT-PCR analysis of mRNA expression MMP-2 and MMP-9 in hHCC-SP8 cells (SP8) or its control (CRT), with GAPDH as an internal control, showing reduced MMPs in hHCC-SP8 cells.

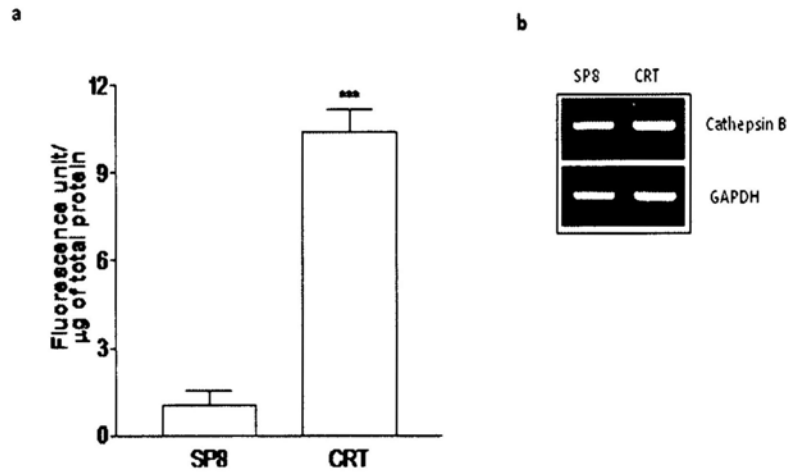


Figure 5.9 Suppressed mean cathepsin B activity (S.D., $n = 3$, *** $p < 0.001$) in hHCC-SP8 cell line (SP8) as compared to its control (CRT), with no difference in mRNA expression of cathepsin B (ii) with GAPDH as an internal control.

capacity of hHCC-SP8 cells was significantly lowered by 60% as compared to the vector control ($n = 3$, $** p < 0.01$, Figure 5.10). The capacity of NYD-SP8 in reducing cancer cell invasion could be a result from inhibition of ECM degradation by inhibiting the three classes of proteases.

5.3.5 NYD-SP8 inhibits cancer invasion and metastasis *in vivo*

To further demonstrate the inhibitory effect of NYD-SP8 on cancer invasion/metastasis *in vivo*, hHCC-SP8 cells were injected into athymic nude mice by i.p. inoculation to examine the presence of metastasized cancer cells in various parts of the body. 5×10^5 cells of hHCC, hHCC-vector and hHCC-SP8 were separately injected into three groups of nude mice intra-peritoneally (i.p.) ($n = 12/\text{group}$). All mice receiving hHCC or hHCC-vector inoculation formed tumors (12 out of 12) 30 days after, whereas only 67% (8 out of 12) of mice inoculated with hHCC-SP8 grew tumors (Figure 5.11).

To examine the effect of NYD-SP8 on tumor invasion, the lungs, hearts and lymph nodes were excised from the nude mice receiving hHCC-SP8 and hHCC-vector i.p. and semi-quantitative RT-PCR was performed to examine the relative expression of human GAPDH, as a metastatic marker, in the organ tissues of the nude mice. The results showed that hHCC-SP8 treated mice had 50% fewer lung micro-metastasis than that of the vector control (Figure 5.12b). No significant difference in expression of human GAPDH was detected in the heart between hHCC-SP8 and hHCC-vector (Figure 5.12a), which could also serve as a control excluding possible contamination of blood vessel perfusion in the observed lung result, suggesting that the presence of human GAPDH in the lung was due to migration and lung extravasations of the human cancer cells. These results have indicated an inhibitory effect of NYD-SP8 on cancer invasion /metastasis *in vivo*.

To further demonstrate the inhibitory effect of NYD-SP8 on cancer metastasis, 2×10^6 of hHCC-SP8 or hHCC-vector cells were injected intravenously (i.v.) into the lateral tail vein of nude mice to produce experimental lung metastasis, bypassing tumor formation at the primary sites. Before i.v. injection, cancer cells (hHCC-SP8 or

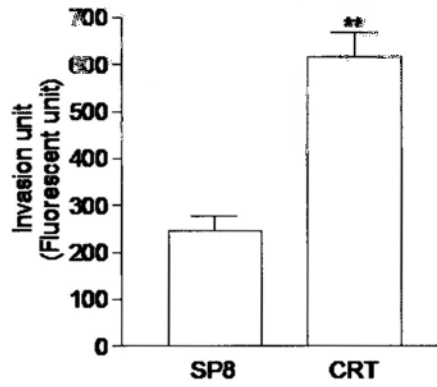


Figure 5.10 Suppression of cancer invasion and metastasis *in vitro*. Summary of matrigel invasion assay showing reduced invasion of hHCC-SP8 cell line (SP8) as compared to control (CRT) after 48 hours of incubation (S.E.M., $n = 3$, $**p < 0.01$).

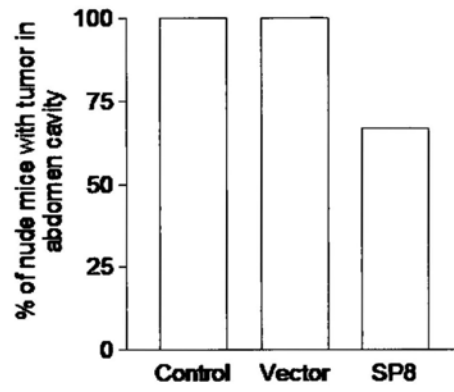


Figure 5.11 Bar chart showing the percentage of nude mice forming tumors 30 days after ip inoculation. All mice receiving hHCC or hHCC-vector inoculation formed tumors (12 out of 12) while only 67% (8 out of 12) of mice inoculated with hHCC-SP8 grew tumors.

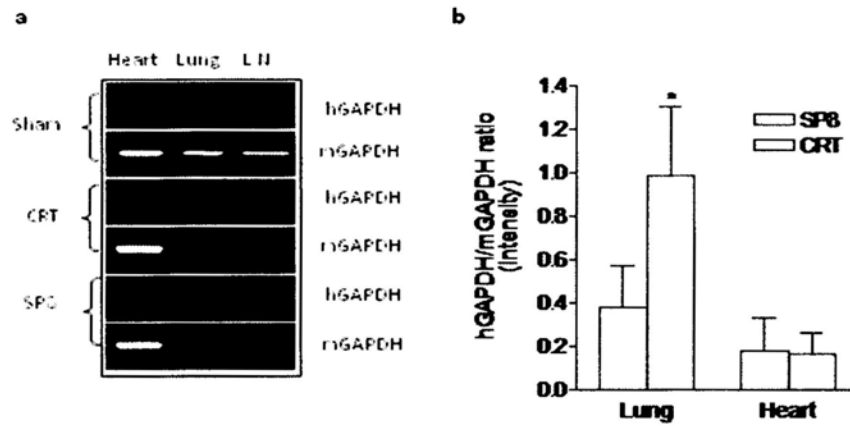


Figure 5.12 NYD-SP8 suppresses experimental metastasis *in vivo*. (a) RT-PCR analysis of mRNA expression of human GAPDH (representing the amount of micro-metastasized human cancer cells) in the heart, lung and lymph node (L.N) of mice 60 days after i.p inoculation of hHCC-SP8 cell line (SP8) or its control (CRT), with mouse GAPDH as an internal control. (b) Corresponding quantitative levels of the mean ratio of human GAPDH/mouse GAPDH mRNA in the lungs and hearts as shown in (a), showing significantly higher levels in the lungs of the control group than that of NYD-SP8 group indicating suppressed metastasis by NYD-SP8 (S.D., $n = 3$, $*p < 0.05$).

hHCC-vector) were either stained with the red fluorescent dye CMRA or green fluorescent dye CMFDA and mixed at a 1:1 ratio (Figure 5.13a).

Figure 5.13b and Figure 5.13c shows two groups of high magnification fluorescence micrographs of labeled cancer cells in the lungs detected 6 hours after injection, with consistently fewer hHCC-SP8 detected as compared to the hHCC-vector, and regardless of the fluorescent dye used. The total number of cells at 10 minutes and 6 hours after injection was also counted, showing similar cell counts in both cases, red or green, at 6 hours but no fluorescent cells detected in the lungs at 10 minutes, consistent with insufficient metastasis within this short period of time, which could also serve as a negative control.

Taken together, the decrease in cancer invasion and metastasis *in vitro* and *in vivo* in NYD-SP8 expressing cells is consistent with the finding that NYD-SP8 is a potent suppressor of multiple ECM-degrading proteases known to be involved in cancer metastasis.

5.4 Discussion

In this chapter, NYD-SP8 demonstrated a novel proteases inhibiting function. NYD-SP8 suppresses both tumor cell invasion and metastasis *in vitro* and *in vivo* by interacting with and inhibiting multi-classes of tumor associated proteases. Proteolysis on tumor cell surface enhances ECM not only regulated by tumor associated proteases but also anti-proteases to prevent unwarranted digestion of the ECM, which cause a loss of cell attachment³⁵ and leading to anoikis. It would be interesting to study the effect of NYD-SP8 in those anti-proteases.

NYD-SP8 directly binds and inhibits uPA activity. While NYD-SP8 was not found to bind MMP-2, NYD-SP8 suppresses active MMP-2 and MMP-9 activities. It is generally accepted that uPA system is involved in regulating pro-MMP-2 and pro-MMP-9 activation^{4,225} Concerning the inhibition of both uPA activity and MMP-9 activity by NYD-SP8, the present data support the implication of uPA system

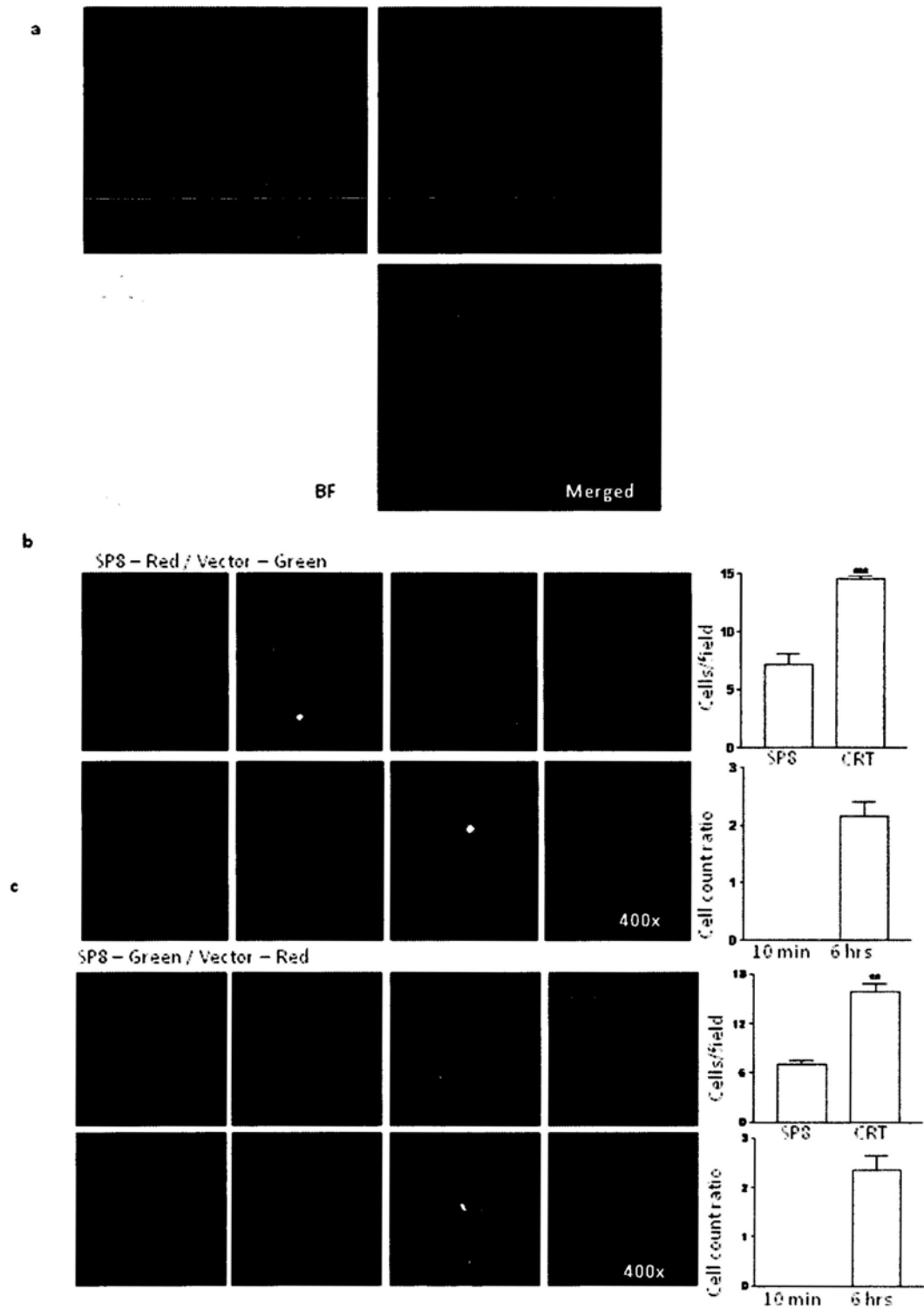


Figure 5.13 Suppressed lung extravasations and metastasis of NYD-SP8-overexpressed cancer cells after tail vein injection.(a) Fluorescence microscopy of CMRA-labelled hHCC-SP8 cell line (SP8-Red) mixed in 1:1 ratio with CMFDA-labelled control hHCC cells (Vector-Green) before tail vein injection. The ratios of cell count ratio were measured by counting in a fluorescence microscope. (b) Confocal

fluorescence microscopy of randomly selected fields from frozen sections of mouse lungs at 6 hours after tail vein injection of 1:1 mixed cells with NYD-SP8 (red) and control (green) cells with tumour cell count ratio (green/red) and number of cells per 4 random microscope fields in lung at 10 minutes and 6 hours after tail vein injection. (c) Reversed labelling in (b). (S.E.M., $n = 3$ for 10 minutes group, $n = 6$ for 6 hours group, $***p < 0.001$).

in MMPs processing. However, whether or not expression of NYD-SP8 directly suppresses uPA-mediated MMPs activation remains unclear. It is because overexpression of NYD-SP8 led to a dramatic decrease in mRNA transcripts of both MMP-2 and MMP-9, at least, *in vitro*. Lowered active MMP-2 and MMP-9 production as detected in gelatin zymography assay could also be a result of lowered mRNA transcripts. Additionally, NYD-SP8 has no effects on Emmprin in both transcriptional and translational level, indicating that NYD-SP8 may directly regulate MMP-2 and MMP-9 production or indirectly by other signaling mechanisms. Further investigation of NYD-SP8 and its effects in MMPs production/activation using uPA-independent system could provide hints in illustrating the mechanisms behind MMPs inhibition.

Cathepsin B is also suggested to be an important upstream regulator in the activation of pro-uPA, plasminogen and pro-MMPs, thereby indirectly involved in mediating ECM degradation.¹⁷³ In this study, NYD-SP8 was shown to lower cathepsin B activity and suppresses uPA activity and MMP-9 activity. An interesting question is that if NYD-SP8 exerts its suppressing effect in one sequential order or in parallel levels. Also, further investigation to understand the specific contribution of NYD-SP8 on individual proteases provides details mechanisms in regulating ECM degradation.

Although the detailed mechanisms by which NYD-SP8 suppresses the activities of the three major classes of ECM-degrading proteases require further studies, the presently demonstrated potent inhibitory effects of NYD-SP8 on tumor associated proteases as well as cancer invasion/metastasis *in vitro* and *in vivo* indicate its therapeutic potentials for suppressing cancer metastasis.

uPAR protein is a heavily glycosylated extracellular proteins that is covalently linked to the outer layer cell membrane via a GPI-anchored and does not possess a transmembrane domain.^{83,126} The GPI-moiety allows high flexibility of uPAR in contact with cell surface receptors and in turn regulates various intracellular signaling. Consequently, it is interesting to know if NYD-SP8 also interferes with other uPAR-related protein-protein interactions and its effect on the downstream

signaling pathways.

According to Chapter 3, NYD-SP8 is suggested to be a CT antigen and it has unknown functions in cancer development. The demonstrated protease-inhibiting and metastasis-suppressing role of NYD-SP8 in this chapter as well as its expression in cancers but not normal tissues except the testis suggest that it could be a host defence mechanism against cancer metastasis. Interestingly, we found that the mRNA expression level of NYD-SP8 in a couple of less invasive hepatocellular cancer cell lines was much higher than its negligible expression in the more invasive hHCC cell line (Figure 5.6). This raises an interesting notion that the expression profile of NYD-SP8 may vary with different stages of cancer development and be correlated with different metastatic potentials. Further detailed studies on NYD-SP8 expression profiles in different cancer tissues and the elucidation of the molecular mechanism regulating its expression may provide new insight into cancer development as well as new diagnostic and treatment strategies for cancer metastasis.

Chapter 6 Involvement of NYD-SP8 in Epithelial and Mesenchymal Transition

6.1. Introduction

In Chapters 4 and 5, NYD-SP8 has been demonstrated to have a very intriguing behavior in tumor progression. On the one hand, NYD-SP8 promotes cell growth and protects cells from apoptosis. On the other hand, NYD-SP8 suppresses proteases activity and in turn inhibits cancer invasion and metastasis. The contrasting functions of NYD-SP8 in early and late cancer development bring out an important question: what happens to NYD-SP8 during the transitional stage of tumor progression from early tumor development to advanced tumor development? And what is the cause and biological significance of this change? In addition, preliminary data in our laboratory suggests that NYD-SP8 may be associated with stage-specific expression during tumor progression. Therefore, it would be interesting to know the molecular events of NYD-SP8 during the transitional stage of tumor progression, which is known as the epithelial-mesenchymal transitions (EMTs).

6.1.1 Epithelial-mesenchymal transitions

EMTs refers to the morphological and molecular changes that epithelial cells undergo as they lose differentiated phenotypes, such as strong cell-cell adhesion and apical-basal polarity, and gain mesenchymal characteristics such as loss of junctional and intercellular adhesion proteins, induction of cytoskeletal reorganization, gain of mesenchymal markers, increase of cell motility, invasion and resistance to apoptosis¹⁵² (Figure 6.1). EMTs is an important biological event during embryonic development, tissue remodeling, restitution and wound healing.¹⁷⁰ However, increasing evidence has suggested that EMTs are one of the key regulations in cancer invasion and metastatic dissemination.^{14,70,195} De-differentiation, loss of adhesive constraints, cell motility and invasion are

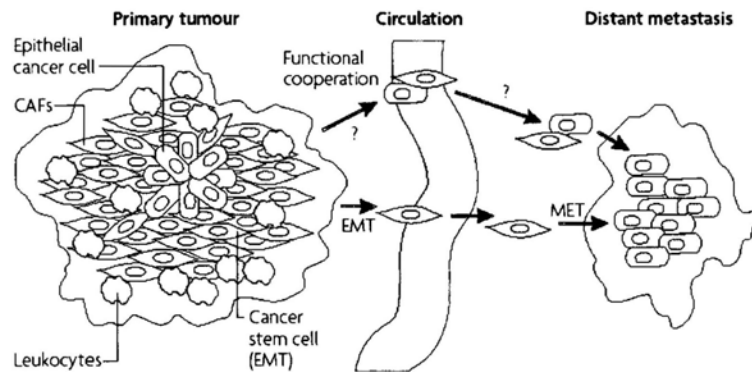


Figure 6.1 Transitions between epithelial and mesenchymal states during carcinoma progression. Interactions with stromal cells induce EMTs and promote growth and survival in cancer cells with mesenchymal phenotype, which are more likely to metastasize and more frequently detected in the circulation and in micro-metastasis. However, macroscopic distant metastasis is more frequently composed of more differentiated epithelial cancer cells. This can be explained by the reversal of EMT through MET after micrometastasis grow, due to local selective pressure for the outgrowth of cancer cells with more epithelial feature or to the absence of EMT-inducing signals at sites of dissemination (Adapted from ¹⁵²).

all aggressive phenotypes of tumor cells. Consequently, novel molecules or proteins that inhibit EMTs may become an attractive strategy for anti-cancer therapy.^{8,85,196,218} There is also significant interest in identifying the underlying mechanisms that contribute to this complex processes.

6.1.2 Induction and signaling mechanisms of EMTs

Although the exact mechanisms of EMTs are still unclear, multiple extracellular signals such as growth factors, ECM components and even MMPs have been implicated in triggering and/or modulating EMTs.^{17,70,118,158,194,195,199} One of the best characterized EMTs inducers is the Transforming growth factor β (TGF β) ligand^{13,55,65,110,136,153}. TGF β is a prototype cytokine that induces EMTs *in vitro* and *in vivo* frequently in conjunction with other cytokines and signaling pathways.¹³⁵ Recent reports have suggested that the molecular interactions between TGF β , Notch, Wnt and receptor tyrosine kinase signaling pathways modulate EMTs.¹⁹³ Other signaling pathways such as Ras, MAPK, PIP3K, Rho, Rac and Src are involved in EMTs (Figure 6.2).^{17,70,195} EMTs can also be modulated by proteolytic degradation of the ECM and the basement membrane.¹⁵⁵

6.1.3 *In vitro* model of EMTs - The LIM1863 cell lines model

The complexity and multiplicity of molecular mechanisms in different tumors cause significant challenges for studying EMTs *in vivo*.¹⁹⁴ For that reason, several cell line models were established in the past 20 years to allow *in vitro* study of EMTs. The best described model is the colon carcinoma LIM1863 cell lines. The LIM1863 cell line was established by Whitehead's group in 1987.²¹³ The LIM1863 cell line grows as three-dimensional free-floating multicellular spheres. The well polarized and morphologically differentiated columnar and goblet cells are arranged around a central lumen²¹³ while the less differentiated cells are lined around the periphery of spheres (Figure 6.3a). Upon TGF β stimulation or TGF β /TNF α co-stimulation,⁷ the 3D LIM1863 organoids undergo EMTs and trans-differentiate into adherent monolayer cells (Figure 6.3b). This observable morphological change enables

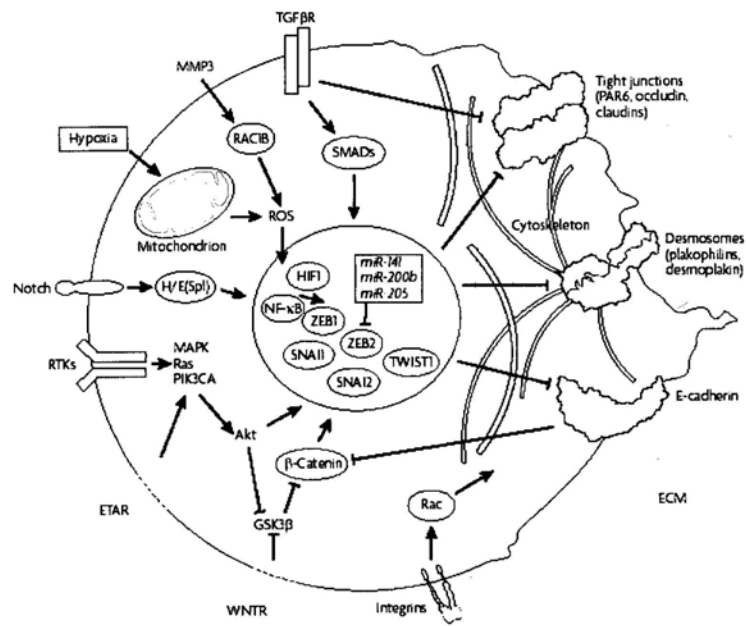


Figure 6.2 Signaling networks regulating epithelial-mesenchymal transitions (EMTs). The receptor tyrosine kinases (RTKs), transforming growth factor- β (TGF β), Notch, Integrins, Wnt, hypoxia and matrix metalloproteinases (MMPs) induce EMT (Adapted from ¹⁵²).

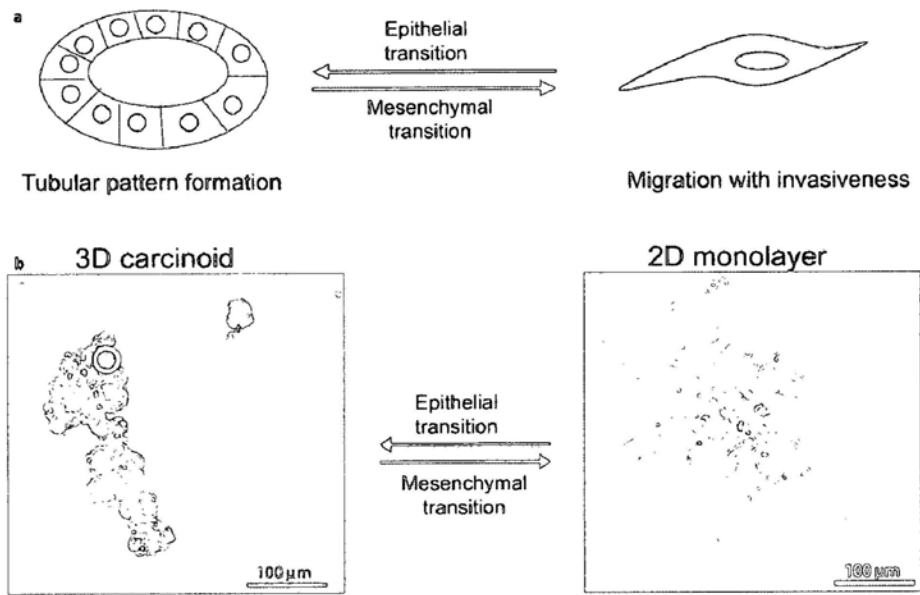


Figure 6.3 *In vitro* model of EMT using LIM1863 cell lines (Adapted from ⁷²).

real-time monitoring of EMTs *in vitro*. In addition, the LIM1863 cells constantly express a high degree of morphological differentiation. This consistent maturation of cells suggests that these cells are very similar to the cells of normal intestinal crypts and is an ideal model system to study EMTs *in vitro*.²¹⁴

Apart from morphological changes, there are molecular hallmarks of EMTs which detection of EMTs at the transcriptional level. They include (1) downregulation/translocation of E-Cadherin which decreases cell-cell contact and adherences junctions, (2) up-regulation of matrix-degrading proteases and mesenchymal-related proteins such as vimentin and N-cadherin and (3) reorganization of actin cytoskeleton mediated by Rho small GTPases to facilitate cell motility^{194,196}.

6.1.4 Cell matrix interactions in EMTs

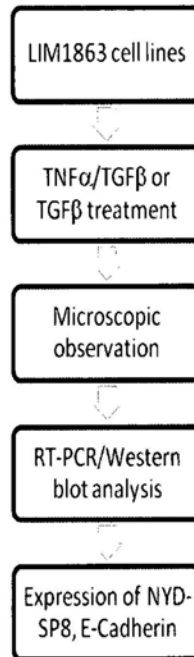
Cancer cells undergo EMTs to gain cell motility for migration, invasion and metastasis. An enhanced cell-matrix interaction is critical in driving tumor cells to penetrate through the basement membrane and carry on proteolysis. Interestingly, the maximum cell motility takes place at moderate levels of adhesiveness. Too low a level of adhesiveness cannot generate sufficient force to direct cell migration while too high a level of adhesiveness cannot break the cell-matrix contact and are therefore leaves the cells immobile. The ability to move depends on a delicate relationship between cell-cell and cell-matrix adhesion through a family of cell surface receptors such as Integrins. Several Integrins have been associated with EMTs and have been reported to increase cell-matrix interactions by forming large multi-protein clusters that link the ECM to the actin network of tumor cells^{6,124,185}. Among the Integrin family members, the $\beta 1$ integrin subfamily has the largest number of members involved in cell to matrix interaction. These members include $\alpha_2\beta_1$, which is a type IV collagen and type I collagen receptor, $\alpha_3\beta_1$, which is a laminin receptor, and $\alpha_5\beta_1$, which is a fibronectin receptor. Cell-matrix interaction is studied using the cell adhesion assay, which is performed on cellular coated supports that mimic the ECM such as collagen, laminin and fibronectin.

6.1.5 Objectives

The aim of this study is to (1) to set up an *in vitro* EMT model in our laboratory using Lim1863 cell line; (2) to study the expression profile of NYD-SP8 during EMTs; and (3) to investigate the potential involvement/function of NYD-SP8 in EMT.

6.2 Experimental plan

Detailed materials and methods are described in Chapter 2. A schematic diagram of experimental plan is shown below.



6.3 Results

6.3.1 Induction of EMTs by TGF β in LIM1863 organoids

In the first set of experiments, LIM1863 cells were cultured in 2ng/mL TGF β for 8 days. The morphological changes of LIM1863 cell lines undergoing EMTs were captured at different time points. Microscopic pictures showed that LIM1863 cells trans-differentiated from free-floating spheres to adherent monolayer cells, indicating that EMTs had occurred (Figure 6.4a). However, in contrast to Bates and Mercurio's 2003 findings,⁷ individual migrating cells were not observed and cell-cell contact remained integral²⁰⁶ (Figure 6.4a). The monolayer LIM1863 cells were then harvested for Western blot analysis.

The expression level of E-Cadherin and NYD-SP8 was tested in LIM1863 cells at different time points after TGF β treatment. Western blot analysis showed that the endogenous expression of NYD-SP8 was significantly decreased 8 days after TGF β treatment (Figure 6.4b), indicating that NYD-SP8 may play a role during TGF β -induced EMTs. To investigate the mechanism of NYD-SP8 protein reduction during EMTs and to study the progress of EMTs in LIM1863 cell lines, cells cultured in 2ng/mL TGF β and total RNA and protein were collected at different time points. The mRNA and protein expression of E-Cadherin and NYD-SP8 were assessed. RT-PCR results showed that the endogenous expression of NYD-SP8 was transcriptionally silenced from Day 3 onwards, and mRNA expression level remained unchanged until Day 6 (Figure 6.4c). Western blot analysis showed a delayed onset of reduction of NYD-SP8 protein at Day 6, which could be explained by the slow turnover rate of membrane proteins (Figure 6.4c). However, in contrast to Bates and Mercurio's 2003 findings, the mRNA and protein expression level of E-Cadherin did not have significant changes from Day 0 to Day 6 after TGF β treatment. This could be explained by (1) this cell line model mimics the very early cell dispersion phase of EMTs¹⁹⁶ and; (2) this version of LIM cell lines is programmed to preserve cell-cell adhesion and cell-matrix contact to avoid apoptosis.¹⁹⁶

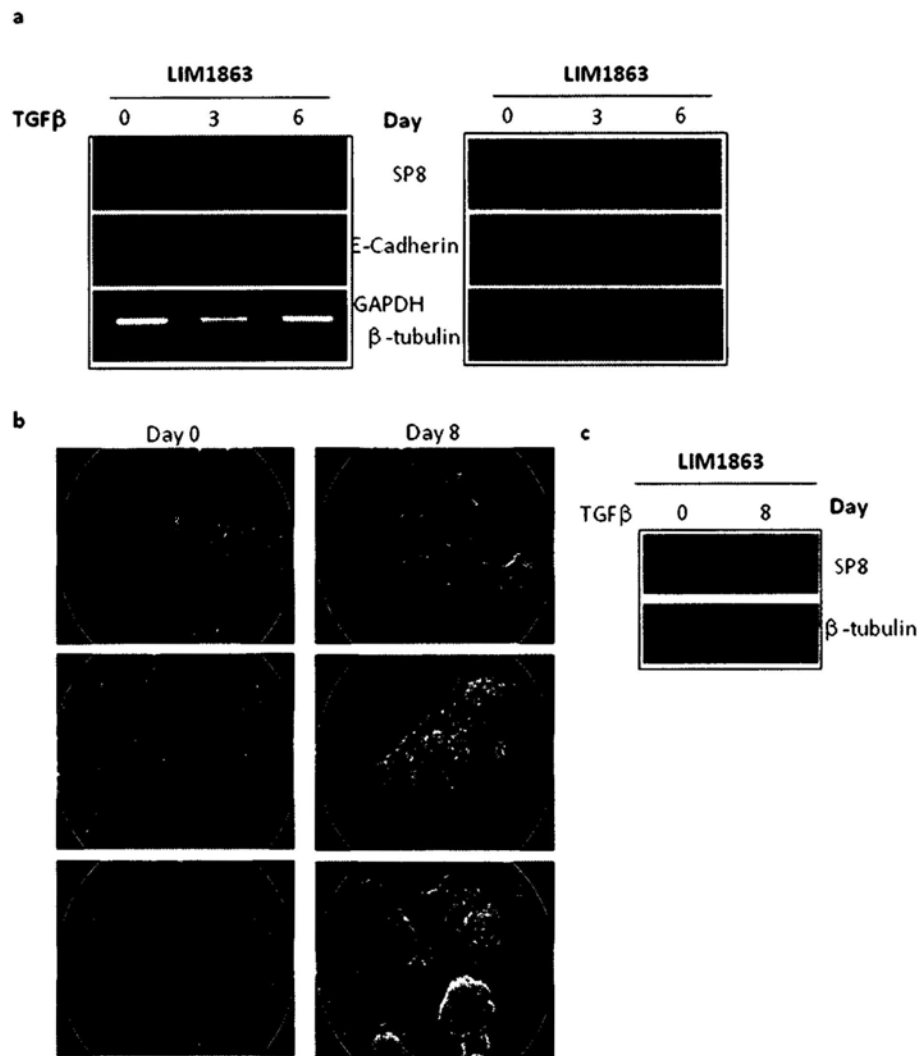


Figure 6.4 LIM1863 cells undergo EMT after addition of TGFβ (2ng/mL). (a) RT-PCR and Western blot analysis showing gradually decrease in NYD-SP8 and E-Cadherin expression from Day 3 to Day 6 after TGFβ treatment. Equal loading control was confirmed by GAPDH (for RT-PCR) and β-tubulin (for Western blot analysis). (b) Morphological changes were documented by light microscopy using phase contrast optics at 0 and 8d after TGFβ treatment. (c) Western blot analysis showing complete loss of NYD-SP8 after addition of TGFβ for 8 day. Equal protein loading was confirmed by β-tubulin.

6.3.2 Accelerated EMTs under TNF α /TGF β treatment in LIM1863 organoids

In the second set of experiments, LIM1863 cells were cultured in TGF β /TNF α (2ng/mL and 10ng/mL, respectively) for 24 hours. Results showed that the induced EMTs were accelerated as described in Bates and Mercurio's 2003 findings (Figure 6.5a). However, the transcriptional changes of E-Cadherin increased, but not decreased, during EMTs. The highest E-Cadherin expression was observed 12 hours after TGF β /TNF α co-stimulations (Figure 6.5b). But still, the expression of NYD-SP8 decreased 24 hours after TGF β /TNF α co-stimulation (Figure 6.5b).

Taken together, the results indicate that NYD-SP8 plays a role during TGF β and also TGF β /TNF α induced EMTs. In addition, the transcriptional silencing event of NYD-SP8 is much earlier than the onset of E-Cadherin silencing during TGF β induced EMTs in LIM1863 cells.

6.3.3 NYD-SP8 affects cell-matrix interaction

An enhanced cell-matrix interaction is critical in directing tumor cells to migrate in EMTs. Moreover, tumor cells activate anti-apoptotic mechanisms in order to survive and grow up in the adverse ECM microenvironment. Recent literature reviews have suggested that enhanced cell-matrix interactions lead to the activation of pro-survival signaling and thus inhibition of apoptosis. As NYD-SP8 confers pro-survival functions as demonstrated in Chapter 4, we would like to investigate the cell-matrix interactions in NYD-SP8 overexpressing cells using *in vitro* cell attachment assays. The results demonstrated that NYD-SP8 significantly enhances the adhesion ability of hHCC cells towards Laminin and Fibronectin (Figure 6.6), indicating that NYD-SP8 may promote cell-matrix interactions. Since the $\alpha_3\beta_1$ and $\alpha_5\beta_1$ integrins are the major receptors responsible for the laminin and fibronectin binding, and both of them contain β_1 integrin subunits, it is possible that NYD-SP8 may be involved in regulating β_1 integrin and thereby affecting the cell-matrix interactions and anti-apoptotic functions of tumor cells in cancer development, especially in the EMT process.

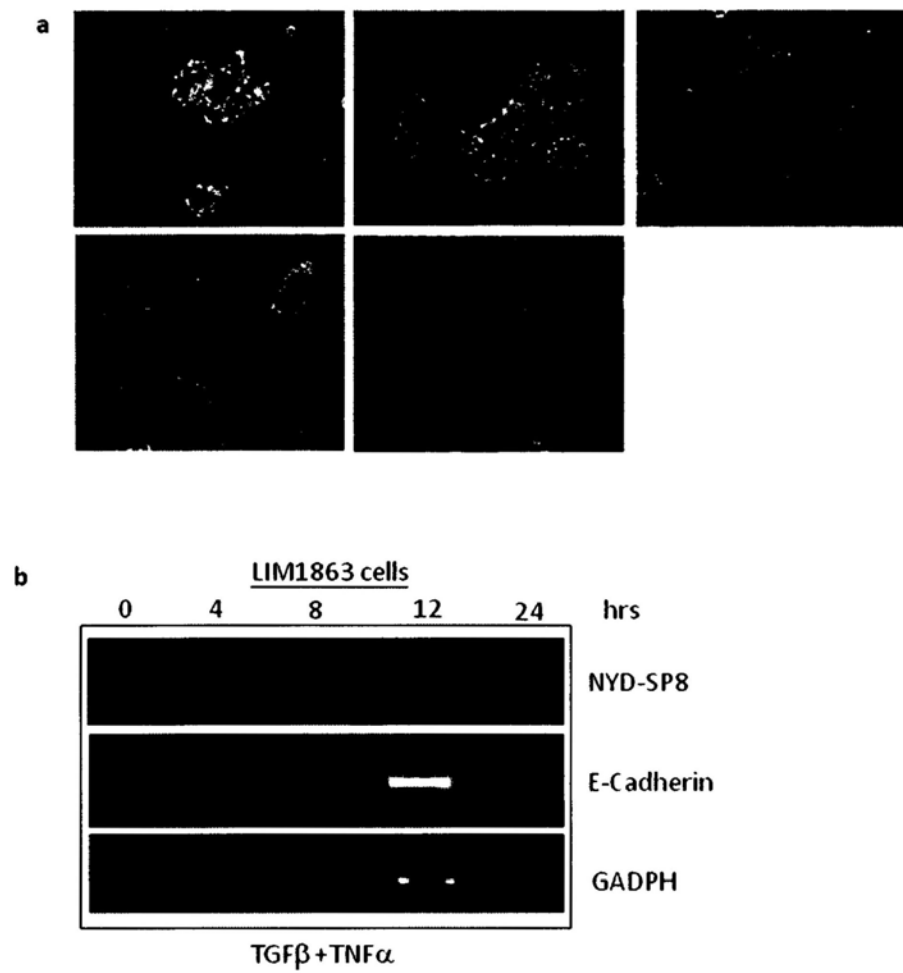


Figure 6.5 LIM1863 cells undergo EMT after addition of TGFβ/TNFα co-stimulation. (a) Morphological changes were documented by light microscopy using phase contrast optics from 0 to 24 hours after TGFβ /TNFα co-stimulation. (b) RT-PCR showing gradually decrease in NYD-SP8 and changes in E-Cadherin expression from 0 to 24 hours after TGFβ /TNFα co-stimulation. Loading control was confirmed by GAPDH.

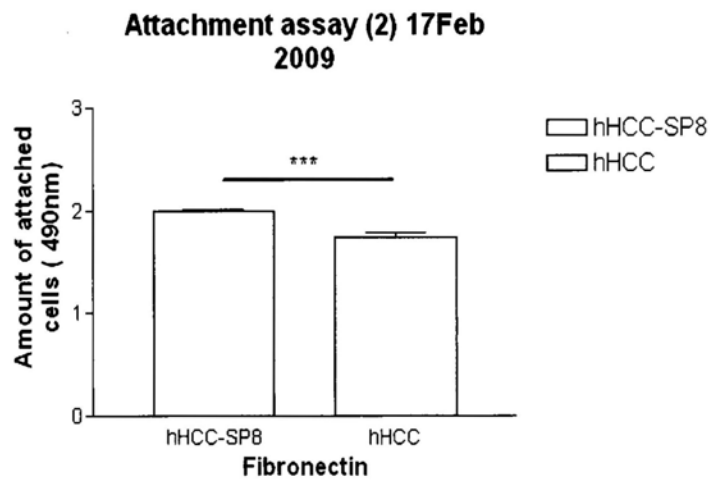
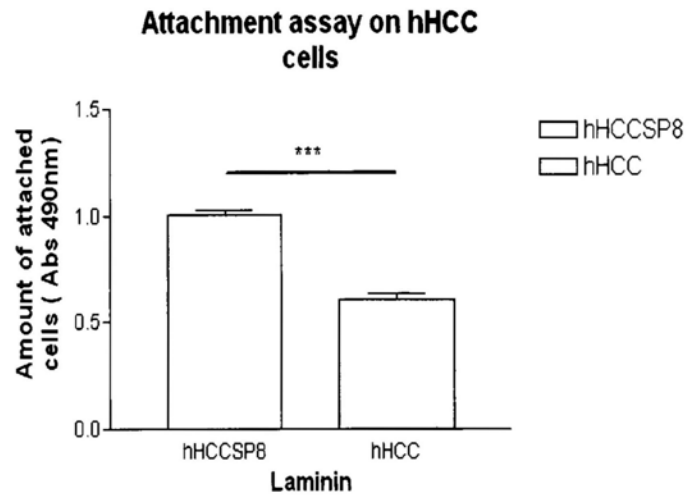


Figure 6.6 Attachment assay of hHCC cells in Laminin and Fibronectin coated plate for 2 hours.

6.4 Discussion

6.4.1 Loss of NYD-SP8 may be a pre-requisite for EMTs

In this chapter, the results have demonstrated that NYD-SP8 is silenced when LIM1863 cells are undergoing TGF β -induced EMTs. Since the results presented in Chapter 5 suggest that NYD-SP8 inhibits cancer invasion and metastasis by suppressing multiple protease functions, expression of NYD-SP8 may keep cancer cells at the primary region and promotes tumor growth as described in Chapter 4. Therefore, the loss of NYD-SP8 may be a pre-requisite for EMTs, which is a critical stage of cancer development in which cancer cells gain their motility to migrate.

In fact, increasing evidence suggests that EMTs are central controllers of cellular plasticity in cancer cells and have important role in metastasis progression as well as therapeutic resistance. However, it remains unclear which signaling pathways are involved in controlling the process. The present findings, together with those presented in previous chapters, suggest an important molecular mechanism by NYD-SP8 governing EMTs and the cancer development. While NYD-SP8 was silenced in EMTs, overexpression of NYD-SP8 affects cell-matrix interactions in hHCC cells. It is interesting to know if knockdown of NYD-SP8 is able to induce EMTs and if overexpression of NYD-SP8 could block EMTs.

6.4.2 Overexpression of NYD-SP8 results in immobilization of cancer cells

Interestingly, CT antigens have been suggested to inhibit trans-differentiation process.¹⁷⁷ The present results show that NYD-SP8 enhances cell-matrix interactions by increasing binding affinity to various ECM proteins. This may result in the immobilization of cancer cells at the local basement membrane and inhibition of cancer cell migration, invasion and metastasis. Integrin clustering and relocalization are the major mechanisms that can alter ECM binding affinity. It would be interesting to know if NYD-SP8 affects Integrin expression and localization.

6.4.3 NYD-SP8 may serve as a new molecular marker of EMT

In consistent with Bates and Mercurio's 2003 finding, the RT-PCR and Western blot

analysis results in our studies showed that expression of E-Cadherin was not decreased during EMT process. In many instances, loss of E-Cadherin is considered a molecular hallmark of EMTs that initiates a series of signaling events and major cytoskeletal reorganization. However, the loss of E-Cadherin should not be considered the only crucial event in EMTs, since knockdown of E-Cadherin expression does not induce a complete EMTs and E-Cadherin overexpression does not restore the epithelial phenotype in spindle carcinoma cells and does not reverse induced EMTs processes.¹³⁴ Therefore, other molecular markers such as the Twist and the Snails family^{42,137,217} have been proposed to be required to monitor the status of EMTs. The present results also indicate that NYD-SP8 could be a potential molecular marker of EMTs. Further investigation on the upstream regulation of NYD-SP8 may provide hints on molecular mechanisms determining cell fate in cancer development.

In conclusion, these data have demonstrated that NYD-SP8 affects cell-matrix interactions, and thus may affect EMTs in cancer progression. The results also suggest that NYD-SP8 may serve as a novel stage-specific biomarker for EMTs.

Chapter 7 Final Discussion and Conclusion

In this study, the structural characteristics and biological functions of NYD-SP8 in cancer development were investigated. NYD-SP8 exhibits a stage-dependent expression in tumor tissues, and more importantly, NYD-SP8 has stage-specific biological functions during cancer development.

7.1 Stage-specific expression of NYD-SP8

Expression of NYD-SP8 is restricted in human and mouse germ lines in normal tissues. However, expression of NYD-SP8 is re-activated in multiple cancer tissues. Our results have shown that the expression of NYD-SP8 is stronger in more differentiated cell lines such as the LIM1863 cells and less invasive cancer cell lines such as the NP1, NP2 and SMMC-7721 cell lines. These data indicate that the expression of NYD-SP8 may be correlated with both the differentiation status and invasiveness of tumor cells. Our results have also shown that the expression of NYD-SP8 is decreased when tumor cells undergo EMTs and gain cell motility to migrate. These data indicate that the expression of NYD-SP8 may be stage-specific which may be associated with unique functions at different stages of cancer development.

7.2 Stage-specific biological functions of NYD-SP8 in cancer development

In this study, the biological functions of NYD-SP8 in different stages of cancer development have been investigated. On the one hand, NYD-SP8 promotes cell proliferation and tumor growth by regulating programmed cell death possibly via the p53-dependent NFkB related signaling pathways as demonstrated in Chapter 4. On the other hand, NYD-SP8 inhibits cell invasion and metastasis by regulating major tumor associated proteases as described in Chapter 5. NYD-SP8 may also be involved in regulating the EMTs as described in Chapter 6. These unique but contrasting functions of NYD-SP8 have suggested that NYD-SP8 is a key controller in fine-tuning different stages of tumor progression.

When normal cells become transformed cells, expression of NYD-SP8 promotes

cell proliferation and tumor growth at the primary site of tumor development. Increased expression of NYD-SP8 protects tumor cells against apoptosis. The presence of NYD-SP8 also prevents transformed cells from migration and invasion, conferring the dormancy of tumor growth when nutrient supply in tumor microenvironment is limited.

However, the adverse tumor microenvironment such as limited availability of nutrients and oxygen, basement membrane and ECM barriers, and attacked by the immune system select for an aggressive phenotype of tumor cells. Tumor cells respond to these external pressures by enhancing their metastatic potential. Most of the epithelial tumors undergo EMTs to diminish their intercellular adhesiveness and increase their cell motility and migration ability as they progress towards malignancy.²⁴ The re-activated expression of NYD-SP8 in tumor cells may be silenced again at this transitional period as their protease inhibiting function work against the metastatic phenotype.

From the present results and hypothesis, NYD-SP8 is predicted to be expressed again when cancer cells become successfully metastasized and start growing in the new organ. Further investigation in the functions of NYD-SP8 in METs (mesenchymal-epithelial transitions) process and more advanced stages of cancer development may answer the question.

7.3 Relationship between NYD-SP8 and uPAR

The reason why NYD-SP8 has such an interesting stage-specific expression profile and stage-dependent biological functions in tumor biology remains unknown. However, some hints may be obtained from the structural homology and functional relationship between NYD-SP8 and uPAR. The uPAR expression level is correlated with different stages of cancer progression. In normal cells, uPAR expression is very low or even undetectable. In the early stages of tumor development, uPAR expression levels are relatively low. NYD-SP8 become dominant in promoting tumor growth and cell survival as demonstrated in Chapter 4. While the uPAR expression level increases in more advanced stage of tumor, NYD-SP8 expression is silenced as

described in Chapter 6 to prevent antagonistic function against uPAR and thereby favor cancer invasion and metastasis, as demonstrated in Chapter 5. It is still unknown the intrinsic relationship between NYD-SP8 and uPAR. But definitely understanding their relationship provides important benefits to tumor biology.

7.4 NYD-SP8 and its implications

7.4.1 NYD-SP8 may serve as a potential biomarker for early onset of tumor development and EMTs.

Our results showed that NYD-SP8 is silenced in normal tissues except germ lines but re-activated in various cancer tissues. The present findings suggest that NYD-SP8 may be a potential biomarker for diagnosis of early tumor development. More importantly, NYD-SP8 is a soluble protein. NYD-SP8 could be shed off by PI-PLC and detected in the serum or circulating system of cancer patients. Compared to those tumor antigens and biomarkers which required pathological studies on biopsy, NYD-SP8 it may be a convenient biomarker for detecting the early onset of tumor development in the circulation system of cancer patients. Further investigation of the correlations between the expression levels of NYD-SP8 in the serum of cancer patients and survival rate of cancer patients may provide better understanding on the use of NYD-SP8 as circulating tumor biomarker. Secondly, NYD-SP8 is silenced in EMTs. While there are no promising molecular markers for detecting EMTs *in vivo* at this moment, NYD-SP8 may serve as a potential biomarkers for early onset of EMTs in the circulating system of patients.

7.4.2 NYD-SP8 may serve as a potential immunotherapeutic target.

Our studies have demonstrated the potent inhibitory effects of NYD-SP8 on the tumor associated proteases and cancer invasion/metastasis. Although the detailed mechanisms by which NYD-SP8 suppresses the activities of the three major classes of ECM-degrading proteases require further studies, the present finding suggests its therapeutic potentials for suppressing cancer metastasis and immunogenic anti-cancer therapy.

7.5 Future studies

The present findings have demonstrated on the biological functions of NYD-SP8 in human cancer development. However, more in-depth investigations on the underlying mechanisms leading to the observed phenotypes are required. There are several important questions.

Firstly, how is NYD-SP8 re-activated in multiple cancer tissues? Our data have shown that NYD-SP8 responds to EMTs much faster than E-Cadherin *in vitro*. It is possible that NYD-SP8 may be upstream of E-Cadherin and communicate and crosstalk with those well-known EMTs initiators such as Twist and Snails. Further investigation of the relationships between the well-known EMTs signaling pathway such as TGF β , Notch, Wnt and NYD-SP8 may provide some hints on the initiation of NYD-SP8 expression in cancer development. Besides, NYD-SP8 is re-activated in early tumor development. It would be interesting to know if NYD-SP8 is involved more early steps of tumor formation, such as immortalization and transformation.

Secondly, how does NYD-SP8 trigger its downstream signaling pathway in cancer cells? The results in Chapter 4 suggest that NYD-SP8 may depend on the interaction with uPAR or other trans-membrane receptors in order to trigger the downstream signaling pathways. However, it is still possible NYD-SP8 may communicate with the cytosolic proteins by other trafficking mechanisms such as endocytosis and internalization of NYD-SP8. It would be interesting to study the molecular mechanisms leading to activation of NYD-SP8-related signaling pathways.

7.6 Conclusion

To conclude, a novel and biologically important CT gene, NYD-SP8, has been introduced. The present findings on NYD-SP8 open up a new line of research in the functional relationship between CT gene and protease activities. NYD-SP8 may be a future immunotherapeutic target for cancer patients. Further understanding the detailed regulatory mechanisms of NYD-SP8 is important in developing new strategies towards diagnosis and treatment of cancer.

Reference List

- ¹ P. A. Andreasen, *et al.*, "The urokinase-type plasminogen activator system in cancer metastasis: a review," *Int. J. Cancer* **72**(1), 1 (1997).
Ref Type: Journal
- ² Angeliki Voulgari and Alexander Pintzas, "Epithelial Mesenchymal Transition in Cancer Metastasis: Mechanisms, Markers and Strategies to Overcome Drug Resistance in the Clinic," in .
- ³ S. J. Baker and E. P. Reddy, "Modulation of life and death by the TNF receptor superfamily," *Oncogene* **17**(25), 3261 (1998).
Ref Type: Journal
- ⁴ E. N. Baramova, *et al.*, "Involvement of PA/plasmin system in the processing of pro-MMP-9 and in the second step of pro-MMP-2 activation," *FEBS Lett.* **405**(2), 157 (1997).
Ref Type: Journal
- ⁵ P. Basset, *et al.*, "Matrix metalloproteinases as stromal effectors of human carcinoma progression: therapeutic implications," *Matrix Biol.* **15**(8-9), 535 (1997).
Ref Type: Journal
- ⁶ R. C. Bates, *et al.*, "Transcriptional activation of integrin beta6 during the epithelial-mesenchymal transition defines a novel prognostic indicator of aggressive colon carcinoma," *J. Clin. Invest* **115**(2), 339 (2005).
Ref Type: Journal
- ⁷ R. C. Bates and A. M. Mercurio, "Tumor necrosis factor-alpha stimulates the epithelial-to-mesenchymal transition of human colonic organoids," *Mol. Biol. Cell* **14**(5), 1790 (2003).
Ref Type: Journal
- ⁸ B. Baum, J. Settleman, and M. P. Quinlan, "Transitions between epithelial and mesenchymal states in development and disease," *Semin Cell Dev. Biol.* **19**(3), 294 (2008).

Ref Type: Journal

- ⁹ A. A. Beg and D. Baltimore, "An essential role for NF-kappaB in preventing TNF-alpha-induced cell death," *Science* **274**(5288), 782 (1996).
Ref Type: Journal
- ¹⁰ J. Benting, *et al.*, "Acyl and alkyl chain length of GPI-anchors is critical for raft association in vitro," *FEBS Lett.* **462**(1-2), 47 (1999).
Ref Type: Journal
- ¹¹ E. J. Bernhard, S. B. Gruber, and R. J. Muschel, "Direct evidence linking expression of matrix metalloproteinase 9 (92-kDa gelatinase/collagenase) to the metastatic phenotype in transformed rat embryo cells," *Proc. Natl. Acad. Sci. U. S. A* **91**(10), 4293 (1994).
Ref Type: Journal
- ¹² R. Besch, *et al.*, "Inhibition of urokinase-type plasminogen activator receptor induces apoptosis in melanoma cells by activation of p53," *Cell Death. Differ.* **14**(4), 818 (2007).
Ref Type: Journal
- ¹³ N. A. Bhowmick, *et al.*, "Transforming growth factor-beta1 mediates epithelial to mesenchymal transdifferentiation through a RhoA-dependent mechanism," *Mol. Biol. Cell* **12**(1), 27 (2001).
Ref Type: Journal
- ¹⁴ C. Birchmeier, W. Birchmeier, and B. Brand-Saberi, "Epithelial-mesenchymal transitions in cancer progression," *Acta Anat. (Basel)* **156**(3), 217 (1996).
Ref Type: Journal
- ¹⁵ C. Biswas, *et al.*, "The human tumor cell-derived collagenase stimulatory factor (renamed Emmprin) is a member of the immunoglobulin superfamily," *Cancer Res.* **55**(2), 434 (1995).
Ref Type: Journal
- ¹⁶ F. Blasi and P. Carmeliet, "uPAR: a versatile signalling orchestrator," *Nat. Rev. Mol. Cell Biol.* **3**(12), 932 (2002).
Ref Type: Journal

- ¹⁷ B. Boyer, A. M. Valles, and N. Edme, "Induction and regulation of epithelial-mesenchymal transitions," *Biochem. Pharmacol.* **60**(8), 1091 (2000).
Ref Type: Journal
- ¹⁸ C. E. Brinckerhoff and L. M. Matrisian, "Matrix metalloproteinases: a tail of a frog that became a prince," *Nat. Rev. Mol. Cell Biol.* **3**(3), 207 (2002).
Ref Type: Journal
- ¹⁹ P. C. Brooks, *et al.*, "Localization of matrix metalloproteinase MMP-2 to the surface of invasive cells by interaction with integrin alpha v beta 3," *Cell* **85**(5), 683 (1996).
Ref Type: Journal
- ²⁰ E. Burstein and C. S. Duckett, "Dying for NF-kappaB? Control of cell death by transcriptional regulation of the apoptotic machinery," *Curr. Opin. Cell Biol.* **15**(6), 732 (2003).
Ref Type: Journal
- ²¹ H. Buth, *et al.*, "Cathepsin B is essential for regeneration of scratch-wounded normal human epidermal keratinocytes," *Eur. J. Cell Biol.* **86**(11-12), 747 (2007).
Ref Type: Journal
- ²² E. Campo, *et al.*, "Cathepsin B expression in colorectal carcinomas correlates with tumor progression and shortened patient survival," *Am. J. Pathol.* **145**(2), 301 (1994).
Ref Type: Journal
- ²³ P. Carmeliet, *et al.*, "Urokinase-generated plasmin activates matrix metalloproteinases during aneurysm formation," *Nat. Genet.* **17**(4), 439 (1997).
Ref Type: Journal
- ²⁴ U. Cavallaro and G. Christofori, "Multitasking in tumor progression: signaling functions of cell adhesion molecules," *Ann. N. Y. Acad. Sci.* **1014**, 58 (2004).
Ref Type: Journal
- ²⁵ D. Cavallo-Medved, *et al.*, "Caveolin-1 mediates the expression and

localization of cathepsin B, pro-urokinase plasminogen activator and their cell-surface receptors in human colorectal carcinoma cells," *J. Cell Sci.* **118**(Pt 7), 1493 (2005).

Ref Type: Journal

- ²⁶ A. F. Chambers, A. C. Groom, and I. C. MacDonald, "Dissemination and growth of cancer cells in metastatic sites," *Nat. Rev. Cancer* **2**(8), 563 (2002).
Ref Type: Journal
- ²⁷ A. F. Chambers and L. M. Matrisian, "Changing views of the role of matrix metalloproteinases in metastasis," *J. Natl. Cancer Inst.* **89**(17), 1260 (1997).
Ref Type: Journal
- ²⁸ H. A. Chapman and Y. Wei, "Protease crosstalk with integrins: the urokinase receptor paradigm," *Thromb. Haemost.* **86**(1), 124 (2001).
Ref Type: Journal
- ²⁹ F. Chen, *et al.*, "New insights into the role of nuclear factor-kappaB, a ubiquitous transcription factor in the initiation of diseases," *Clin. Chem.* **45**(1), 7 (1999).
Ref Type: Journal
- ³⁰ Y. T. Chen, *et al.*, "Identification of cancer/testis-antigen genes by massively parallel signature sequencing," *Proc. Natl. Acad. Sci. U. S. A* **102**(22), 7940 (2005).
Ref Type: Journal
- ³¹ D. Collen and H. R. Lijnen, "Basic and clinical aspects of fibrinolysis and thrombolysis," *Blood* **78**(12), 3114 (1991).
Ref Type: Journal
- ³² I. Collins and M. D. Garrett, "Targeting the cell division cycle in cancer: CDK and cell cycle checkpoint kinase inhibitors," *Curr. Opin. Pharmacol.* **5**(4), 366 (2005).
Ref Type: Journal
- ³³ F. F. Costa, Blanc K. Le, and B. Brodin, "Concise review: cancer/testis antigens, stem cells, and cancer," *Stem Cells* **25**(3), 707 (2007).
Ref Type: Journal

- ³⁴ T. G. Cotter, "Apoptosis and cancer: the genesis of a research field," *Nat. Rev. Cancer* **9**(7), 501 (2009).
Ref Type: Journal
- ³⁵ L. M. Coussens, B. Fingleton, and L. M. Matrisian, "Matrix metalloproteinase inhibitors and cancer: trials and tribulations," *Science* **295**(5564), 2387 (2002).
Ref Type: Journal
- ³⁶ E. Creemers, *et al.*, "Disruption of the plasminogen gene in mice abolishes wound healing after myocardial infarction," *Am. J. Pathol.* **156**(6), 1865 (2000).
Ref Type: Journal
- ³⁷ C. W. Crowley, *et al.*, "Prevention of metastasis by inhibition of the urokinase receptor," *Proc. Natl. Acad. Sci. U. S. A* **90**(11), 5021 (1993).
Ref Type: Journal
- ³⁸ N. N. Danial and S. J. Korsmeyer, "Cell death: critical control points," *Cell* **116**(2), 205 (2004).
Ref Type: Journal
- ³⁹ K. Dano, *et al.*, "Plasminogen activators, tissue degradation, and cancer," *Adv. Cancer Res.* **44**, 139 (1985).
Ref Type: Journal
- ⁴⁰ K. Dass, *et al.*, "Evolving role of uPA/uPAR system in human cancers," *Cancer Treat. Rev.* **34**(2), 122 (2008).
Ref Type: Journal
- ⁴¹ B. Davidson, *et al.*, "Expression of metalloproteinases and their inhibitors in adenocarcinoma of the uterine cervix," *Int. J. Gynecol. Pathol.* **17**(4), 295 (1998).
Ref Type: Journal
- ⁴² Craene B. De, *et al.*, "The transcription factor snail induces tumor cell invasion through modulation of the epithelial cell differentiation program," *Cancer Res.* **65**(14), 6237 (2005).
Ref Type: Journal

- ⁴³ C. Dehay and H. Kennedy, "Cell-cycle control and cortical development," *Nat. Rev. Neurosci.* **8**(6), 438 (2007).
Ref Type: Journal
- ⁴⁴ Rosso M. Del, G. Fibbi, and Cerinic M. Matucci, "The urokinase-type plasminogen activator system and inflammatory joint diseases," *Clin. Exp. Rheumatol.* **17**(4), 485 (1999).
Ref Type: Journal
- ⁴⁵ G. Devitt, *et al.*, "Serological analysis of human renal cell carcinoma," *Int. J. Cancer* **118**(9), 2210 (2006).
Ref Type: Journal
- ⁴⁶ R. O. Dillman, S. R. Selvan, and P. M. Schiltz, "Patient-specific dendritic-cell vaccines for metastatic melanoma," *N. Engl. J. Med.* **355**(11), 1179 (2006).
Ref Type: Journal
- ⁴⁷ A. Dohchin, *et al.*, "Immunostained cathepsins B and L correlate with depth of invasion and different metastatic pathways in early stage gastric carcinoma," *Cancer* **89**(3), 482 (2000).
Ref Type: Journal
- ⁴⁸ P. Drane, *et al.*, "Accumulation of an inactive form of p53 protein in cells treated with TNF alpha," *Cell Death. Differ.* **9**(5), 527 (2002).
Ref Type: Journal
- ⁴⁹ M. J. Duffy, P. M. McGowan, and W. M. Gallagher, "Cancer invasion and metastasis: changing views," *J. Pathol.* **214**(3), 283 (2008).
Ref Type: Journal
- ⁵⁰ H. F. Dvorak, "Tumors: wounds that do not heal. Similarities between tumor stroma generation and wound healing," *N. Engl. J. Med.* **315**(26), 1650 (1986).
Ref Type: Journal
- ⁵¹ Y. Eeckhout and G. Vaes, "Further studies on the activation of procollagenase, the latent precursor of bone collagenase. Effects of lysosomal cathepsin B, plasmin and kallikrein, and spontaneous activation," *Biochem. J.* **166**(1), 21 (1977).

Ref Type: Journal

- ⁵² M. Egeblad and Z. Werb, "New functions for the matrix metalloproteinases in cancer progression," *Nat. Rev. Cancer* **2**(3), 161 (2002).
Ref Type: Journal
- ⁵³ B. Eisenhaber, P. Bork, and F. Eisenhaber, "Sequence properties of GPI-anchored proteins near the omega-site: constraints for the polypeptide binding site of the putative transamidase," *Protein Eng* **11**(12), 1155 (1998).
Ref Type: Journal
- ⁵⁴ B. Eisenhaber, P. Bork, and F. Eisenhaber, "Post-translational GPI lipid anchor modification of proteins in kingdoms of life: analysis of protein sequence data from complete genomes," *Protein Eng* **14**(1), 17 (2001).
Ref Type: Journal
- ⁵⁵ V. Ellenrieder, *et al.*, "Transforming growth factor beta1 treatment leads to an epithelial-mesenchymal transdifferentiation of pancreatic cancer cells requiring extracellular signal-regulated kinase 2 activation," *Cancer Res.* **61**(10), 4222 (2001).
Ref Type: Journal
- ⁵⁶ S. M. Ellerbroek and M. S. Stack, "Membrane associated matrix metalloproteinases in metastasis," *Bioessays* **21**(11), 940 (1999).
Ref Type: Journal
- ⁵⁷ M. R. Emmert-Buck, *et al.*, "Increased gelatinase A (MMP-2) and cathepsin B activity in invasive tumor regions of human colon cancer samples," *Am. J. Pathol.* **145**(6), 1285 (1994).
Ref Type: Journal
- ⁵⁸ Y. Z. Fan, *et al.*, "Expression of MMP-2, TIMP-2 protein and the ratio of MMP-2/TIMP-2 in gallbladder carcinoma and their significance," *World J. Gastroenterol.* **8**(6), 1138 (2002).
Ref Type: Journal
- ⁵⁹ N. Fankhauser and P. Maser, "Identification of GPI anchor attachment signals by a Kohonen self-organizing map," *Bioinformatics.* **21**(9), 1846 (2005).
Ref Type: Journal

- ⁶⁰ M. A. Ferguson, "The structure, biosynthesis and functions of glycosylphosphatidylinositol anchors, and the contributions of trypanosome research," *J. Cell Sci.* **112 (Pt 17)**, 2799 (1999).
Ref Type: Journal
- ⁶¹ M. A. Ferguson, "The structure, biosynthesis and functions of glycosylphosphatidylinositol anchors, and the contributions of trypanosome research," *J. Cell Sci.* **112 (Pt 17)**, 2799 (1999).
Ref Type: Journal
- ⁶² A. Frenzel, *et al.*, "Bcl2 family proteins in carcinogenesis and the treatment of cancer," *Apoptosis.* **14(4)**, 584 (2009).
Ref Type: Journal
- ⁶³ R. Frlan and S. Gobec, "Inhibitors of cathepsin B," *Curr. Med. Chem.* **13(19)**, 2309 (2006).
Ref Type: Journal
- ⁶⁴ E. Frohlich, *et al.*, "Activity, expression, and transcription rate of the cathepsins B, D, H, and L in cutaneous malignant melanoma," *Cancer* **91(5)**, 972 (2001).
Ref Type: Journal
- ⁶⁵ K. Fujimoto, *et al.*, "Transforming growth factor-beta1 promotes invasiveness after cellular transformation with activated Ras in intestinal epithelial cells," *Exp. Cell Res.* **266(2)**, 239 (2001).
Ref Type: Journal
- ⁶⁶ H. Gali-Muhtasib and N. Bakkar, "Modulating cell cycle: current applications and prospects for future drug development," *Curr. Cancer Drug Targets.* **2(4)**, 309 (2002).
Ref Type: Journal
- ⁶⁷ Y. Ge and M. T. Elghetany, "Urokinase plasminogen activator receptor (CD87): something old, something new," *Lab Hematol.* **9(2)**, 67 (2003).
Ref Type: Journal
- ⁶⁸ I. Ghiran, L. B. Klickstein, and A. Nicholson-Weller, "Calreticulin is at the surface of circulating neutrophils and uses CD59 as an adaptor molecule," *J. Biol. Chem.* **278(23)**, 21024 (2003).

Ref Type: Journal

- ⁶⁹ V. Gocheva, *et al.*, "Distinct roles for cysteine cathepsin genes in multistage tumorigenesis," *Genes Dev.* **20**(5), 543 (2006).
Ref Type: Journal
- ⁷⁰ J. Gotzmann, *et al.*, "Molecular aspects of epithelial cell plasticity: implications for local tumor invasion and metastasis," *Mutat. Res.* **566**(1), 9 (2004).
Ref Type: Journal
- ⁷¹ F. L. Graham, *et al.*, "Characteristics of a human cell line transformed by DNA from human adenovirus type 5," *J. Gen. Virol.* **36**(1), 59 (1977).
Ref Type: Journal
- ⁷² D. R. Green and J. C. Reed, "Mitochondria and apoptosis," *Science* **281**(5381), 1309 (1998).
Ref Type: Journal
- ⁷³ A. Gross, J. M. McDonnell, and S. J. Korsmeyer, "BCL-2 family members and the mitochondria in apoptosis," *Genes Dev.* **13**(15), 1899 (1999).
Ref Type: Journal
- ⁷⁴ H. Guo, *et al.*, "Stimulation of matrix metalloproteinase production by recombinant extracellular matrix metalloproteinase inducer from transfected Chinese hamster ovary cells," *J. Biol. Chem.* **272**(1), 24 (1997).
Ref Type: Journal
- ⁷⁵ G. P. Gupta and J. Massague, "Cancer metastasis: building a framework," *Cell* **127**(4), 679 (2006).
Ref Type: Journal
- ⁷⁶ W. C. Hahn, *et al.*, "Integrative genomic approaches to understanding cancer," *Biochim. Biophys. Acta* **1790**(6), 478 (2009).
Ref Type: Journal
- ⁷⁷ J. W. Harbour and D. C. Dean, "Rb function in cell-cycle regulation and apoptosis," *Nat. Cell Biol.* **2**(4), E65-E67 (2000).
Ref Type: Journal

- ⁷⁸ L. H. Hartwell and T. A. Weinert, "Checkpoints: controls that ensure the order of cell cycle events," *Science* **246**(4930), 629 (1989).
Ref Type: Journal
- ⁷⁹ H. H. Heidtmann, *et al.*, "Cathepsin B and cysteine proteinase inhibitors in human lung cancer cell lines," *Clin. Exp. Metastasis* **15**(4), 368 (1997).
Ref Type: Journal
- ⁸⁰ K. J. Heppner, *et al.*, "Expression of most matrix metalloproteinase family members in breast cancer represents a tumor-induced host response," *Am. J. Pathol.* **149**(1), 273 (1996).
Ref Type: Journal
- ⁸¹ J. Herz, D. E. Clouthier, and R. E. Hammer, "LDL receptor-related protein internalizes and degrades uPA-PAI-1 complexes and is essential for embryo implantation," *Cell* **71**(3), 411 (1992).
Ref Type: Journal
- ⁸² N. M. Hooper, "Foreword: lipid rafts/biophysics, cell signalling, trafficking and processing," *Mol. Membr. Biol.* **23**(1), 1 (2006).
Ref Type: Journal
- ⁸³ Q. Huai, *et al.*, "Structure of human urokinase plasminogen activator in complex with its receptor," *Science* **311**(5761), 656 (2006).
Ref Type: Journal
- ⁸⁴ S. J. Hughes, *et al.*, "A novel amplicon at 8p22-23 results in overexpression of cathepsin B in esophageal adenocarcinoma," *Proc. Natl. Acad. Sci. U. S. A* **95**(21), 12410 (1998).
Ref Type: Journal
- ⁸⁵ H. Hugo, *et al.*, "Epithelial--mesenchymal and mesenchymal--epithelial transitions in carcinoma progression," *J. Cell Physiol* **213**(2), 374 (2007).
Ref Type: Journal
- ⁸⁶ H. Ikezawa, *et al.*, "Studies on phosphatidylinositol phosphodiesterase (phospholipase C type) of *Bacillus cereus*. I. purification, properties and phosphatase-releasing activity," *Biochim. Biophys. Acta* **450**(2), 154 (1976).
Ref Type: Journal

- ⁸⁷ Y. Itoh, *et al.*, "Plasma membrane-bound tissue inhibitor of metalloproteinases (TIMP)-2 specifically inhibits matrix metalloproteinase 2 (gelatinase A) activated on the cell surface," *J. Biol. Chem.* **273**(38), 24360 (1998).
Ref Type: Journal
- ⁸⁸ E. Jager, *et al.*, "Induction of primary NY-ESO-1 immunity: CD8+ T lymphocyte and antibody responses in peptide-vaccinated patients with NY-ESO-1+ cancers," *Proc. Natl. Acad. Sci. U. S. A* **97**(22), 12198 (2000).
Ref Type: Journal
- ⁸⁹ C. Jedeszko and B. F. Sloane, "Cysteine cathepsins in human cancer," *Biol. Chem.* **385**(11), 1017 (2004).
Ref Type: Journal
- ⁹⁰ H. Jin, *et al.*, "Molecular characterization of a germ-cell-specific antigen, TEX101, from mouse testis," *Zygote*. **14**(3), 201 (2006).
Ref Type: Journal
- ⁹¹ M. Johnsen, *et al.*, "Cancer invasion and tissue remodeling: common themes in proteolytic matrix degradation," *Curr. Opin. Cell Biol.* **10**(5), 667 (1998).
Ref Type: Journal
- ⁹² J. A. Joyce, *et al.*, "Cathepsin cysteine proteases are effectors of invasive growth and angiogenesis during multistage tumorigenesis," *Cancer Cell* **5**(5), 443 (2004).
Ref Type: Journal
- ⁹³ J. A. Joyce and J. W. Pollard, "Microenvironmental regulation of metastasis," *Nat. Rev. Cancer* **9**(4), 239 (2009).
Ref Type: Journal
- ⁹⁴ T. Kanekura, X. Chen, and T. Kanzaki, "Basigin (CD147) is expressed on melanoma cells and induces tumor cell invasion by stimulating production of matrix metalloproteinases by fibroblasts," *Int. J. Cancer* **99**(4), 520 (2002).
Ref Type: Journal
- ⁹⁵ M. H. Kang and C. P. Reynolds, "Bcl-2 inhibitors: targeting mitochondrial apoptotic pathways in cancer therapy," *Clin. Cancer Res.* **15**(4), 1126 (2009).

Ref Type: Journal

- ⁹⁶ H. Kataoka, *et al.*, "Tumor cell-derived collagenase-stimulatory factor increases expression of interstitial collagenase, stromelysin, and 72-kDa gelatinase," *Cancer Res.* **53**(13), 3154 (1993).
Ref Type: Journal
- ⁹⁷ J. F. Kerr, A. H. Wyllie, and A. R. Currie, "Apoptosis: a basic biological phenomenon with wide-ranging implications in tissue kinetics," *Br. J. Cancer* **26**(4), 239 (1972).
Ref Type: Journal
- ⁹⁸ R. Khosravi-Far and M. D. Esposti, "Death receptor signals to mitochondria," *Cancer Biol. Ther.* **3**(11), 1051 (2004).
Ref Type: Journal
- ⁹⁹ M. Klaric, *et al.*, "Cysteine cathepsins are not critical for TNF-alpha-induced cell death in T98G and U937 cells," *Biochim. Biophys. Acta* (2009).
Ref Type: Journal
- ¹⁰⁰ J. Kos, *et al.*, "Cathepsins B, H, and L and their inhibitors stefin A and cystatin C in sera of melanoma patients," *Clin. Cancer Res.* **3**(10), 1815 (1997).
Ref Type: Journal
- ¹⁰¹ E. Krepela, "Cysteine proteinases in tumor cell growth and apoptosis," *Neoplasma* **48**(5), 332 (2001).
Ref Type: Journal
- ¹⁰² D Kronegg, "[Http://Www.Expasy.Ch/Tools/](http://www.Expasy.Ch/Tools/)," in 1999).
- ¹⁰³ A. Kurita, *et al.*, "Identification, cloning, and initial characterization of a novel mouse testicular germ cell-specific antigen," *Biol. Reprod.* **64**(3), 935 (2001).
Ref Type: Journal
- ¹⁰⁴ T. T. Lah, *et al.*, "Stefins and lysosomal cathepsins B, L and D in human breast carcinoma," *Int. J. Cancer* **50**(1), 36 (1992).
Ref Type: Journal
- ¹⁰⁵ S. S. Lakka, *et al.*, "Specific interference of urokinase-type plasminogen

activator receptor and matrix metalloproteinase-9 gene expression induced by double-stranded RNA results in decreased invasion, tumor growth, and angiogenesis in gliomas," *J. Biol. Chem.* **280**(23), 21882 (2005).

Ref Type: Journal

- ¹⁰⁶ S. S. Lakka, *et al.*, "Adenovirus-mediated antisense urokinase-type plasminogen activator receptor gene transfer reduces tumor cell invasion and metastasis in non-small cell lung cancer cell lines," *Clin. Cancer Res.* **7**(4), 1087 (2001).
Ref Type: Journal
- ¹⁰⁷ O. Laptenko and C. Prives, "Transcriptional regulation by p53: one protein, many possibilities," *Cell Death. Differ.* **13**(6), 951 (2006).
Ref Type: Journal
- ¹⁰⁸ G. Lauc and M. Heffer-Lauc, "Shedding and uptake of gangliosides and glycosylphosphatidylinositol-anchored proteins," *Biochim. Biophys. Acta* **1760**(4), 584 (2006).
Ref Type: Journal
- ¹⁰⁹ M. H. Lee and H. Y. Yang, "Regulators of G1 cyclin-dependent kinases and cancers," *Cancer Metastasis Rev.* **22**(4), 435 (2003).
Ref Type: Journal
- ¹¹⁰ R. Lehmann and E. D. Schleicher, "Molecular mechanism of diabetic nephropathy," *Clin. Chim. Acta* **297**(1-2), 135 (2000).
Ref Type: Journal
- ¹¹¹ G. Leto, *et al.*, "Lysosomal cathepsins B and L and Stefin A blood levels in patients with hepatocellular carcinoma and/or liver cirrhosis: potential clinical implications," *Oncology* **54**(1), 79 (1997).
Ref Type: Journal
- ¹¹² N. B. Liabakk, *et al.*, "Matrix metalloprotease 2 (MMP-2) and matrix metalloprotease 9 (MMP-9) type IV collagenases in colorectal cancer," *Cancer Res.* **56**(1), 190 (1996).
Ref Type: Journal
- ¹¹³ I. T. Lim, *et al.*, "Strategy in inhibition of cathepsin B, a target in tumor invasion

and metastasis," J. Am. Chem. Soc. **126**(33), 10271 (2004).

Ref Type: Journal

- ¹¹⁴ J. H. Lim, *et al.*, "Activation of human cancer/testis antigen gene, XAGE-1, in tumor cells is correlated with CpG island hypomethylation," Int. J. Cancer **116**(2), 200 (2005).
Ref Type: Journal
- ¹¹⁵ L. A. Liotta and W. G. Stetler-Stevenson, "Tumor invasion and metastasis: an imbalance of positive and negative regulation," Cancer Res. **51**(18 Suppl), 5054s (1991).
Ref Type: Journal
- ¹¹⁶ S. Liptay, *et al.*, "Related subunits of NF-kappa B map to two distinct loci associated with translocations in leukemia, NFKB1 and NFKB2," Genomics **13**(2), 287 (1992).
Ref Type: Journal
- ¹¹⁷ A. Lochter and M. J. Bissell, "An odyssey from breast to bone: multi-step control of mammary metastases and osteolysis by matrix metalloproteinases," APMIS **107**(1), 128 (1999).
Ref Type: Journal
- ¹¹⁸ A. Lochter, *et al.*, "Matrix metalloproteinase stromelysin-1 triggers a cascade of molecular alterations that leads to stable epithelial-to-mesenchymal conversion and a premalignant phenotype in mammary epithelial cells," J. Cell Biol. **139**(7), 1861 (1997).
Ref Type: Journal
- ¹¹⁹ C. Lopez-Otin and L. M. Matrisian, "Emerging roles of proteases in tumour suppression," Nat. Rev. Cancer **7**(10), 800 (2007).
Ref Type: Journal
- ¹²⁰ A. R. Mackay, *et al.*, "Basement membrane type IV collagen degradation: evidence for the involvement of a proteolytic cascade independent of metalloproteinases," Cancer Res. **50**(18), 5997 (1990).
Ref Type: Journal
- ¹²¹ S. Maddika, *et al.*, "Cell survival, cell death and cell cycle pathways are interconnected: implications for cancer therapy," Drug Resist. Updat.

10(1-2), 13 (2007).

Ref Type: Journal

- ¹²² S. Marastoni, *et al.*, "Extracellular matrix: a matter of life and death," *Connect. Tissue Res.* **49(3)**, 203 (2008).

Ref Type: Journal

- ¹²³ M. Marchand, *et al.*, "Tumor regressions observed in patients with metastatic melanoma treated with an antigenic peptide encoded by gene MAGE-3 and presented by HLA-A1," *Int. J. Cancer* **80(2)**, 219 (1999).

Ref Type: Journal

- ¹²⁴ S. Maschler, *et al.*, "Tumor cell invasiveness correlates with changes in integrin expression and localization," *Oncogene* **24(12)**, 2032 (2005).

Ref Type: Journal

- ¹²⁵ S. Mayor and H. Riezman, "Sorting GPI-anchored proteins," *Nat. Rev. Mol. Cell Biol.* **5(2)**, 110 (2004).

Ref Type: Journal

- ¹²⁶ A. P. Mazar, "The urokinase plasminogen activator receptor (uPAR) as a target for the diagnosis and therapy of cancer," *Anticancer Drugs* **12(5)**, 387 (2001).

Ref Type: Journal

- ¹²⁷ A. P. Mazar, J. Henkin, and R. H. Goldfarb, "The urokinase plasminogen activator system in cancer: implications for tumor angiogenesis and metastasis," *Angiogenesis.* **3(1)**, 15 (1999).

Ref Type: Journal

- ¹²⁸ F. Mbeunkui and D. J. Johann, Jr., "Cancer and the tumor microenvironment: a review of an essential relationship," *Cancer Chemother. Pharmacol.* **63(4)**, 571 (2009).

Ref Type: Journal

- ¹²⁹ B. McMahon and H. C. Kwaan, "The plasminogen activator system and cancer," *Pathophysiol. Haemost. Thromb.* **36(3-4)**, 184 (2008).

Ref Type: Journal

- ¹³⁰ H. Y. Min, *et al.*, "Urokinase receptor antagonists inhibit angiogenesis and

primary tumor growth in syngeneic mice," *Cancer Res.* **56**(10), 2428 (1996).

Ref Type: Journal

- ¹³¹ M. J. Murnane, *et al.*, "Stage-specific increases in cathepsin B messenger RNA content in human colorectal carcinoma," *Cancer Res.* **51**(4), 1137 (1991).

Ref Type: Journal

- ¹³² G. Murphy, *et al.*, "Physiological mechanisms for metalloproteinase activation," *Matrix Suppl* **1**, 224 (1992).

Ref Type: Journal

- ¹³³ J. Myllyharju and K. I. Kivirikko, "Collagens, modifying enzymes and their mutations in humans, flies and worms," *Trends Genet.* **20**(1), 33 (2004).

Ref Type: Journal

- ¹³⁴ P. Navarro, E. Lozano, and A. Cano, "Expression of E- or P-cadherin is not sufficient to modify the morphology and the tumorigenic behavior of murine spindle carcinoma cells. Possible involvement of plakoglobin," *J. Cell Sci.* **105 (Pt 4)**, 923 (1993).

Ref Type: Journal

- ¹³⁵ A. Nawshad, *et al.*, "Transforming growth factor-beta signaling during epithelial-mesenchymal transformation: implications for embryogenesis and tumor metastasis," *Cells Tissues. Organs* **179**(1-2), 11 (2005).

Ref Type: Journal

- ¹³⁶ M. Oft, K. H. Heider, and H. Beug, "TGFbeta signaling is necessary for carcinoma cell invasiveness and metastasis," *Curr. Biol.* **8**(23), 1243 (1998).

Ref Type: Journal

- ¹³⁷ T. Ohkubo and M. Ozawa, "The transcription factor Snail downregulates the tight junction components independently of E-cadherin downregulation," *J. Cell Sci.* **117**(Pt 9), 1675 (2004).

Ref Type: Journal

- ¹³⁸ T. Ohsawa, T. Higashi, and T. Tsuji, "The secretion of high molecular weight

cathepsin B from cultured human liver cancers," *Acta Med. Okayama* **43**(1), 9 (1989).

Ref Type: Journal

- ¹³⁹ Y. Okumura, *et al.*, "Proteolytic activation of the precursor of membrane type 1 matrix metalloproteinase by human plasminogen A possible cell surface activator," *FEBS Lett.* **402**(2-3), 181 (1997).

Ref Type: Journal

- ¹⁴⁰ K. Olszynski and M. Zimowska, "[Structure and function of matrix metalloproteinases]," *Postepy Biochem.* **55**(1), 76 (2009).

Ref Type: Journal

- ¹⁴¹ Z. N. Oltvai, C. L. Millman, and S. J. Korsmeyer, "Bcl-2 heterodimerizes in vivo with a conserved homolog, Bax, that accelerates programmed cell death," *Cell* **74**(4), 609 (1993).

Ref Type: Journal

- ¹⁴² M. J. Omaetxebarria, *et al.*, "Isolation and characterization of glycosylphosphatidylinositol-anchored peptides by hydrophilic interaction chromatography and MALDI tandem mass spectrometry," *Anal. Chem.* **78**(10), 3335 (2006).

Ref Type: Journal

- ¹⁴³ P. Orlean and A. K. Menon, "Thematic review series: lipid posttranslational modifications. GPI anchoring of protein in yeast and mammalian cells, or: how we learned to stop worrying and love glycosphospholipids," *J. Lipid Res.* **48**(5), 993 (2007).

Ref Type: Journal

- ¹⁴⁴ L. Ossowski and J. A. Guirre-Ghiso, "Urokinase receptor and integrin partnership: coordination of signaling for cell adhesion, migration and growth," *Curr. Opin. Cell Biol.* **12**(5), 613 (2000).

Ref Type: Journal

- ¹⁴⁵ H. Pappot, *et al.*, "Elevated plasma levels of urokinase plasminogen activator receptor in non-small cell lung cancer patients," *Eur. J. Cancer* **33**(6), 867 (1997).

Ref Type: Journal

- ¹⁴⁶ M. T. Park and S. J. Lee, "Cell cycle and cancer," *J. Biochem. Mol. Biol.* **36**(1), 60 (2003).
Ref Type: Journal
- ¹⁴⁷ R. B. Parmigiani, *et al.*, "Characterization of a cancer/testis (CT) antigen gene family capable of eliciting humoral response in cancer patients," *Proc. Natl. Acad. Sci. U. S. A* **103**(48), 18066 (2006).
Ref Type: Journal
- ¹⁴⁸ N. D. Perkins, "Regulation of NF-kappaB by atypical activators and tumour suppressors," *Biochem. Soc. Trans.* **32**(Pt 6), 936 (2004).
Ref Type: Journal
- ¹⁴⁹ M. Ploug, "Structure-function relationships in the interaction between the urokinase-type plasminogen activator and its receptor," *Curr. Pharm. Des* **9**(19), 1499 (2003).
Ref Type: Journal
- ¹⁵⁰ M. Ploug and V. Ellis, "Structure-function relationships in the receptor for urokinase-type plasminogen activator. Comparison to other members of the Ly-6 family and snake venom alpha-neurotoxins," *FEBS Lett.* **349**(2), 163 (1994).
Ref Type: Journal
- ¹⁵¹ M. Ploug, *et al.*, "Peptide-derived antagonists of the urokinase receptor. affinity maturation by combinatorial chemistry, identification of functional epitopes, and inhibitory effect on cancer cell intravasation," *Biochemistry* **40**(40), 12157 (2001).
Ref Type: Journal
- ¹⁵² K. Polyak and R. A. Weinberg, "Transitions between epithelial and mesenchymal states: acquisition of malignant and stem cell traits," *Nat. Rev. Cancer* **9**(4), 265 (2009).
Ref Type: Journal
- ¹⁵³ G. Portella, *et al.*, "Transforming growth factor beta is essential for spindle cell conversion of mouse skin carcinoma in vivo: implications for tumor invasion," *Cell Growth Differ.* **9**(5), 393 (1998).
Ref Type: Journal

- ¹⁵⁴ K. T. Preissner, S. M. Kanse, and A. E. May, "Urokinase receptor: a molecular organizer in cellular communication," *Curr. Opin. Cell Biol.* **12**(5), 621 (2000).
Ref Type: Journal
- ¹⁵⁵ D. C. Radisky, *et al.*, "Rac1b and reactive oxygen species mediate MMP-3-induced EMT and genomic instability," *Nature* **436**(7047), 123 (2005).
Ref Type: Journal
- ¹⁵⁶ J. S. Rao, "Molecular mechanisms of glioma invasiveness: the role of proteases," *Nat. Rev. Cancer* **3**(7), 489 (2003).
Ref Type: Journal
- ¹⁵⁷ J. C. Reed and M. Pellicchia, "Apoptosis-based therapies for hematologic malignancies," *Blood* **106**(2), 408 (2005).
Ref Type: Journal
- ¹⁵⁸ M. Reichert, T. Muller, and W. Hunziker, "The PDZ domains of zonula occludens-1 induce an epithelial to mesenchymal transition of Madin-Darby canine kidney I cells. Evidence for a role of beta-catenin/Tcf/Lef signaling," *J. Biol. Chem.* **275**(13), 9492 (2000).
Ref Type: Journal
- ¹⁵⁹ S. A. Rempel, *et al.*, "Cathepsin B expression and localization in glioma progression and invasion," *Cancer Res.* **54**(23), 6027 (1994).
Ref Type: Journal
- ¹⁶⁰ S. Ricard-Blum and F. Ruggiero, "The collagen superfamily: from the extracellular matrix to the cell membrane," *Pathol. Biol. (Paris)* **53**(7), 430 (2005).
Ref Type: Journal
- ¹⁶¹ M. L. Roberts, *et al.*, "Microarray analysis of the differential transformation mediated by Kirsten and Harvey Ras oncogenes in a human colorectal adenocarcinoma cell line," *Int. J. Cancer* **118**(3), 616 (2006).
Ref Type: Journal
- ¹⁶² J. Romer, B. S. Nielsen, and M. Ploug, "The urokinase receptor as a potential target in cancer therapy," *Curr. Pharm. Des* **10**(19), 2359 (2004).

Ref Type: Journal

- ¹⁶³ S. Rosenberg, "New developments in the urokinase-type plasminogen activator system," *Expert. Opin. Ther. Targets.* **5**(6), 711 (2001).
Ref Type: Journal
- ¹⁶⁴ S. A. Rosenberg, *et al.*, "Immunologic and therapeutic evaluation of a synthetic peptide vaccine for the treatment of patients with metastatic melanoma," *Nat. Med.* **4**(3), 321 (1998).
Ref Type: Journal
- ¹⁶⁵ S. Roshy, B. F. Sloane, and K. Moin, "Pericellular cathepsin B and malignant progression," *Cancer Metastasis Rev.* **22**(2-3), 271 (2003).
Ref Type: Journal
- ¹⁶⁶ E. K. Rowinsky, "Targeted induction of apoptosis in cancer management: the emerging role of tumor necrosis factor-related apoptosis-inducing ligand receptor activating agents," *J. Clin. Oncol.* **23**(36), 9394 (2005).
Ref Type: Journal
- ¹⁶⁷ B. Saile, *et al.*, "The bcl, NFkappaB and p53/p21WAF1 systems are involved in spontaneous apoptosis and in the anti-apoptotic effect of TGF-beta or TNF-alpha on activated hepatic stellate cells," *Eur. J. Cell Biol.* **80**(8), 554 (2001).
Ref Type: Journal
- ¹⁶⁸ T. Sameshima, *et al.*, "Glioma cell extracellular matrix metalloproteinase inducer (Emmprin) (CD147) stimulates production of membrane-type matrix metalloproteinases and activated gelatinase A in co-cultures with brain-derived fibroblasts," *Cancer Lett.* **157**(2), 177 (2000).
Ref Type: Journal
- ¹⁶⁹ N. Sasi, *et al.*, "Regulated cell death pathways: new twists in modulation of BCL2 family function," *Mol. Cancer Ther.* **8**(6), 1421 (2009).
Ref Type: Journal
- ¹⁷⁰ P. Savagner, "Leaving the neighborhood: molecular mechanisms involved during epithelial-mesenchymal transition," *Bioessays* **23**(10), 912 (2001).
Ref Type: Journal

- ¹⁷¹ M. J. Scanlan, A. J. Simpson, and L. J. Old, "The cancer/testis genes: review, standardization, and commentary," *Cancer Immun.* **4**, 1 (2004).
Ref Type: Journal
- ¹⁷² K. A. Schafer, "The cell cycle: a review," *Vet. Pathol.* **35**(6), 461 (1998).
Ref Type: Journal
- ¹⁷³ M. Schmitt, *et al.*, "Tumor-associated urokinase-type plasminogen activator: biological and clinical significance," *Biol. Chem. Hoppe Seyler* **373**(7), 611 (1992).
Ref Type: Journal
- ¹⁷⁴ G. K. Schwartz and M. A. Shah, "Targeting the cell cycle: a new approach to cancer therapy," *J. Clin. Oncol.* **23**(36), 9408 (2005).
Ref Type: Journal
- ¹⁷⁵ J. Sha, *et al.*, "Identification of testis development and spermatogenesis-related genes in human and mouse testes using cDNA arrays," *Mol. Hum. Reprod.* **8**(6), 511 (2002).
Ref Type: Journal
- ¹⁷⁶ R. M. Siegel, "Caspases at the crossroads of immune-cell life and death," *Nat. Rev. Immunol.* **6**(4), 308 (2006).
Ref Type: Journal
- ¹⁷⁷ A. J. Simpson, *et al.*, "Cancer/testis antigens, gametogenesis and cancer," *Nat. Rev. Cancer* **5**(8), 615 (2005).
Ref Type: Journal
- ¹⁷⁸ S. Singh, *et al.*, "Expression and functional role of CCR9 in prostate cancer cell migration and invasion," *Clin. Cancer Res.* **10**(24), 8743 (2004).
Ref Type: Journal
- ¹⁷⁹ H. Solberg, *et al.*, "The murine receptor for urokinase-type plasminogen activator is primarily expressed in tissues actively undergoing remodeling," *J. Histochem. Cytochem.* **49**(2), 237 (2001).
Ref Type: Journal
- ¹⁸⁰ P. S. Steeg, "Tumor metastasis: mechanistic insights and clinical challenges," *Nat. Med.* **12**(8), 895 (2006).

Ref Type: Journal

- ¹⁸¹ I. Stefanova, *et al.*, "GPI-anchored cell-surface molecules complexed to protein tyrosine kinases," *Science* **254**(5034), 1016 (1991).
Ref Type: Journal
- ¹⁸² V. V. Stepanova and V. A. Tkachuk, "Urokinase as a multidomain protein and polyfunctional cell regulator," *Biochemistry (Mosc.)* **67**(1), 109 (2002).
Ref Type: Journal
- ¹⁸³ S. Stevanovic, "Identification of tumour-associated T-cell epitopes for vaccine development," *Nat. Rev. Cancer* **2**(7), 514 (2002).
Ref Type: Journal
- ¹⁸⁴ A. Strasser, "Apoptosis. Death of a T cell," *Nature* **373**(6513), 385 (1995).
Ref Type: Journal
- ¹⁸⁵ L. Strizzi, *et al.*, "Epithelial mesenchymal transition is a characteristic of hyperplasias and tumors in mammary gland from MMTV-Cripto-1 transgenic mice," *J. Cell Physiol* **201**(2), 266 (2004).
Ref Type: Journal
- ¹⁸⁶ T. Suda, *et al.*, "Identification of secernin 1 as a novel immunotherapy target for gastric cancer using the expression profiles of cDNA microarray," *Cancer Sci.* **97**(5), 411 (2006).
Ref Type: Journal
- ¹⁸⁷ S. R. Sunyaev, *et al.*, "PSIC: profile extraction from sequence alignments with position-specific counts of independent observations," *Protein Eng* **12**(5), 387 (1999).
Ref Type: Journal
- ¹⁸⁸ M. Sutinen, *et al.*, "Expression of matrix metalloproteinases (MMP-1 and -2) and their inhibitors (TIMP-1, -2 and -3) in oral lichen planus, dysplasia, squamous cell carcinoma and lymph node metastasis," *Br. J. Cancer* **77**(12), 2239 (1998).
Ref Type: Journal
- ¹⁸⁹ K. Szoltysek, *et al.*, "TNFalpha-induced activation of NFkappaB protects against UV-induced apoptosis specifically in p53-proficient cells," *Acta Biochim.*

Pol. **55**(4), 741 (2008).

Ref Type: Journal

- ¹⁹⁰ K. Tajima, *et al.*, "Expression of cancer/testis (CT) antigens in lung cancer," *Lung Cancer* **42**(1), 23 (2003).
Ref Type: Journal
- ¹⁹¹ C. H. Tang and Y. Wei, "The urokinase receptor and integrins in cancer progression," *Cell Mol. Life Sci.* **65**(12), 1916 (2008).
Ref Type: Journal
- ¹⁹² Y. Tang, *et al.*, "Tumor-stroma interaction: positive feedback regulation of extracellular matrix metalloproteinase inducer (Emmprin) expression and matrix metalloproteinase-dependent generation of soluble Emmprin," *Mol. Cancer Res.* **2**(2), 73 (2004).
Ref Type: Journal
- ¹⁹³ D. Tarin, E. W. Thompson, and D. F. Newgreen, "The fallacy of epithelial mesenchymal transition in neoplasia," *Cancer Res.* **65**(14), 5996 (2005).
Ref Type: Journal
- ¹⁹⁴ J. P. Thiery, "Epithelial-mesenchymal transitions in tumour progression," *Nat. Rev. Cancer* **2**(6), 442 (2002).
Ref Type: Journal
- ¹⁹⁵ J. P. Thiery, "Epithelial-mesenchymal transitions in development and pathologies," *Curr. Opin. Cell Biol.* **15**(6), 740 (2003).
Ref Type: Journal
- ¹⁹⁶ J. P. Thiery and J. P. Sleeman, "Complex networks orchestrate epithelial-mesenchymal transitions," *Nat. Rev. Mol. Cell Biol.* **7**(2), 131 (2006).
Ref Type: Journal
- ¹⁹⁷ B. Tian and A. R. Brasier, "Identification of a nuclear factor kappa B-dependent gene network," *Recent Prog. Horm. Res.* **58**, 95 (2003).
Ref Type: Journal
- ¹⁹⁸ H. Tsukamoto, *et al.*, "Genomic organization and structure of the 5'-flanking region of the TEX101 gene: alternative promoter usage and splicing

generate transcript variants with distinct 5'-untranslated region," *Mol. Reprod. Dev.* **74**(2), 154 (2007).

Ref Type: Journal

- ¹⁹⁹ G. C. Tucker, *et al.*, "Collagen-mediated dispersion of NBT-II rat bladder carcinoma cells," *Cancer Res.* **50**(1), 129 (1990).
Ref Type: Journal
- ²⁰⁰ B. Turk, "Targeting proteases: successes, failures and future prospects," *Nat. Rev. Drug Discov.* **5**(9), 785 (2006).
Ref Type: Journal
- ²⁰¹ T. Turpeenniemi-Hujanen, "Gelatinases (MMP-2 and -9) and their natural inhibitors as prognostic indicators in solid cancers," *Biochimie* **87**(3-4), 287 (2005).
Ref Type: Journal
- ²⁰² S. Udenfriend and K. Kodukula, "How glycosylphosphatidylinositol-anchored membrane proteins are made," *Annu. Rev. Biochem.* **64**, 563 (1995).
Ref Type: Journal
- ²⁰³ S. Ulisse, *et al.*, "The urokinase plasminogen activator system: a target for anti-cancer therapy," *Curr. Cancer Drug Targets.* **9**(1), 32 (2009).
Ref Type: Journal
- ²⁰⁴ J. W. van der Stappen, *et al.*, "Activation of cathepsin B, secreted by a colorectal cancer cell line requires low pH and is mediated by cathepsin D," *Int. J. Cancer* **67**(4), 547 (1996).
Ref Type: Journal
- ²⁰⁵ K. Vermeulen, D. R. Van Bockstaele, and Z. N. Berneman, "The cell cycle: a review of regulation, deregulation and therapeutic targets in cancer," *Cell Prolif.* **36**(3), 131 (2003).
Ref Type: Journal
- ²⁰⁶ E. Vincan, *et al.*, "Frizzled-7 dictates three-dimensional organization of colorectal cancer cell carcinoids," *Oncogene* **26**(16), 2340 (2007).
Ref Type: Journal
- ²⁰⁷ D. G. Walker, L. F. Lue, and T. G. Beach, "Increased expression of the urokinase

plasminogen-activator receptor in amyloid beta peptide-treated human brain microglia and in AD brains," *Brain Res.* **926**(1-2), 69 (2002).
Ref Type: Journal

²⁰⁸ Y. Wang, "The role and regulation of urokinase-type plasminogen activator receptor gene expression in cancer invasion and metastasis," *Med. Res. Rev.* **21**(2), 146 (2001).
Ref Type: Journal

²⁰⁹ Y. Wang, *et al.*, "Structure of the human urokinase receptor gene and its similarity to CD59 and the Ly-6 family," *Eur. J. Biochem.* **227**(1-2), 116 (1995).
Ref Type: Journal

²¹⁰ Y. Wei, *et al.*, "Identification of the urokinase receptor as an adhesion receptor for vitronectin," *J. Biol. Chem.* **269**(51), 32380 (1994).
Ref Type: Journal

²¹¹ T. A. Weinert and L. H. Hartwell, "The RAD9 gene controls the cell cycle response to DNA damage in *Saccharomyces cerevisiae*," *Science* **241**(4863), 317 (1988).
Ref Type: Journal

²¹² Z. Werb, "ECM and cell surface proteolysis: regulating cellular ecology," *Cell* **91**(4), 439 (1997).
Ref Type: Journal

²¹³ R. H. Whitehead, *et al.*, "A new colon carcinoma cell line (LIM1863) that grows as organoids with spontaneous differentiation into crypt-like structures in vitro," *Cancer Res.* **47**(10), 2683 (1987).
Ref Type: Journal

²¹⁴ R. H. Whitehead, *et al.*, "A new colon carcinoma cell line (LIM1863) that grows as organoids with spontaneous differentiation into crypt-like structures in vitro," *Cancer Res.* **47**(10), 2683 (1987).
Ref Type: Journal

²¹⁵ B. Z. Yan, *et al.*, "Role of cathepsin B-mediated apoptosis in fulminant hepatic failure in mice," *World J. Gastroenterol.* **15**(10), 1231 (2009).
Ref Type: Journal

- ²¹⁶ W. Yan, *et al.*, "The hydrophobic domains in the carboxyl-terminal signal for GPI modification and in the amino-terminal leader peptide have similar structural requirements," *J. Mol. Biol.* **275**(1), 25 (1998).
Ref Type: Journal
- ²¹⁷ J. Yang, *et al.*, "Twist, a master regulator of morphogenesis, plays an essential role in tumor metastasis," *Cell* **117**(7), 927 (2004).
Ref Type: Journal
- ²¹⁸ J. Yang and R. A. Weinberg, "Epithelial-mesenchymal transition: at the crossroads of development and tumor metastasis," *Dev. Cell* **14**(6), 818 (2008).
Ref Type: Journal
- ²¹⁹ L. Yang, *et al.*, "Coexistence of high levels of apoptotic signaling and inhibitor of apoptosis proteins in human tumor cells: implication for cancer specific therapy," *Cancer Res.* **63**(20), 6815 (2003).
Ref Type: Journal
- ²²⁰ L. Yin, *et al.*, "A sperm GPI-anchored protein elicits sperm-cumulus cross-talk leading to the acrosome reaction," *Cell Mol. Life Sci.* **66**(5), 900 (2009).
Ref Type: Journal
- ²²¹ H. Yoshitake, *et al.*, "TEX101, a germ cell-marker glycoprotein, is associated with lymphocyte antigen 6 complex locus k within the mouse testis," *Biochem. Biophys. Res. Commun.* **372**(2), 277 (2008).
Ref Type: Journal
- ²²² R. J. Youle and A. Strasser, "The BCL-2 protein family: opposing activities that mediate cell death," *Nat. Rev. Mol. Cell Biol.* **9**(1), 47 (2008).
Ref Type: Journal
- ²²³ Q. Yu and I. Stamenkovic, "Localization of matrix metalloproteinase 9 to the cell surface provides a mechanism for CD44-mediated tumor invasion," *Genes Dev.* **13**(1), 35 (1999).
Ref Type: Journal
- ²²⁴ Q. Zhan, *et al.*, "Induction of bax by genotoxic stress in human cells correlates with normal p53 status and apoptosis," *Oncogene* **9**(12), 3743 (1994).
Ref Type: Journal

- ²²⁵ Y. Zhao, *et al.*, "Urokinase directly activates matrix metalloproteinases-9: a potential role in glioblastoma invasion," *Biochem. Biophys. Res. Commun.* **369**(4), 1215 (2008).
Ref Type: Journal
- ²²⁶ S. J. Zheng, *et al.*, "Distribution and anti-HBV effects of antisense oligodeoxynucleotides conjugated to galactosylated poly-L-lysine," *World J. Gastroenterol.* **9**(6), 1251 (2003).
Ref Type: Journal

Appendix A – Reagents and Chemicals

Reagent	Cat. No	Manufacturer
100bp DNA Ladder 250ug		Gibco
30% Acrylamide/Bis solution, 37.5:1,	161-0158	Bio-Rad
Agarose-High Gel Streng	US75817-500G	Amersham Biosciences
Alkaline Phosphatase, Calf Intestinal (CIP),	M0290S	New England Biolabs, USA
Antibiotic G-418	US11379-5g	Amersham Biosciences
ArrayGrade cRNA Clenup Kit	GA-012	Superaray
Biotin-16-UTP, 250 nM	11388908910	Roche
Brij (R) 35 suitable for Stein-Moore Chromatography 500g	P1254	Sigma
CellTiter 96 AQueous One Solution Cell Proliferation Assay 1000 assays	G3580	Promega
CellTracker Green CMFDA 20x50ug	C-7025	Invitrogen Hong Kong Limited
CellTracker Orange CMRA 20x50ug	C-34551	Invitrogen Hong Kong Limited
dNTP MIX with dttp, 12 PAQ, 10mM	4303442	Applied Biosystems
ECL Plus Western blot analysis Reagents	RPN2132	GE Healthcare
EcoRI (REME)	E1040y	GE Healthcare Bio-sciences
Ethanol absolute, GR, 2.5L	E_100983_2.5	Merck
Fetal Bovine Serum S. American, Qualified, 500ml		Gibco
FideliTaq, 50U # PCR	E71180V	GE Medical Systems Hong Kong Limtied
Fuji Super RX20.3x25.4cm 100S	F50.099	Fuji Medical
GFX PCR DNA, Gel Band Purficiation kit, 250 (PCR)		GE Medical Systems
GoTaq Flexi DNA Polymerase	M8295	Promega
Hemocytometer: "HL" Counting Chamber, bright line, Burker, depth 0.1mm with 2 cover glass	8100201	Zahlkammern
Hybond-ECL	RPN303D	Amersham Bioscience

Hygromycin B, Liquid, 1g		Invitrogen
InnoZyme Cathepsin B Activity Assay Kit, Fluorogenic, 1 kit (Merck)	CBA001-1KIT	Oncogene
LipofectAMINE 2000 Reagent		Invitrogen
Lipofectamine Reagent, 1ml		Invitrogen
Luria Broth, 1kg	75854	USB
Master Mix, TF, 5 Pack Power SYBR Green PCR	4368702	Applied Biosystems
Midi Plus, 25 prep	GDV2001	Viogene
Mini Trans-Blot Electrophoretic Transfer Cell	170-3930	Bio-rad
MMLV Reverse Transcriptase	E70456Z	Amersham Biosciences
Oligo d(T)16 primers	N8080128	Applied Biosystems
Oligo GEArray Bulk Kit	GA-034	SuperArray
Oligo GEArray Human Signal Transduction in Cancer Microarray (HybTube), 4 GEArrays	OHS-044-4	Superarray
Oligo GEArray Human Tumor Metastasis Microarray (set of 4)	OHS-028-4	SuperArray
One shot TOP 10 Electrocomp E. Coli, 20 Rxn	C4040-52	Invitrogen
PCR Master Mix TF, 5x200rxn TaqMan Univ	4364340	Applied Biosystems
Phospholipase C, phosphatidylinositol-specific from Bacillus cereus	P-6466	Molecular Probe, Invitrogen Hong Kong Limited
Primers		Tech Dragon Limited
Protein Assay Dye Reagent Concentrate, 450 ml	500-0006	Bio-Rad
Proteinase K	V3021	Promega
QCM ECMatrix Cell Invasion Assay, Fluorimetric (96 wells)	ECM555	Chemicon
QIAamp DNA Mini Kit	51304	Qiagen
Random Hexamer Primers, 50 uM	N8080127	Invitrogen
Recombinant rainbow molecular 500ul	RPN800E	Amersham Bioscience
RNase Inhibitor, 20Unit/ul, 100Rxn	N8080119	Applied Biosystems
RPMI Medium 1640, Powder		Gibco

T4 DNA Ligase, 500 u (Weiss Units)	M1804	Promega
Taq DNA Polymerase		Amersham Bioscience
Taqman GenExpression Inventoried Assay (Assay ID: Hs00169842_m1), [human IL6 receptor]	4331182	Applied Biosystems
TPP cell scraper L=24cm, 150/case	99002	TPP
Triton X-100 SigmaUltra, 500ml	T9284	Sigma
Trizol Reagent		Invitrogen
Truelabeling-AMP 2.0	GA-030	Superarray
uPA Activity Assay Kit	ECM600	Chemicon
uPA Colorimetric Substrate 5mg	ECM 610	Chemicon
Trypsin-EDTA (0.25% Trypsin, 1mM EDTA4Na) (1x) Liquid		Gibco
Penicillin-Streptomycin		Gibco
RPMI medium 1640, powder, 10x1L		Gibco

Appendix B – Antibodies lists

Antibody	Cat. No	Manufacturer
Bax (B-9) antibodies	sc-7480	Santa Cruz
Bcl-2 (N-19) antibodies	sc-492	Santa Cruz
β-tubulin (H-235)	sc-9104	Santa Cruz
cdc 2 rabbit polyclonal IgG ((C-19)	sc-954	Santa Cruz
CDK4 rabbit polyclonal IgG (C-22)	sc-260	Santa Cruz
C-Jun rabbit polyclonal IgG (H-79)	sc-1694	Santa Cruz
cyclin A rabbit polyclonal IgG (H-432)	sc-751	Santa Cruz
cyclin E rabbit polyclonal IgG (H-145)	sc-20684	Santa Cruz
E-Cadherin (H-108)	sc-7870	Santa Cruz
ECL Mouse IgG, HRP-linked antibody	NA931	Amersham Biosciences
ECL Rabbit IgG, HRP-linked antibody	NA934-1ML	Amersham Biosciences
mouse anti-human uPAR Monoclonal antibody	3937	American Diagnostica
mouse anti-NYD-SP8 polyclonal antibody	-	Prof Sha, NJU
Nomral goat IgG	sc-2028	Santa Cruz
Nomral mouse IgG	sc-2025	Santa Cruz
Nomral rabbit IgG	sc-2027	Santa Cruz
p21 Waf1/Cip1 (DCS60) Mouse monoclonal Ab	2946	CST
PCNA (PC-10) mouse monoclonal IgG2a	sc-56	Santa Cruz
Rabbit antihuman uPAR Polyclonal Antibody	399R	American Diagnostica
Stat Antibody Sampler Kit	9939	Cellsignaling
TEX101 MaxPabPolyclonal antibody (B01)	H00083639-B01	Abnova
uPA (C-20)	sc-6830	Santa Cruz
uPA (H-140)	sc-14019	Santa Cruz
uPAR (FL-290)	sc-10815	Santa Cruz
p53	9282	Cell signaling
MMP-9	ab16306	abcam

Appendix C – Buffers

Lysis Buffer of Sperm

Urea	7 M
Thiourea	2 M
CHAPs	4%
Halt™ protease inhibitor	1X
DTT	2%

RT Buffer 1 (for semi-quantitative PCR)

RT Buffer	1x
dNTPs	0.5 μM
Oligo dT	0.5 μM
MgCl ₂	5 mM
DTT	0.02 μM
MMLV	2.5 U

RT Buffer 2 (for quantitative real time PCR)

RT Buffer	1X
dNTPs	0.5 mM
Random Hexamers	0.5 μM
MgCl ₂	5 mM
DTT	0.02 μM
MuLV	3 U

Semi-quantitative PCR

PCR buffer	1X
dNTPs	0.5 μM
Primer F	0.25 μM
Primer R	0.25 μM
Template	1-10 ng
Taq Polymerase	3 U

RIPA lysis buffer

Tris-HCl (pH 8.0)	50 mM
NaCl	150 mM
NP40	1%
Deoxycholic acid (DOC)	0.50%
SDS	0.10%

uPA lysis buffer

Tween-20	2%
----------	----

Proteinase inhibitors

aprotinin	1 µg/mL
leupeptin	1 µg/mL

6X Sample Buffer

4X Tris-Cl/SDS (pH 6.8)	7 mL
Glycerol	3 mL
SDS	1 g
DTT	0.93 g
Bromophenol blue	1.2 mg

10X SDS-PAGE running buffer**Stacking gel (/gel)**

30% polyacrylamide	0.375 mL
Milli-Q water	2.2 mL
Tris-HCl 1M (pH6.8)	0.375 mL
10%SDS	15 µL
10%APS	15 µL
TEMED	3 µL

Separating gel (/gel)**Example: 12.5%**

30% polyacrylamide	3.2 mL
Milli-Q water	1.5 mL
Tris-HCl 1 M (pH 8.8)	2.8 mL
10% SDS	37.5 µL

10% APS	37.5 μ L
---------	--------------

TEMED	7.5 μ L
-------	-------------

10X TBS

Tris-HCl, 1 M, pH 7.5	5 mL
NaCl 5 M	30 mL
Milli-Q water	1000 mL

1X TBST

Tween-20	1 mL
TBS	1L

1X Blotto

Non-fat dry milk powder	2.5 g
Bovine serum album	1.0 g
TBST	100 mL

Zymography digestion buffer

NaCl	200 mM
Tris	50 mM
CaCl ₂	5 mM
Brij-35 (v/v)	0.02%

Appendix D – Primers list

Primer	Sequence (5'–3')
UPA_F	GCCATCCCGGACTATACAGA
UPA_R	AGGCCATTCTCTCCTTGGT
CATHEPSIN B_F	TCGGATGAGCTGGTCAACTATG
CATHEPSIN B_R	TCCAAGCTTCAGCAGGATAG
MMP-9_F	CGTCCCGGGTGTAGAGGTC
MMP-9_R	ACGGGCTCCTGGCACACG
pEGFP-C2 NYD-SP8 cloning primer_F	ATTGTCCAGCACTCTTCACC
pEGFP-C2 NYD-SP8 cloning primer_R	AGACGACTCAATGCCACC
pQCXIH NYD-SP8 cloning primer_F	CTTGCGGCCGCGATGGGAACCCCTCGTA
pQCXIH NYD-SP8 cloning primer_R	GCCGGATCCTTAGGAAAAGTGAATAA
NYD-SP8_F	ATTGTCCAGCACTCTTCACC
NYD-SP8_R	AGACGACTCAATGCCACC
GAPDH (human)_F	AGG GTC ATC ATC TCT GCC
GAPDH (human)_R	CCA TCA CGC CAC AGT TTC
uPAR_F	CTGGAGCTGGTGGAGAAAAG
uPAR_R	TGTTGCAGCATTTCAGGAAG
PAI-1_F	CGGTCATTCCCAGGTTCTCTA
PAI-1_R	TGCTGGTGAATGCCCTCTACT
NFKB-1_F	AGAAATAGACGGCTCCGAGA
NFKB-1_R	GGCACCCTGGTCAGAGACTC
GAPDH (mouse)_F	GAC CAC AGT CCA TGC CAT CAC TGC
GAPDH (mouse)_R	GCT GTT GAA GTC GCA GGA GAC AAC